UiT
THE ARCTIC UNIVERSITY OF NORWAY

Faculty of Science and Technology

Department of Geoscience

Reconstruction of late Holocene paleoenvironment in Kongsfjorden, West Spitsbergen

based on analysis of benthic foraminifera

—

Kim-André Danielsen

Master's thesis in Marine Geology and Geophysics (GEO-3900)

May 2017

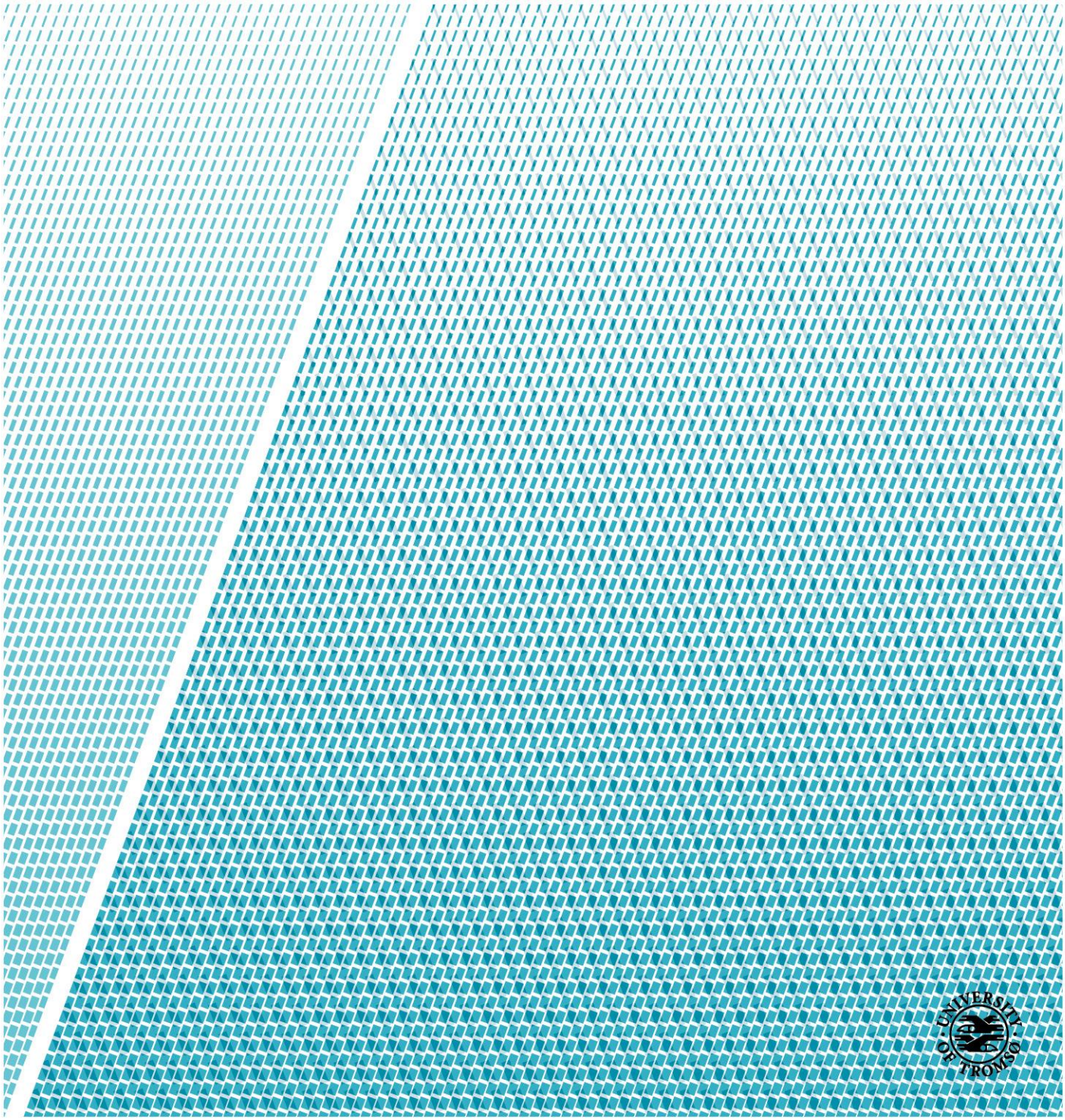

Abstract

The benthic foraminiferal fauna of two marine sediment records from the Kongsfjorden Trough and the inner part of Kongsfjorden were analyzed to reconstruct the paleoenvironmental development throughout the last ~ 2000 years. A generally cold period is evident in both records, lasting from ~ 700 to 1400 CE at the Kongsfjorden Trough and from ~ 350 to 1200 CE in the inner part of Kongsfjorden, with low to moderate influence of Atlantic Water at both sites. However, the record from the inner part of Kongsfjorden show more fluctuating conditions, possibly due to high influence of local water masses. In both records, the cold period is followed by a period of ameliorated conditions, characterized by an abrupt increase of the benthic foraminiferal flux from ~ 1400 to 1650 CE at the Kongsfjorden Trough, and a gradual increase in the relative abundance of *N. labradorica* from ~ 1200 to 1550 CE in the inner part of Kongsfjorden. This indicates increased influence of Atlantic Water at both sites, and is correlated to correspond to the Medieval Warm Period. The record from the Kongsfjorden Trough stops at ~ 1650 CE as the core top is missing. In the inner part of Kongsfjorden a period of rapidly deteriorated conditions follows from ~ 1550 to 1650 CE, characterized by an abrupt increase of % *E. excavatum* f. *clavata* and a corresponding decrease of % *N. labradorica*. From ~ 1650 to 1900 CE the trend changes with gradually improved conditions. The period from ~ 1550 to 1900 CE is correlated to correspond to the Little Ice Age. The last ~ 100 years of the NP14-Kb3 record is characterized by an accelerated increase of % *N. labradorica*, reaching maxima in relative abundance. This possibly indicates the highest influence of Atlantic Water throughout the record, and is correlated to correspond to the Modern Warming.

Table of Contents

List of Tables

List of Figures

Acknowledgements

Eg vil gjerne rette ein stor takk til rettleiarane mine Katrine Husum og Jan Sverre Laberg for veldig god rettleiing i skriveprosessen. I rettleiingsmøta har eg fått mange gode og konstruktive tilbakemeldingar som eg har lært mykje av. Det har vert veldig kjekt og inspirerande å diskutere oppgåva med dykk, og de har alltid vert tilgjengelege for spørsmål.

Takk til Trine Dahl, Ingvild Hald og Karina Monsen for veldig god hjelp og opplæring gjennom labarbeidet!

Takk til medstudentar og vener for ei kjekk tid i Tromsø!

Takk til familie som har vert støttande heile vegen!

Og takk til Nina som har venta på meg i Bergen i to år! :)

Kim-André Danielsen,

Førde, Mai 2017

1 Introduction

1.1 Paleoceanography

Paleoceanography is an interdisciplinary field of science describing how the oceans have developed through history, by combining different geological and biological factors like plate tectonics, ocean circulation, sedimentation, ecology and biological productivity. This is achievable by using so called "proxies", which are physical imprints which can be used as indicators of past oceanic conditions and climate. Example of proxies are corals, ice cores, alkenones and different organisms like diatoms, foraminifera and radiolarians. For this master thesis, benthic foraminifera are used as a proxy. Benthic foraminifera are protists living on the ocean floor building their shells from mostly calcium carbonate, but also agglutinated sediments and silica. Certain species of benthic foraminifera can be connected to specific oceanographic conditions. With this knowledge, it is possible to reconstruct the paleoceanography at a location by analyzing the population dynamics of fossilized foraminifera in a sediment core. Paleoceanography may further provide information on past climatic conditions, known as "paleoclimate".

1.2 Regional paleoceanographic and paleoclimatic development throughout Holocene

According to paleorecords from the Fennoscandian region, the North Atlantic and the Arctic region, climatic fluctuations has occurred several times from the start of Holocene to the present-day (e.g. Hald, et al. 2007; Risebrobakken, et al., 2011; Rasmussen, et al., 2014; Aagaard-Sørensen, et al. 2014; Sejrup, et al, 2016) There are several theories about the forcing factors behind these fluctuations. This includes variability in solar insolation due to orbital forcing, variability in the thermohaline circulation affecting the northward flow of Atlantic Water, increased meltwater fluxes from disintegrating ice sheets, volcanic eruptions and variability in the state of the Arctic Oscillation (AO) and the North Atlantic Oscillation (NAO) (e.g. Risebrobakken, et al., 2011; Sejrup, et al., 2016). The AO is a weather phenomenon created by the difference in atmospheric pressure between the high-pressure zone at mid latitudes and low-pressure zone at high latitudes in the Northern Hemisphere. A positive state of the AO means an increased difference in atmospheric pressure compared to a negative state. The NAO behaves very similar to the AO, but originates from a more localized atmospheric pressure difference in the North Atlantic, between the Azores high and the Icelandic low. Both the AO and the NAO affects the strength of the westerlies, which further influences the strength of the northward flow of Atlantic Water to the Arctic (e.g. Hurrell, 1995; Ambaum, et al., 2001; Goosse & Holland, 2005; Trouet, et al., 2009). When discussing possible forcing factors behind climatic fluctuations in different

paleorecords, it has proven to be important to separate surface proxies from near-surface proxies (Risebrobakken, et al., 2011; Sejrup, et al., 2016).

1.2.1 Paleoceanography and paleoclimate during Holocene in the North-Atlantic and Arctic regions

This section will introduce some of the climatic fluctuations throughout Holocene in the North-Atlantic and Arctic regions, while the next section will describe centennial-scale climatic fluctuations at Svalbard during the last ~ 2000 years. The dated Holocene subdivisions (Early, mid- and late Holocene) are obtained from Slubowska, et al., 2005.

Early Holocene

In terrestrial and marine records from the Nordic Seas and the Arctic region, a shorter period of cooling is documented from ~ 11,3-11,05 ka BP. This is known as the Preboreal Oscillation (PBO) (e.g. Björk, et al., 1997; Hald & Hagen 1998; Husum & Hald 2002; Skirbekk, et al., 2010; Aagaard-Sørensen, et al., 2014; Rasmussen, et al., 2014). Increased meltwater from glaciers, slowing down the North Atlantic Current (NAC), combined with increased export of sea-ice into the Fram Strait, are suggested as possible forcing factors for the PBO (Hald & Hagen, 1998; Fisher, et al., 2002).
Going further into the early Holocene (~ 10,800–6800 cal years B.P.) the climate gradually changes into what is often considered the climate optimum of the Holocene, often referred to as the Holocene Thermal Maximum (HTM). In general, the HTM has been attributed to increased solar insolation due to orbital forcing (Renssen, et al., 2009). However, it has also been suggested that northward advection of Atlantic Water had a major impact on the warm sea surface water temperatures (SST) during the HTM (Kaufman, et al., 2004). By comparing near surface marine proxies (e.g. alkenones and diatoms) and proxies from beneath the summer mixed layer (SML) (e.g. foraminifera and radiolarians), this hypothesis has subsequently been challenged. At the Vøring Plateau, reconstructions of SST based on diatoms and alkenones show warmer temperatures during the HTM, while at the same site, no warming is found in temperature reconstructions based on foraminifera and radiolarians (Risebrobakken, et al., 2011 and references therein). Risebrobakken et al. 2011 concludes that the HTM should solely be attributed to increased solar insolation due to orbital forcing, and consequently, the HTM can only be identified in marine proxies within the SML. According to Risebrobakken et al. 2011, this explains the warming trend from ~ 9 to 6 kyr BP seen in several SST reconstructions from the eastern Nordic Seas (e.g. Koc, et al., 1993; Birks & Koc, 2002; Calvo, et al., 2002; Kim, et al., 2004; Andersen, et al., 2004; Risebrobakken, et al., 2010).
Risebrobakken et al. 2011 further concludes that proxies from beneath the SML, mainly reflects

variability in northward advection of Atlantic Water through the Norwegian Atlantic Current (NwAC). This possibly explains a maximum in temperature at ~ 10 kyr BP, seen in several foraminiferal records from the Nordic Seas and the Barents Sea (e.g Hald, et al., 2007; Aagaard-Sørensen, et al., 2010; Risebrobakken, et al., 2010), and at the west coast of Svalbard (e.g. Hald, et al., 2007; Ebbesen, et al., 2007; Skirbekk, et al., 2010). The increased advection of Atlantic Water is possibly explained by the gradual build-up of an Atlantic subsurface reservoir, due to glacial melting weakening the Atlantic Meridional Overturning Circulation (AMOC) (Knorr & Lohmann, 2007). The AMOC is

Mid-Holocene

Colder conditions during the Mid-Holocene (~ 6800–4500 cal years B.P.) is evident in several time series from the Nordic seas (e.g. Calvo, et al., 2002; Birks & Koc, 2002) and Svalbard and the Fram Strait (e.g. Slubowska, et al., 2005; Slubowska-Woldengen, et al., 2007; Ebbesen, et al., 2007; Hald, et al., 2007; Rasmussen, et al., 2007; Aagaard-Sørensen, et al., 2014), representing both reconstructions of sub sea surface temperatures (sSST) and SST. The changes are possibly due to a combination of decreased solar insolation (Laskar, 1990; Berger & Loutre, 1991), combined with a negative state of the NAO, slowing the inflow of Atlantic Water to the Arctic (Hurrell et al., 1995; Nesje, et al., 2001)

Late Holocene

Several paleorecords from the Nordic Seas show cold sea surface temperatures during late Holocene (~ 4500 cal years B.P. to Present) (e.g. Koc, et al., 1993; Andersen, et al. 2004), generally coinciding with the continuously decreasing Northern Hemisphere insolation at the time. Oppositely, several paleorecords from the Nordic Seas that is based on sub surface proxies, show a warming trend during the same period (e.g. Risebrobakken, et al., 2003; Sarnthein, et al., 2003; Ebbesen, et al., 2007; Andersson, et al., 2010) This can possibly be attributed a positive NAO state after ~ 2 kyr BP (Nesje, et al., 2001; Olsen, et al., 2012).

In paleorecords from Svalbard, based on benthic foraminifera, the late Holocene is generally characterized by cold bottom water conditions (Slubowska, et al., 2005; Slubowska-Woldengen, et al., 2007; Skirbekk, et al., 2010). However, the last ~ 1000 years of the records show ameliorated conditions with increased influence of Atlantic Water. In a more recent study from Kongsfjorden Trough and Hinlopen Trough, the use of high-resolution data from the last 2000 years have shown several centennial climatic changes during the most recent part of Holocene (Jernas, et al., 2013), which will be further discussed in the next section.

1.2.2 Paleoceanography at Svalbard during the last ~ 2000 years

The last ~ 2000 years accounts for some of the most frequent climatic fluctuations throughout Holocene. These fluctuations have been described as several shorter periods of warm and cold climate, and includes among others the "Medieval Warm Period" (MWP), "Little Ice Age" (LIS) and the recent "Modern Warming" (MW) (e.g. Lamb, 1965; Grove, 1988; Mann, et al., 2011; Graham, et al., 2011).

According to Jernas et. al (2013), by interpreting the relative abundance, diversity and productivity of the most dominant benthic foraminiferal species, several centennial-scale climatic fluctuations can be found in foraminiferal records from the Kongsfjorden Trough and the Hinlopen strait. A total of six intervals were found in the Hinlopen record, numbered from I to VI (VI= BC 50-AD 300, V= AD 300-700, IV = AD 700-1200, III= AD 1200-1500, II= AD 1500-1900 and I= AD 1900-present), while only V-I were found in the Kongsfjorden Trough record. The records from the two sites shows similar trends with gradually improved conditions throughout the last ~ 2000 years. However, there are some differences between the records due to the Kongsfjorden Trough being more affected by Atlantic Water from the WSC, and the Hinlopen Strait being affected by the Sea Ice Margin (Jernas, et al., 2013). Wilson et. al (2011) discovered similar findings in the Barents Sea, by studying the benthic foraminiferal fauna south east of Bjørnøya during the last 1400 years.

The first interval, VI, is only present in the record from Hinlopen, and is characterized by moderate influence of Atlantic Water and near presence of the Polar front. This is interpreted from a relative high abundance of *Nonionella labradorica*, which is often connected to high supply of nutrients from Atlantic Water (e.g. Hald & Korsun, 1997; Korsun & Hald, 1998; Korsun & Hald, 2000; Rytter, et al., 2002; Jennings, et al., 2004).

Interval V is related to colder conditions in both records, although more critical for the Hinlopen record. In the IV interval influence of Atlantic water gradually increases again towards interval III, where the foraminiferal flux reaches its maxima. Both periods are characterized by a relatively high abundance of *N. labradorica*. The IV and III intervals are correlated to correspond to the MWP. Interval II represents a new period of deteriorated conditions, not unlike the conditions in interval V, with less AW influence and reoccurrence of perennial sea ice cover. Like in interval V, the climatic conditions are more severe in Hinlopen compared to the Kongsfjorden Trough, as the Kongsfjorden Trough experienced advection of AW during summer. Interval II correlates with the LIA cold period. From AD 1900 the records from Hinlopen generally shows reduced sea ice cover, while the Kongsfjorden records shows stronger advection from AW and increased productivity (Jernas, et al., 2013)

Indications of similar centennial climatic fluctuations throughout the last part of Holocene is also present in several other high-resolution palaeoceanographic records from the Arctic (i.e. Murdmaa, et al., 2004; Majewski, et al., 2009; Bonnett, et al., 2010; Spielhagen, et al., 2011; Werner, et al., 2011) and the Nordic Seas (i.e. Andersson, et al., 2003, 2010; Risebrobakken, et al., 2003; Sejrup, et al. 2010.)

The forcing factors behind the MWP and LIA are debated. Several studies attribute the MWP and the LIA to the state of the Arctic Oscillation (AO) and the North Atlantic Oscillation (NAO). A positive state of the AO/ NAO and a consequently increased strength of the AMOC is suggested to correlate with the MWP, and a more neutral NAO state and weaker AMOC correlates with the LIA (e.g. Shindell, et al., 2001, 2003; Seidenkrantz, et al., 2007; Trouet, et al., 2009, 2011; Mann, et al., 2011). Regarding the LIA, external factors like decreased solar insolation and volcanic activity are also considered to play a major role (e.g. Crowley, 2000; Shindell, et al., 2003; Jiang, et al., 2005, 2015; Miller, et al., 2012; Schleussner, et al., 2015).

1.3 Study area

Together with Krossfjorden, Kongsfjorden is a part of a two-armed fjord system which converges into the Kongsfjorden Trough at the West Spitsbergen Shelf. The fjord system is located between 78°40 and 77°30 N, and 11°3 and 13°6 E (Figure 1.1). Large parts of the area surrounding Kongsfjorden and Krossfjorden are covered by glaciers, and several tidewater glaciers culminates into the fjord system. In Kongsfjorden this includes Kongsbreen, Kongsvegen and Kongsbreen which terminates at the head of Kongsfjorden, and Conwaybreen and Blomstrandsbreen terminating at the northern coast of the fjord (Svendsen, et al., 2002). Kongsfjorden and the Kongsfjorden Trough are the focus for this master thesis.

Figure 1.1: Map of Svalbard. Red square shows the location of the study area. Map adapted and modified from Kartverket.no.

1.4 Objectives

The purpose of this master thesis is to map changes in the oceanography of Kongsfjorden during the last ~ 2000 years, by analyzing changes in the benthic calcareous foraminiferal fauna, and in this way, investigate the causes of climatic and environmental changes. This will contribute to knowledge about how climate will change in the future.

The two sediment cores provided for this master thesis, NP15-Kb0-MC and NP14-Kb3-MC (from here abbreviated "NP15-Kb0" and "NP14-Kb3") were collected during cruises with research vessel, R/V Lance to Kongsfjorden in 2014 and 2015. The location of the NP15-Kb0 record lies within the Kongsfjorden Trough in proximity to the mouth of the Kongsfjorden-Krossfjorden fjord system at 79°02.78'N; 11°08.36'E and at a water depth of 315 m, while the NP14-Kb3 record is located within the inner parts of Kongsfjorden at 79°02.78'N; 11°08.36'E and at water depth of 329 m (Figure 2.1). Both cores were retrieved using a multicorer.

2 Geological setting

2.1 Bathymetry and geology

2.1.1 Bathymetry

Stretching from northwest to southeast, Kongsfjorden measures about 20 km in length and between 4 and 10 km in width. The inner parts of the fjord are relatively shallow with depths below 100 m, while the outer parts are generally deeper with a maximum depth of 394 m (Svendsen, et al., 2002; Howe, et al., 2003) (Figure 2.1). Based on interpretation of multibeam images, parts of the seabed morphology are constituted by glacial landforms like drumlins and glacial flutes, as well as sediments reworked by bottom currents (Howe, et al., 2003). Where the submarine channels of Kongsfjorden and Krossfjorden meet, they form a common glacial basin called "Kongsfjordsrenna" (The Kongsfjorden Through). The Kongsfjorden Trough stretches all the way to the shelf edge. Because of this large submarine through, and lack of distinctive sills at the fjord mouth, Kongsfjorden is largely exposed to incoming currents from the open ocean and coastal water masses, which is highly affecting the hydrophysical and biological systems within the fjord (Svendsen, et al., 2002; Cottier, et al., 2005).

2.1.2 Sedimentary environment

The sedimentary environment of Kongsfjorden is considered glaciomarine and ice-proximal, and sedimentation is largely influenced by the surrounding tidewater glaciers (Elverhøi, et al., 1983; Howe, et al., 2003). The sedimentary environment can be categorized based on water depth: shallow water (<100 m), intermediate environments (250-100 m) and basins (>250 m). The shallow water environment is largely influenced by ice related processes. This includes reworking of sediments by ice berg scouring and deposition of ice rafted sediments. In the intermediate environment, different mass flow processes are dominating, both downslope and along the slope, as well as settling of sediments through the water column. The deeper basins are also affected by mass flow processes, but mainly the sediments are deposited through direct settling from the water column in a low energy environment (Howe, et al., 2003).

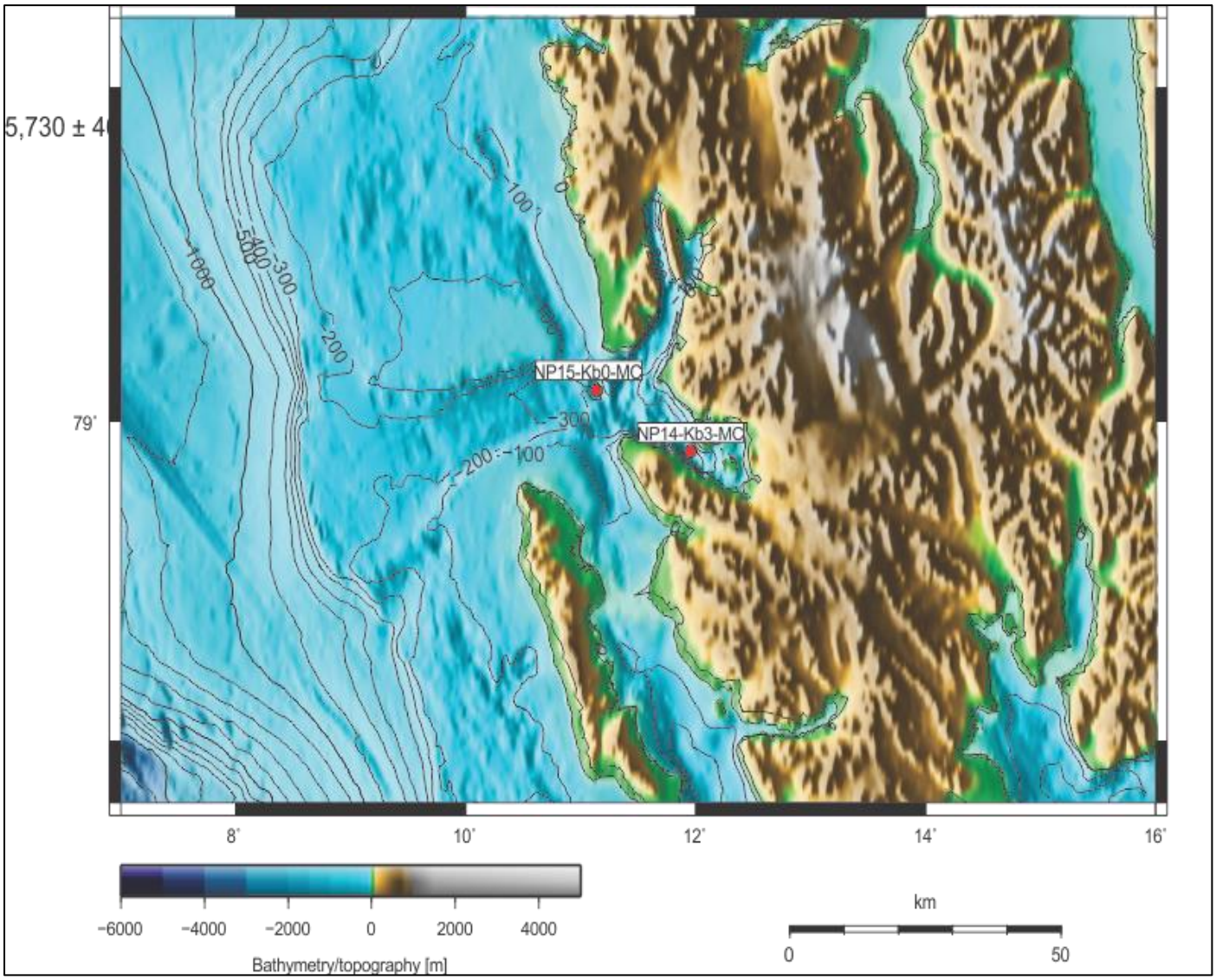

Figure 2.1: Bathymetric map including the Kongsfjorden-Krossfjorden fjord system and the Kongsfjorden Trough, showing the location of sediment cores NP15-Kb0-MC and NP14-Kb3-MC.

2.2 Recent Oceanography

The North Atlantic Current (NAC) is an extension of the Gulf stream and a part of the global thermohaline circulation. The thermohaline circulation is a global system driven by density differences in the oceans, generally caused by difference in temperature and salinity. Warm and saline Atlantic Water (AW) is transported by the NAC from the equatorial Atlantic Ocean to the cold polar areas of Northwestern Europe (Saloranta & Hauan, 2001).

The Norwegian-Atlantic Current is a continuation of the NAC, and follows the Norwegian coast until its northernmost tip, where it splits into the North Cape Current and the West Spitsbergen Current (WSC) (Saloranta & Hauan, 2001). The WSC, defined as AW with T > 3°C and S > 34.9‰ (Hopkins, 1991), continues northwards where it finally reaches the continental margin of Svalbard (Figure 2.1). Going northwards along the western coast of Svalbard, the water masses of the WSC are gradually cooled down, resulting in an increasingly denser current. This eventually leads to the WSC sinking below colder and fresher Arctic Water (ArW) at approximately 78 °N. Further the current follows the slope bathymetry of the shelf slope, along the west coast of Svalbard, resulting in a nearly ice-free area west of the shelf (Aagaard, et al., 1987; Gascard, et al., 1995). Based on several studies, the WSC is estimated to transport somewhere between 28 and 70 TW of heat to the Arctic (Cisewski, et al., 2003; Schauer, et al., 2004; Walczowski, et al., 2005), and is considered the main contributor of AW to the Arctic seas (Saloranta & Hauan, 2001; Vinje, 2001).

Another external current influencing the west coast of Svalbard is the East Svalbard Current (ESC). Originating from the Arctic Ocean, the ESC transports cold ArW (T < 0°C and S 34.4 – 34.7‰ (Loeng, 1991)) to the Barents Sea. The current follows the shelf of Svalbard, going from the east to the west coast, and along the west coast of Svalbard, it is called the Coastal Current (CC). Because of mixing with outflowing water masses from the fjords, ArW from the CC is freshened as the current progresses northward (Cottier, et al., 2005).

The density difference between the WSC and the CC forms a boundary between the currents, called the Arctic Front. Seasonal variations in the strength of the Arctic Front makes advection of Atlantic water into the shelf possible (Tverberg & Nøst, 2009), influencing several fjord systems at the western coast of Svalbard by the inflow of warm and saline AW (Svendsen, et al., 2002; Cottier, et al., 2005; Nilsen, et al., 2008) (Figure 2.1) One of the fjords affected by the WSC is Kongsfjorden, where increasing temperatures of AW recently has resulted in a general rise of summer and winter temperatures (Cottier, et al., 2007). However, poor stratification of the water column in Kongsfjorden during winter season, due to surface cooling and convection, AW is normally prevented from entering the fjord. This changes towards summer as meltwater improves the stratification, and advection of Atlantic water into Kongsfjorden becomes possible around mid-summer (Svendsen, et al., 2002). The inflow of AW to the shelf and continuously into Kongsfjorden, can be seen in figure 2.3 and 2.4.

A third source of water influencing Kongsfjorden, is freshwater supplied by surrounding glaciers, rivers, ground water and snow melting. The five tidewater glaciers located at the inner parts of Kongsfjorden are the major contributors for this water source (Svendsen, et al., 2002; Cottier, et al., 2005). Together, all the freshwater sources provide a mean total discharge of about 1,4 km^3, with 90 % being supplied to the fjord in the period from June to August (Svendsen, et al., 2002). This makes freshwater account for 5% of the total mass balance relative to the fjord volume of 29.4 km^3 (Ito & Kudoh, 1997).

2.2.1 Water masses, circulation and seasonal sea-ice in Kongsfjorden and the Kongsfjorden Trough

A total of seven different water masses are present in Kongsfjorden and the Kongsfjorden Trough. This includes AW and ArW originating from the continental shelf and slope (external water masses), Surface Water (SW), Local Water (LW) and Winter Cooled Water (WCW) locally produced within Kongsfjorden (internal water masses), and Intermediate Water (IW) and Transformed Atlantic Water (TAW) (mixed water masses) (Svendsen, et al., 2002; Cottier, et al., 2005). The interaction between these water masses results in large seasonal variations throughout the year, changing from dominance of cold and fresh Arctic Water during winter to warm and saline Atlantic Water during summer (Svendsen, et al., 2002).

Glacial melting during late spring and summer supplies a large amount of meltwater to the fjord. This meltwater is called SW, and has a wide range of temperatures, much due to its high sediment content which increases the effectiveness of solar warming (Svendsen, et al., 2002; Cottier, et al., 2005). The salinity generally increases from ~ 28 close to the glacier termini to a maximum of 34 further into the fjord. As SW flows towards the fjord mouth, it gradually decreases in thickness. Simultaneously, SW is mixing with underlying AW and TAW, resulting in the formation of IW (Svendsen, et al., 2002; Cottier, et al., 2005).

During autumn and winter cooling of SW and IW in Kongsfjorden, results in formation of LW ($T < 1°C$ and S 0.5 – 1 psu (Cottier, et al., 2005)). When LW reaches its freezing point, production of sea ice increases its salinity, making it denser. This ultimately results in the formation of Winter Cooled Water (WCW). The process of LW and WCW becoming progressively denser eventually leads to convection and mixing with the underlying TAW, resulting in further increased salinity and temperature of the water masses. When reaching a salinity of >34,5 at freezing point, WCW bypasses the density of TAW, and further mixes with TAW as it sinks to the bottom. WCW can remain at the bottom throughout the year, although some of it eventually mixes with surface water during summer resulting in formation of IW (Svendsen, et al., 2002; Cottier, et al., 2005; Nilsen, et al., 2008).

When AW flows across the shelf towards Kongsfjorden, parts of it mixes with ArW from the CC. This results in a mix between AW and ArW called Transformed Atlantic Water (TAW) (Cottier, et al.,

2005). Because of its higher salinity, AW and TAW usually enters the Kongsfjorden Trough below ArW, as a subsurface current (Svendsen, et al., 2002).

The relatively high inflow of AW and TAW to Kongsfjorden keeps large parts of the fjord free of sea-ice all year round. However, a seasonal sea ice cover emerges during the winter season (December/January) and further develops throughout the spring, consisting of a combination of Fast Ice, Drift Ice and Young Ice. The extent of the seasonal sea ice cover varies annually, but is generally limited to the inner part of Kongsfjorden (Figure 2.5) (Svendsen, et al., 2002).

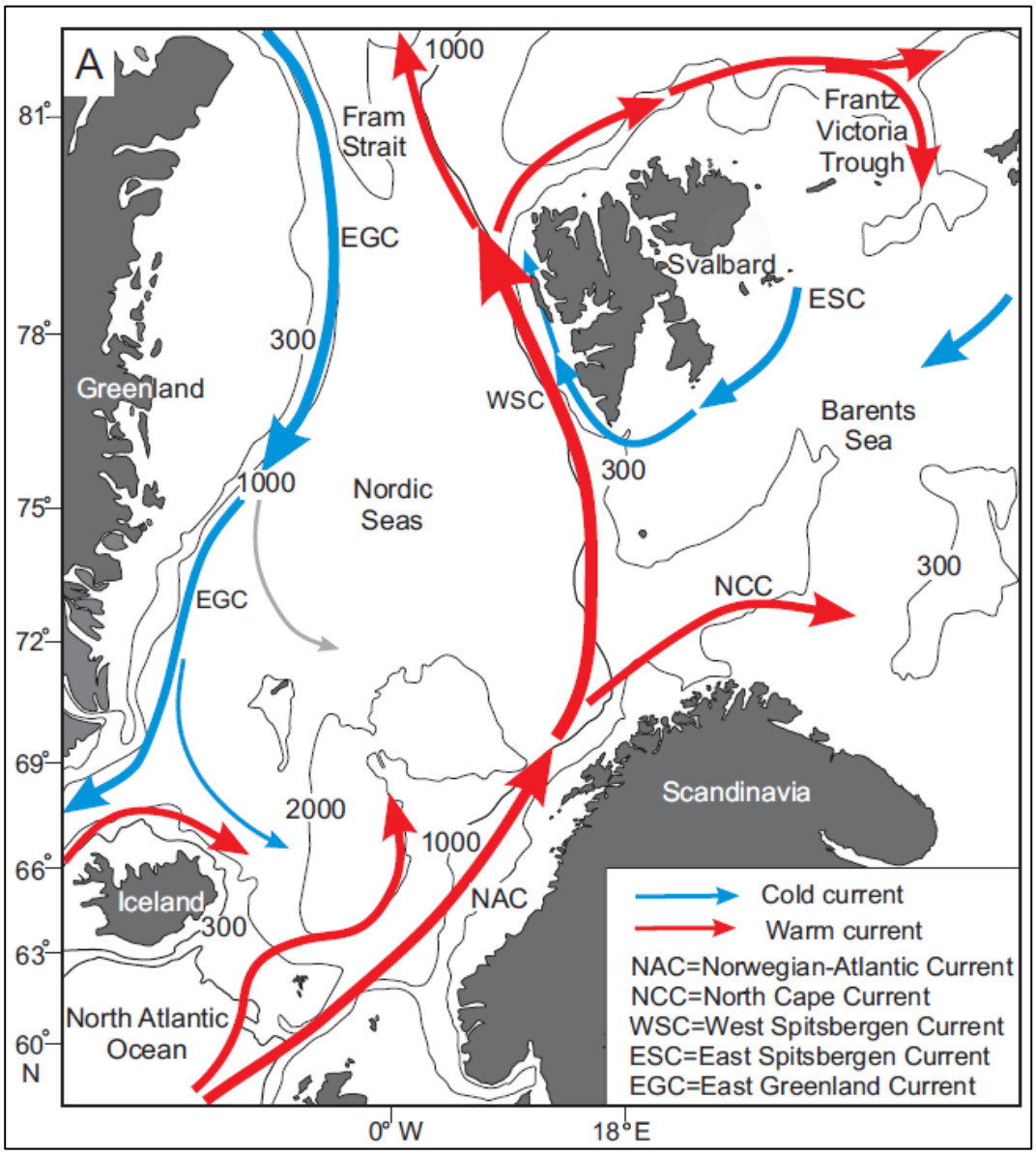

Figure 2.2: A map showing the major surface currents affecting the western coast of Svalbard. Adapted by Rasmussen et al. (2014).

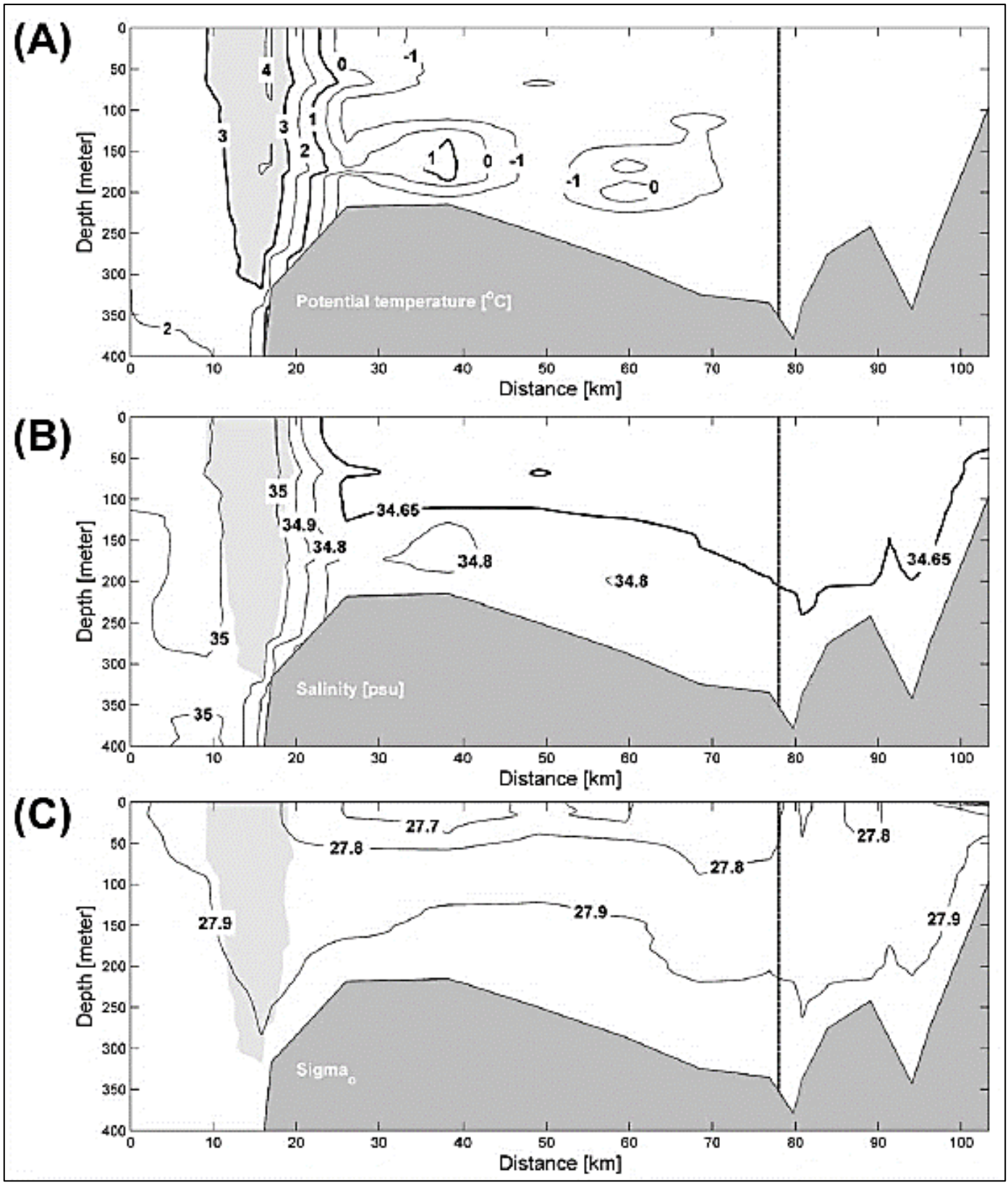

Figure 2.3: (A) Temperature, (B) Salinity and (C) Density sections (April 2002), in a profile stretching from the Kongsfjorden trough to the inner parts of Kongsfjorden. The fjord mouth is represented by the dotted line and the shaded area represents AW. Adapted by Cottier, et al., 2005.

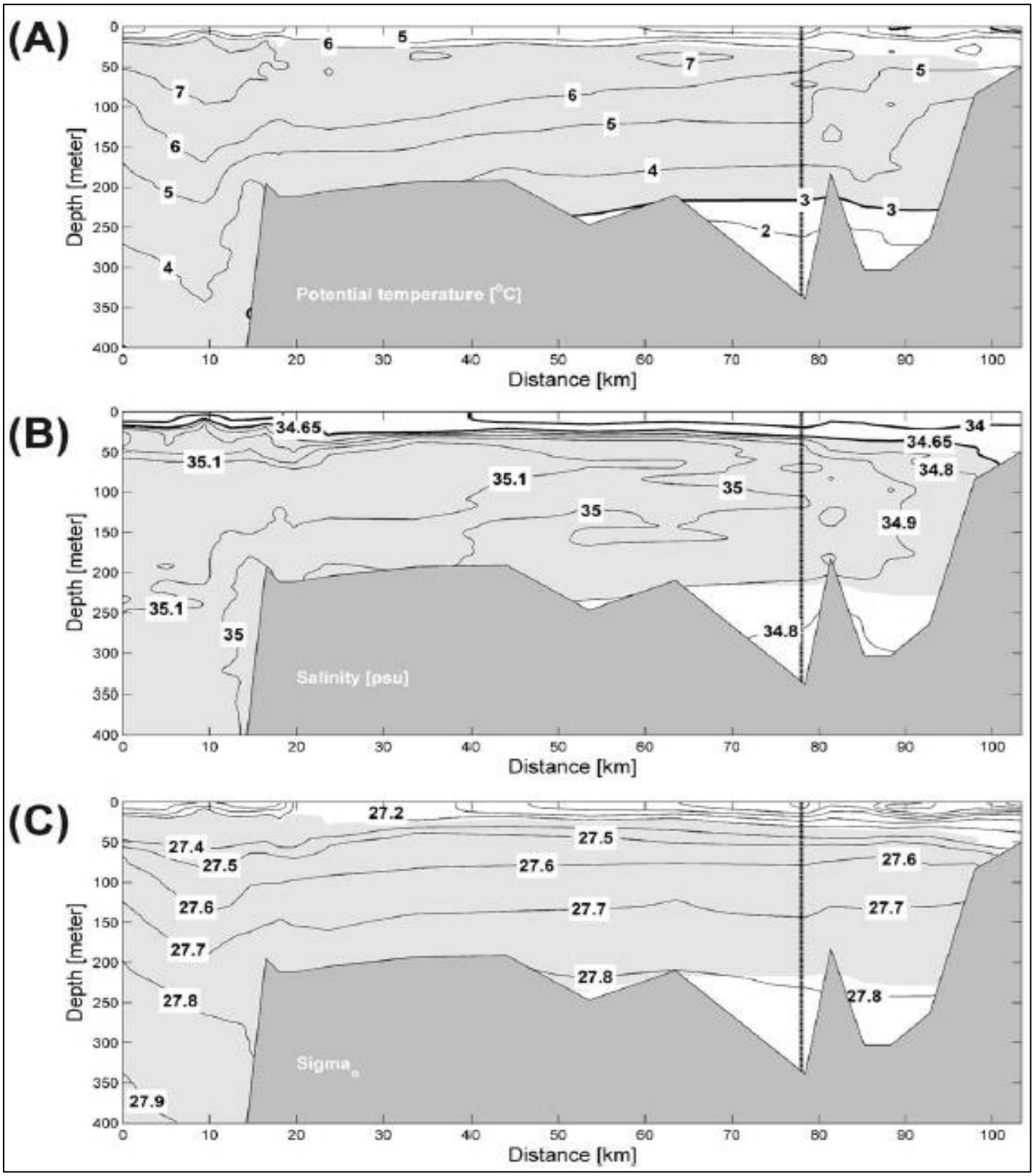

Figure 2.4: (A) Temperature, (B) Salinity and (C) Density sections (September 2002), in a profile stretching from the Kongsfjorden trough to the inner parts of Kongsfjorden. The fjord mouth is represented by the dotted line and the shaded area represents AW. Adapted by Cottier, et al., 2005.

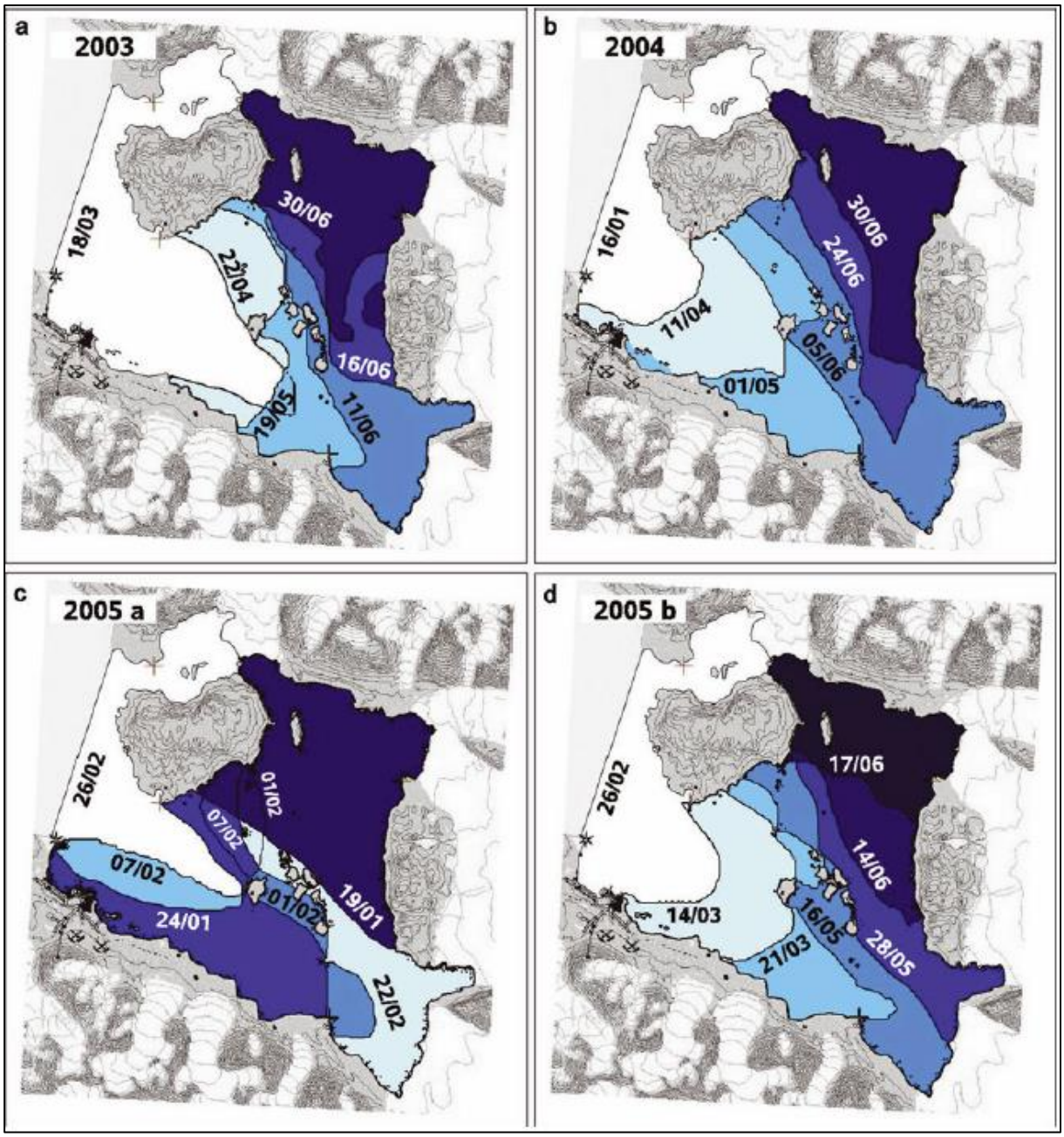

Figure 2.5: Ice-extent for 2003 (a), 2004 (b) and 2005 (c), with dates corresponding to the different positions of the fast ice-edges throughout the year. Adapted by Gerland & Renner, 2007.

3 Material and methods

3.1 Sediment cores

The samples providing the data for this master thesis, NP15-Kb0-MC and NP14-Kb3-MC, were already prepared in advance, and only needed to be dry-sieved to extract the >100 um fraction.
One multicore, HH13-25 MC, from Greenland, was originally intended for this master thesis. Samples from the core were freeze-dried, wet-sieved, heat dried and weighed as described below. However, further analysis of the samples by my supervisor, Katrine Husum, showed that the number of benthic foraminifera was insufficient for extracting statistically significant data of the benthic fauna. Hence this core was abandoned for this study, and new cores, NP15-Kb0-MC and NP14-Kb3-MC, from the Kongsfjorden Trough and Kongsfjorden in Svalbard, were investigated instead. The samples from these cores had already been prepared by a research assistant following the same procedures as HH13-25 MC. All the methods for core preparation will be mentioned in the methods, as I went through a similar preparation process with the HH13-25 MC core.

3.2 Field work

3.2.1 Multi Corer

A multi corer is a device used for collecting sediment cores from the upper parts of the seafloor. The multi corer consists of a metal frame with 1 ton of weight at the top, and the possibility to attach six plastic tubes to it. These tubes are about one meter in length, and behind each tube there is a core catcher. The multi corer is lowered to the sea surface using a winch. When the multi corer hits the seafloor, the weight of the device pushes the tubes into the sediments. As the tubes are filled with sediment the core catchers are released, preventing the sediments from escaping. The multi corer is then hoisted back to the vessel. On deck, the tubes are carefully removed from the multi corer and transferred to a lid. This is done as smoothly as possible to prevent loss of data. A similar lid is also put on the top of the tube. Finally, the cores are stored safely in a vertical position. During the whole process, it is important to keep the cores in a vertical position to preserve the stratigraphy.

3.3 Lab work

3.3.1 Sub sampling

The cores were subsampled using a core extruder. This method works by placing the core on the extruder, and then pushing the tube down carefully. When the desired amount of sediment is measured, the measured part is cut using two metal plates. Every 1-cm of the cores were subsampled. The samples were stored in marked plastic bags and preserved in a freezer.

3.3.2 Freeze-drying

Freeze-drying is a method used to gently dry sediment samples. The method uses sublimation to transform frozen water directly from solid phase to gas phase. Freeze-drying preserves the foraminiferal tests in a better way than heat drying in an oven, and makes it easier to sieve the samples later.

3.3.3 Sieving

The samples were first weighed, before washed and wet sieved using 63 and 1000 μm sieves. The >63 μm fraction were put into a filter paper, while the >1000 μm fraction were put into dram glasses. All the filter papers and dram glasses were labeled with core number, core depth and size fraction. A spray bottle with distilled water was used to make sure all the sediment got transferred from the sieves. The sieves were washed using an ultrasonic cleaner between the sieving of each sample to avoid contamination. After sieving all the samples, they were dried in an oven at 50 °C for about one day. All the samples were then weighed and transferred to labeled dram glasses. Later the 63 μm fraction was dry sieved on the 100 μm sieve for benthic foraminiferal analysis (Appendix 3, 4).

3.3.4 Foraminiferal analysis

The >100 μm size-fraction were used for picking and counting of benthic foraminifera. Because all the samples were relatively large compared to what is needed for species analysis, the >100 μm size-fractions were divided into smaller parts by using a core splitter. A core splitter works by splitting the cores into two equally large parts. The desired fraction of the sample is then equally distributed across a picking tray with 45 squares, with a collection tray below.

The benthic calcareous foraminifera were counted and identified by species name, before transferred to the underlying collection tray through small holes in the picking tray. Square by square were counted until reaching a total of at least 300 benthic calcareous tests. The relative abundance of each species was calculated as the percentage of the total number of benthic foraminiferal specimens in each sample (Appendix 1.3 and 2.3). Planktic and agglutinated foraminifera were not identified, as the amount were insufficient for further analysis.

To calculate the concentration and flux of calcareous benthic foraminifera for each sample the following formulas were applied (Appendix 1.2, 1.4 and 2.2, 2.4):

1. $$Concentration\ \left[\frac{No.of x}{g}\right] = \frac{45}{No.of\ counted\ squares} \times \frac{No.of\ x \times No.of\ splits * 2}{Tot\ wt.\ dry\ sediment}$$

2. $$Flux\ \left[\frac{No.of\ x}{cm^2 \times kyr}\right] = Concentration\left[\frac{No.of x}{g}\right] \times bulk\ dry\ sediment\ density\left[\frac{g}{cm^3}\right] \times sedimentation\ rate\left[\frac{cm}{kyr}\right]$$

Where *x* = total number of calcareous benthic foraminifera. A dry bulk density of 0.5 g cm^{-3} were obtained from Jernas et al., 2013.

3.4 Radiocarbon dating

3.4.1 AMS radiocarbon dating

Some specimens of *N. labradorica* from selected samples in the NP15-Kb0 core were sent to the Poznan Radiocarbon Laboratory for AMS (Accelerator Mass Spectrometry) radiocarbon dating (Table 5.1, Appendix 3). Radiocarbon dating generally works by counting the relative abundance of ^{14}C-atoms compared to ^{12}C-atoms. Because ^{14}C is a radioactive isotope, it decays at a constant speed. Knowing that the half-life of ^{14}C is about 5,730 ± 40 years, it is possible to estimate the age of dead organic material, as dead plants and animals are no longer exchanging carbon with its surroundings. The AMS method works by accelerating ions towards a magnetic field, with high energy. The heaviest ions will be less deflected by the magnetic field. In this way, it is possible to separate the amount of the heavier ^{14}C isotopes from the lighter ^{12}C isotopes.

3.4.2 Marine reservoir age

Carbon is exchanged from the atmosphere to the ocean through dissolution of carbon dioxide. The carbon is further transported to the deep ocean as part of the thermohaline circulation, and ultimately brought back to the surface by upwelling. During this circulation process, the radioactive isotope ^{14}C is decaying at a constant speed, meaning that the water masses are gradually aging. This aging ultimately leads to a difference between the radiocarbon content of the surface water and the atmosphere, called the marine reservoir age, and has a global average value of ~ 400 years (Reimer, et al., 2013). The marine reservoir age varies among regions, which is important to correct for when calibrating ^{14}C ages to calendar years (e.g. Mangerund, et al., 2006).

4 Benthic foraminifera

Benthic foraminifera are a group of single celled protists living mainly in marine environments. They often build tests (internal shells) composed of calcium carbonate, in which case the tests are calcareous. Unlike planktic foraminifera which floats in the water column, benthic foraminifera live either upon (epifaunal) or within (infaunal) the seafloor sediments. Because benthic foraminifera are sensitive to environmental changes, it can be used as a proxy for palaeoceanographic reconstructions (Murray, 2001). The distribution of living benthic foraminifera has been mapped at several locations to learn about the preferred ecology of each specie (i.e. Steinsund, et al., 1994; Hald & Steinsund, 1992; Korsun & Hald, 2000; Jennings, et al., 2004). Assuming this relationship has remained unchanged through time, palaeoceanographic reconstructions are possible by studying the fossilized benthic foraminifera in a sediment core.

4.1 Ecology

The term "ecology" is described as the interactions between living organisms and the environment they live in. The preferred ecology of different benthic foraminiferal species is controlled by physical, chemical and biological parameters. Examples of physical parameters are temperature and turbidity; salinity and alkalinity are chemical parameters and supply of nutrients is a biological parameter. Some benthic foraminiferal species are specific about their preferred habitat and environmental conditions, for example preferring low water temperatures with low salinity, or preferring coarse sediments in a high-energy environment. Other species are more opportunistic and adaptable to fluctuating conditions (Murray, 2001).

4.2 Ecological preferences of benthic foraminiferal species

The ecological preferences of the most common benthic species of NP15-Kb0 and NP14-Kb3 will be described in the following section.

4.2.1 *Elphidium excavatum* (Terquem) forma *clavata* Cushman, 1930

Foraminiferal fauna studies from several fjords on Svalbard and off the coast of Novaya Zemlya concludes that *E. excavatum* f. *clavata* occur most frequently in glacier proximal environments, which is an environment associated with high turbidity and sedimentation rates, fluctuating salinity and limited access to nutrients (e.g. Hald & Korsun, 1997; Korsun & Hald, 1998; Korsun & Hald, 2000; Polyak, et al., 2002). However, the species also appears in more glacier distal environments, where it has been connected to cold water masses (e.g. LW, IW, WCW and ArW) and heavy sea ice cover (Hald, et al., 1994; Hald & Korsun, 1997). Generally, the areas in which *E. excavatum* f. *clavata* dominates, is characterized by largely fluctuating and unfavorable conditions, indicating that the species is opportunistic (e.g. Steinsund, et al. 1994).

4.2.2 *Nonionellina labradorica* (Dawson, 1860)

N. labradorica is an epifaunal species, preferring temperatures of <1 °C and salinities in the range 33-34 psu (Steinsund, et al., 1994). The species is mainly associated with high supply of high-quality nutrients and is consequently often found in proximity to oceanic fronts. This is concluded based on studies from fjords on Svalbard and Novaya Zemlya, where *N. labradorica* is most abundant in the outer, deeper parts of the fjords, where the environmental conditions are characterized by high influence of TAW (Korsun et al. 1995; Hald & Korsun, 1997; Korsun & Hald, 1998; Korsun & Hald, 2000; Rytter, et al., 2002). Findings suggests that *N. labradorica* prefers to feed on diatoms (Cedhagen, 1991; Bernhard & Bowser, 1999)

4.2.3 *Cassidulina reniforme* Nørvang, 1945

C. reniforme prefers cold bottom water with temperatures ranging from <1 to <3 °C. The tolerance of low salinity is high, but preferably >30 ‰ (Steinsund, et al., 1994). Studies from Svalbard and Novaya Zemlya shows that *C. reniforme* is most abundant in the glacier proximal environments, further away from the glacier terminus than *E. excavatum* f. *clavata,* (Korsun, et al., 1995; Hald & Korsun, 1997; Korsun & Hald, 1998). In the studies from Svalbard *C. reniforme* correlates with Local Water and Winter-cooled Water (Hald & Korsun, 1997; Korsun & Hald, 1998).

4.2.4 *Cibicides lobatulus* (Walker & Jacob, 1798)

Several studies show that *C. lobatulus* correlates positively to content of coarser sediments (sand and gravel) (Steinsund, et al., 1994; Hald & Korsun, 1997). This can be explained by *C. lobatulus* being an epifaunal species that attaches to coarse particles and feeds on suspended nutrients (Steinsund, et al., 1994). On Svalbard, the species is mainly located among coarse sediments in the outer parts of the fjord, indicating that the specie prefers a high-energy environment (Hald & Korsun, 1997).

4.2.5 *Buccella spp.*

Buccella spp. includes *Buccella frigida* (Cushman, 1922), together with a low abundance of *Buccella tennerima* (Bandy, 1950). The species are epifaunal, or dwelling in the shallow parts of the sediments, and thrives in temperatures of 0-1 °C and salinities in the range 33-34 ‰. High occurrence of *Buccella* spp. is connected to high organic productivity caused by seasonal ice covers or proximity to the Polar Front. This can be explained by the species feeding on both ice edge algal blooms as well as phyto-detritus transported by Atlantic currents (Steinsund, et al., 1994). However, a more recent study suggests that *Buccella* spp. is primarily an indicator of increased food availability, and thus not necessarily and indicator of sea-ice (Seidenkrantz, 2013).

4.2.6 *Astrononion gallowayi* Loeblich & Tappan, 1953

Astronion gallowayi is an epifaunal species that prefer low temperatures below 1 °C and high salinities, preferably >33 ‰. The species is associated with shallow areas with coarse sediments, and is for that reason often observed together with *C. lobatulus* (Steinsund, et al., 1994).

4.2.7 *Islandiella norcrossi* (Cushman, 1933)

Islandiella norcrossi is considered an epifaunal or shallow infaunal species. The species prefers fine grained sediments at water depths ranging from 200 – 400 m (Steinsund, et al., 1994). Studies from Novaya Zemlya shows that *I. norcrossi* increases in abundance towards glacial-distal environments (Korsun & Hald, 1998). The species is sometimes grouped together with *Islandiella helenae,* due to their morphological similarity (see section 4.2.8).

4.2.8 *Islandiella helenae* Feyling-Hanssen & Buzas, 1976

I. helenae and *I. norcrossi* often occurs together, although dominance of *I. helenae* is connected to shallower and less stable environments than *I. norcrossi* (Steinsund, et al., 1994). *I. helenae* has, sometimes together with *I. norcrossi,* been considered an indicator of sea-ice and ice-edge algal blooming (Korsun & Polyak, 1989; Steinsund, et al., 1994; Hald & Steinsund, 1996). However, it is uncertain if the species is a direct indicator of ice production or a general indicator of increased food supply.

4.2.9 *Stainforthia loeblichi* Feyling-Hanssen, 1954

A study from the Barents and Kara Sea show that the species prefers water temperatures lying around 0 °C. The same study suggests a connection between S. *loeblichi* and seasonal sea-ice cover (Steinsund, et al., 1994). However, *S. loeblichi* cannot be considered a true sea-ice indicator (Seidenkrantz, 2013).

4.2.10 *Trifarina angulosa* (Williamson, 1858)

A study from the southwestern Barents Sea shows that *T. angulosa* thrives in sediments rich in carbonate and prefer high temperatures (Hald & Steinsund, 1992).

4.2.11 *Elphidium bartletti* Cushman, 1933

E. bartletti is associated with near coastal brackish environments, and connected to coarse grained sediments (Steinsund, et al., 1994; Polyak, et al., 2002)

4.2.12 *Nonionella auricula* Heron-Allen & Earland, 1930

N. auricula is morphologically similar to *N. labradorica.* The species is connected to environments with high primary productivity, in sediments with a high content of organic carbon (Austin & Evans, 2000).

5 Results

5.1 Chronology

5.1.1 Chronology and age model for NP15-Kb0

The chronology and age model for core NP15-Kb0 is established using linear interpolation between three AMS radiocarbon dates from three levels (Table 5.1). To make the age model, the three radiocarbon ages were calibrated from 14C years to calendar years using Common Era/ Before Common Era (CE/BCE), using the calibration software CALIB 7.10 with the calibration set "marine13". The reservoir age used for the calibration set is 405 ± 22 (Reimer, et al., 2013). To correct for the regional reservoir age at Svalbard, a value of $\Delta R = 105 \pm 24$ were applied (Mangerud, et al., 2006).

A constant sedimentation rate between 2,5 cm and 20,5 cm, and 20,5 cm and 34,5 cm was assumed to create the age model (Figure 5.1). The sedimentation rate for the interval 2,5 to 20,5 cm is calculated to 89,55 cm/ kyr, and 18,97 cm/ kyr for the interval 20,5 to 34,5 cm.
For unknown reasons, the top of the core is missing. A possible explanation is that the top was lost during the coring process or after the preparation process, or there was very little sedimentation during the present.

Lab code	**Core name**	**Depth (cm)**	**Material**	**^{14}C years (BP)**	**Calibrated age range ± 2σ (CE)**	**Calibrated age range ± 1σ (CE)**	**Calibrated age used in age model (CE)**
Poz-83769	NP15-Kb0	2,5	*N. labradorica*	750 ± 50	1526 - 1811	1569- 1706	1656
Poz-83770	NP15-Kb0	20,5	*N. labradorica*	980 ± 60	1327- 1579	1407- 1509	1455
Poz-83771	NP15-Kb0	34,5	*N. labradorica*	1780 ± 50	611- 847	668- 771	717

Table 5.1: Radiocarbon years and calibrated ages for NP15-Kb0.

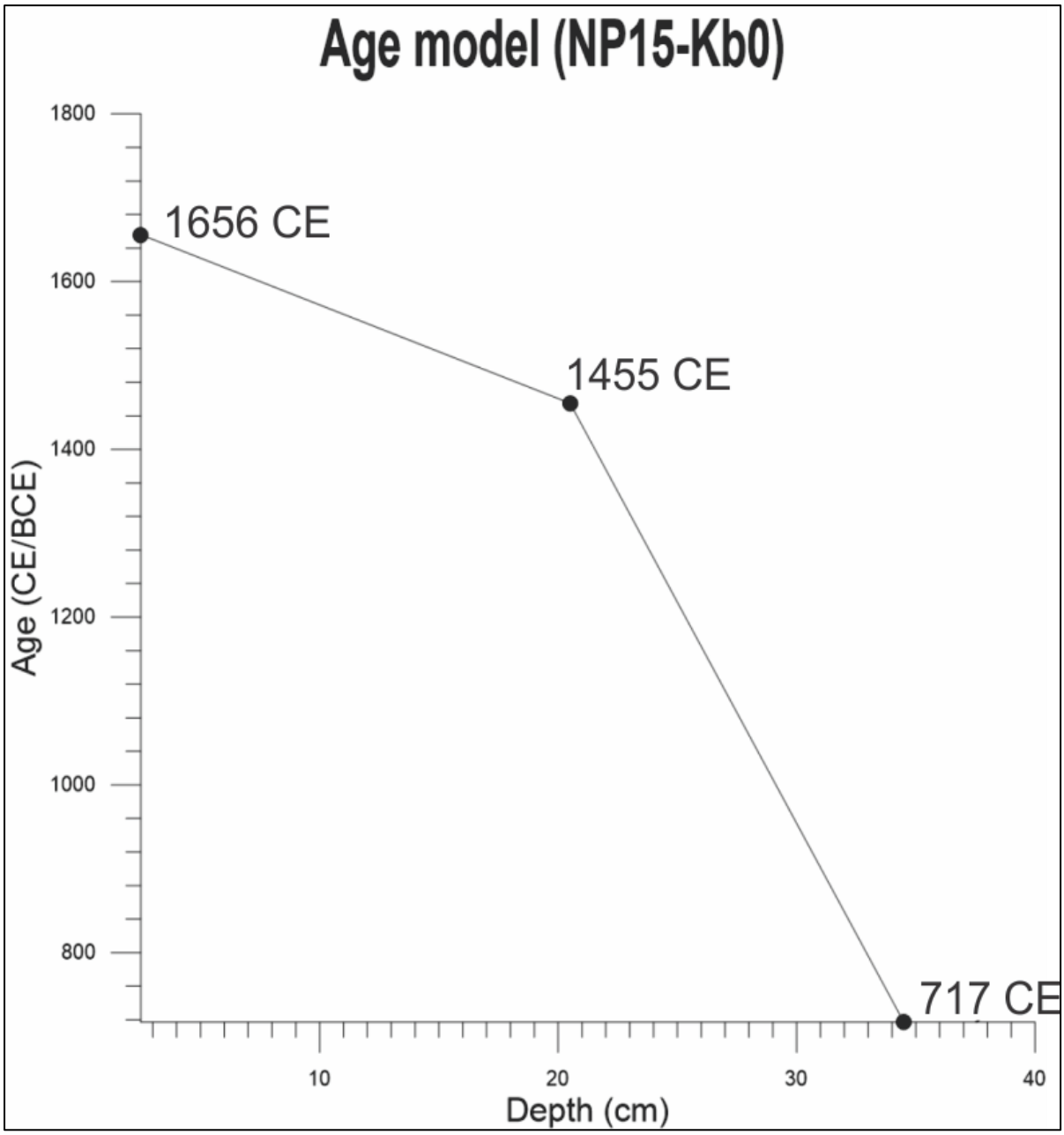

Figure 5.1: Age model for NP15-Kb0. Black dots are indicating the dated intervals.

5.1.2 Chronology and age model for NP14-Kb3

There are no radiocarbon dates from NP14-Kb3. Analysis of $\Delta^{13}C$ and $\Delta^{15}N$ of the NP14-Kb3 shows that the core top represents the time of retrieval, 2014 CE (Miettinen, pers.com). The chronology for NP14-Kb3 was established by correlating to the study by Jernas et al. (2013) obtaining an age for one level in NP14-Kb3 (Table 5.2). Zone 3 of NP14-Kb3 (25 - 15,5 cm) has been correlated to correspond with interval III (CE 1200-1500) of NP05-21. This correlation is based upon a general increase of the relative abundance of *Nonionellina labradorica* entering this period. The start of zone 3 is thus correlated to 1200 CE. A constant sedimentation rate between 25 and 2 cm is assumed to make the age model (Figure 5.2), and the same sedimentation rate is assumed to continue to the bottom of the core at 50 cm. The sedimentation rate is calculated to 28,26 cm/ kyr.

Core name	Depth (cm)	Dating method	Calibrated years (CE)
NP14-Kb3	2 cm	$\Delta^{13}C$ and $\Delta^{15}N$ dating (Miettinen, pers.com).	2014
NP14-Kb3	25,5 cm	Correlation with NP05-21 (Jernas, et al., 2013).	1200

Table 5.2: Calibrated years (CE) for NP14-Kb3

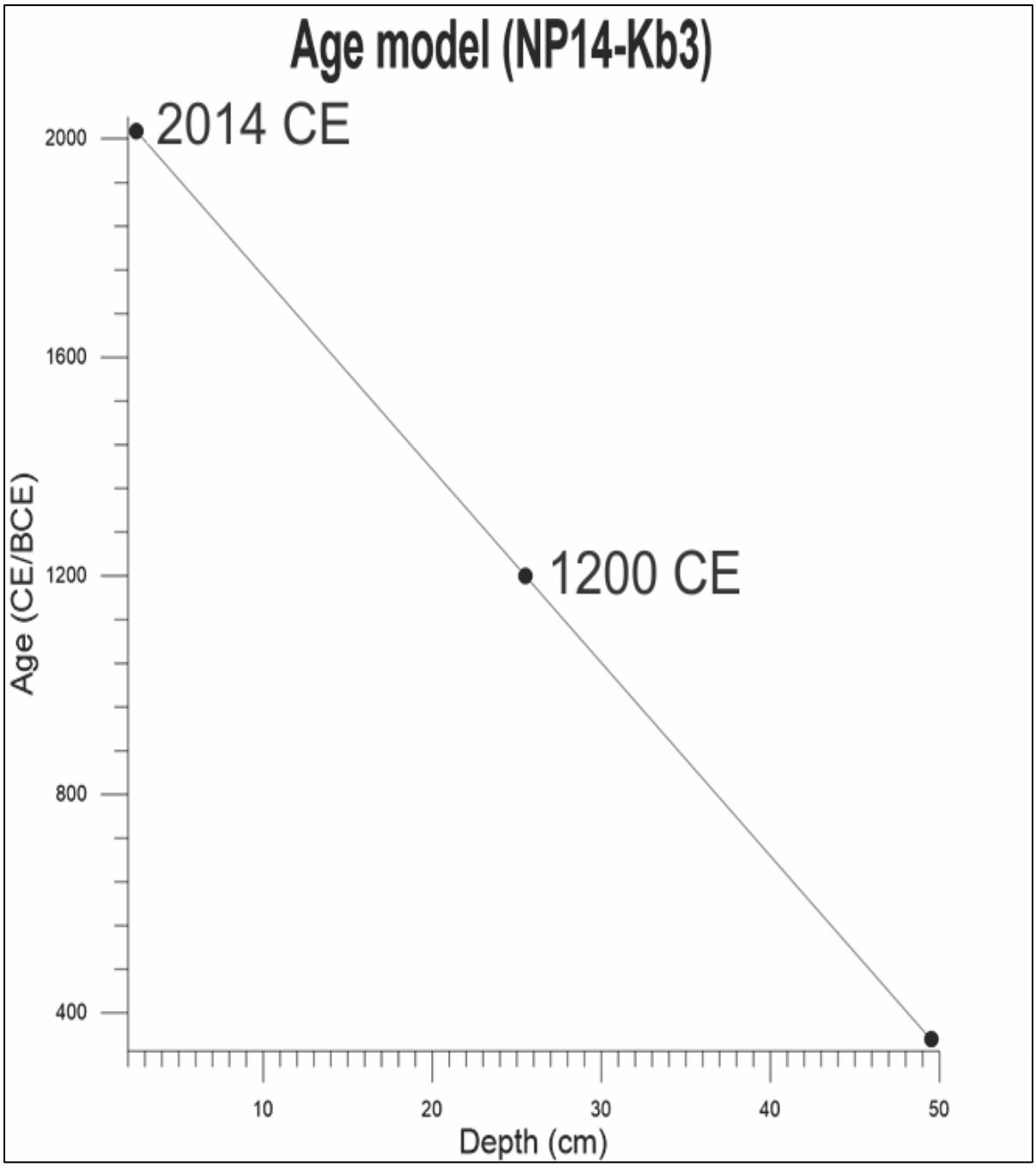

Figure 5.2: Age model for NP14-Kb3.

5.2 Biozones in core NP15-Kb0

In sediment core NP15-Kb0, 22 species were identified (Table 5.3; Appendix 1.1) and two assemblage zones defined (Figure 5.3, 5.4).

5.2.1 Assemblage zone 2: *E. excavatum* f. *clavata* zone (~ 35 - 21 cm, ~ 720 – 1400 CE)

The dominant species of assemblage zone 2 is *Elphidium excavatum* f. *clavata*, with a mean value of ~ 36 % (Figure 5.3, 5.4). The species has a maximum value of 42% at 33,5 cm/ 770 CE and has a generally decreasing trend towards the top of the zone, where it reaches a minimum relative abundance of 30 % at 19,5 cm. Although the general trend shows a gradual decline in abundance, there are also some minor fluctuations within the zone, with most fluctuations lying within a range of ± 5 %. The species flux is stable at an average value of 869 spec./cm2/yr.

Nonionella labradorica is the second most abundant species of the zone with an average abundance of ~ 20 %. It ranges between 16 % and 20 % with no major fluctuations throughout the zone. The flux is stable at an average of 436 spec./cm2/yr. *Cibicides lobatulus* is another abundant species within the zone, and it has an average value of ~ 16 %. Its frequency fluctuates strongly, but it shows a generally increasing trend towards 25,5 cm/ 1191 CE, reaching a value of 25 %. After this point, the frequency of *C. lobatulus* decreases to approximately 10 % towards the top of the zone. The flux follows a similar fluctuating trend with a minimum and maximum value of 236 and 697 spec./cm2/yr., respectively. *Cassidulina reniforme* is the least abundant of the most occurring species ranging between 7 – 13 %. In general, it shows a minor increase in abundance towards the top of the zone. The flux is stable at an average value of 222 spec./cm2/yr.

The most common species of the less abundant species in zone 2 is *Buccella* spp. with an average abundance of ~ 5 % and minimum and maximum abundance of 3 and 8 %. The species is remaining relatively stable throughout the zone with some minor fluctuations. The flux is low with an average value of 124 spec./cm2/yr.

Islandiella helenae is fluctuating throughout the zone with values between 1 and 6 %, and an average flux of 76 spec./cm2/yr. *Islandiella norcrossi* decreases abruptly from a maximum of 8 % at the start of zone 2 to ca 1 % at 30,5 cm/ 928 CE – 16,5 cm/ 1500 CE. The flux follows a similar decrease. *Elphidium bartletti* starts to occur at 23,5 cm/ 1297 CE and increases to a maximum of 8 % at 20,5 cm/ 1455 CE, before decreasing to 5 % at the top of the zone. The two least abundant species of the zone are *Astrononion gallowayi* and *Nonionella auricula*. *A. gallowayi* is nearly absent until 20,5 cm/ 1455 CE, where it appears at a mean value of 5 % towards the end of the zone. The abundance of *N. auricula* is generally low throughout the zone with an average of 2 %.

5.2.2 Assemblage zone 1: *E. excavatum* f. *clavata* - *N. labradorica* zone (~ 21 – 0 cm, ~ 1400 – 1660 CE)

E. excavatum f. *clavata* and *N. labradorica* are the most abundant species of this zone, with average abundances of 21 and 22 %, respectively (Figure 5.3, 5.4). *E. excavatum* f. *clavata* decreases abruptly in the transition between zone 2 and 1, from 34 % to 25 %. The species continuous to slightly decrease towards 10,5 cm, reaching a minimum abundance of 17 %, before increasing to a maximum abundance of 28% towards the top of the zone. The flux abruptly increases entering zone 2, from a mean value of 869 spec./cm2/yr. in zone 1 to a mean value of 2618 spec./cm2/yr. in zone 2. Within zone 2 the flux increases towards a maximum of 5827 spec./cm2/yr. at 16,5 cm/ 1500 CE, followed by a rapid decrease towards 411 spec./cm2/yr. at 11,5 cm/ 1556 CE. Throughout the remaining zone, the flux fluctuates around the mean value.

N. labradorica shows an increasing trend in relative abundance towards 5,5 cm, reaching a maximum of 27 %, apart from an anomaly of 29 % at 12,5 cm. The trend reverses after 5,5 cm descending to a relative abundance of 19 % at the top of the zone. *N. labradorica* shows a similar flux trend as *E. excavatum* f. *clavata.* There are however some differences. The flux is abruptly increasing from 411 spec./cm2/yr. at 21,5 cm/ 1402 CE to 2099 spec./cm2/yr. at 20,5 cm/ 1455 CE; continuing to increase towards 3646 spec./cm2/yr. at 12,5 cm/ 1544 CE. This is followed by an abrupt decrease to 455 spec./cm2/yr. at 11,5 cm/ 1556 CE, before increasing to 4126 spec./cm2/yr. at 7,5 cm/ 1600 CE and decreasing again towards the top.

% *C. lobatulus* generally stays at a stable level of ~ 12 % until it starts to increase from 5,5 cm until the top of the zone and reaches a maximum value of 16 %. *C. reniforme* shows an opposite trend of *C. lobatulus.* The relative abundance remains at an average of 12 % until decreasing to an average of 7 % from 6,5 cm towards the top of the zone. Among the less abundant species, *Buccella* spp. shows a clear increase at the transition between zone 2 and 1. The average abundance increases to 8 %, and reaches 11 % towards the top of the zone. *A. gallowayi* is clearly increasing in relative abundance going into zone 1, with an average value of 6 %. The relative abundance slightly fluctuates throughout the zone, with maximum fluctuations of ± 3 %, and minimum and maximum values of 4 % and 9%. There is also a slightly decreasing trend with lower values towards the top of the zone. *N. auricula* has an increasing trend towards 10,5 cm/ 1567 CE, going from a relative abundance of 3 % to 6 %, before starting to decrease towards 1 % at the top of the zone. *C. lobatulus, A. gallowayi* and *Buccella* spp. generally shows the same flux trends as *N. labradorica*, while *C. reniforme* shows a similar trend as *E. excavatum* f. *clavata*.

Both *I. helenae and I. norcrossi* increases in average relative abundance going from zone 2 to 1. *I. helenae* is fluctuating with a minimum and maximum relative abundance of 1 % and 7 %, while *I.*

norcrossi is more stable throughout the zone. *I norcrossi* shows a similar flux trend as *N. labradorica*, while *I. helenae* is more similar to *E. excavatum* f. *clavata*. The average relative abundance of *E. bartletti* decreases to below 2 % in zone 1. Apart from one anomaly of 6 % at 6,5 cm/ 1611 CE, the species stays at values between 0 % and 3 % throughout the zone. *Stainforthia loeblichi* and *Trifarnia angulosa* are low in relative abundance and fluctuating chaotically throughout the zone.

SPECIES LIST

Benthic foraminiferal species identified in NP15-Kb0:

Astrononion gallowayi Loeblich & Tappan, 1953
Bolivina pseudopunctata Höglund, 1947
Buccella frigida (Cushman, 1922)
Buccella tenerrima (Bandy, 1950)
Casidulina neoteretis Seidenkrantz, 1995
Casidulina reniforme Nørvang, 1945
Cibicides lobatulus (Walker & Jacob, 1798)
Elphidium bartletti Cushman, 1933
Elphidium excavatum forma *clavata* Cushman, 1930
Globobulimina auriculata (Bailey, 1894)
Islandiella helenae Feyling-Hanssen & Buzas, 1976
Islandiella norcrossi (Cushman, 1933)
Melonis barleeanum (Williamson, 1858)
Nodosariida sp
Nonionella auricula Heron-Allen & Earland, 1930
Nonionella labradorica (Dawson, 1860)
Nonionellina turgida (Williamson, 1858)
Oolina melo d'Orbigny, 1839
Oolina williamsoni (Alcock, 1865)
Pullenia sp.
Stainforthia concava (Höglund, 1947)
Stainforthia fusiformis (Williamson, 1848)
Stainforthia loeblichi (Feyling-Hanssen, 1954)
Trifarina angulosa (Malumian 1982)

Table 5.3: Species list including all the identified benthic taxa of core NP15-Kb3 (a total of 24 benthic taxa were identified)

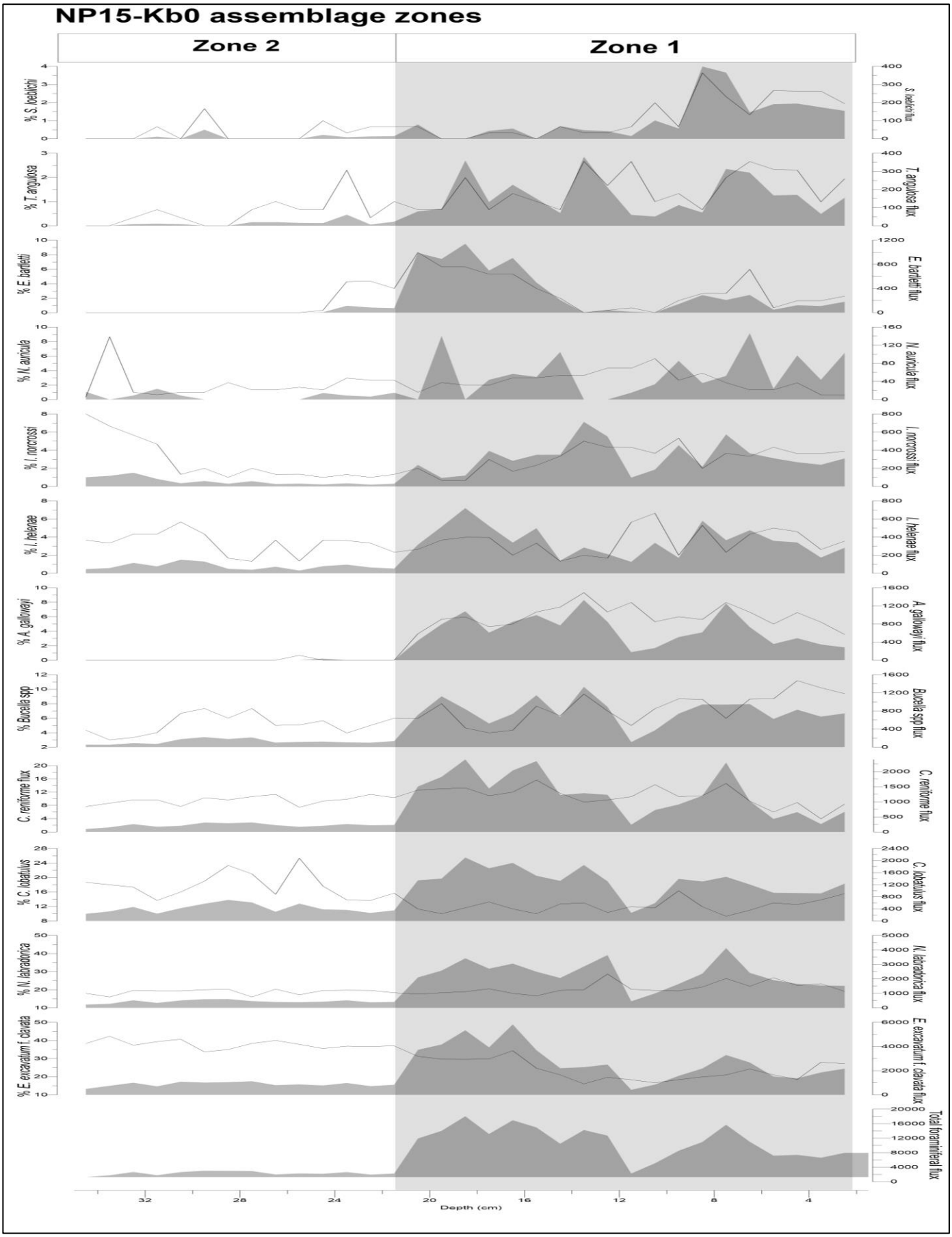

Figure 5.3: Relative abundances (left scale, line) and fluxes (right scale, shading) plotted against depth for NP15-Kb0.

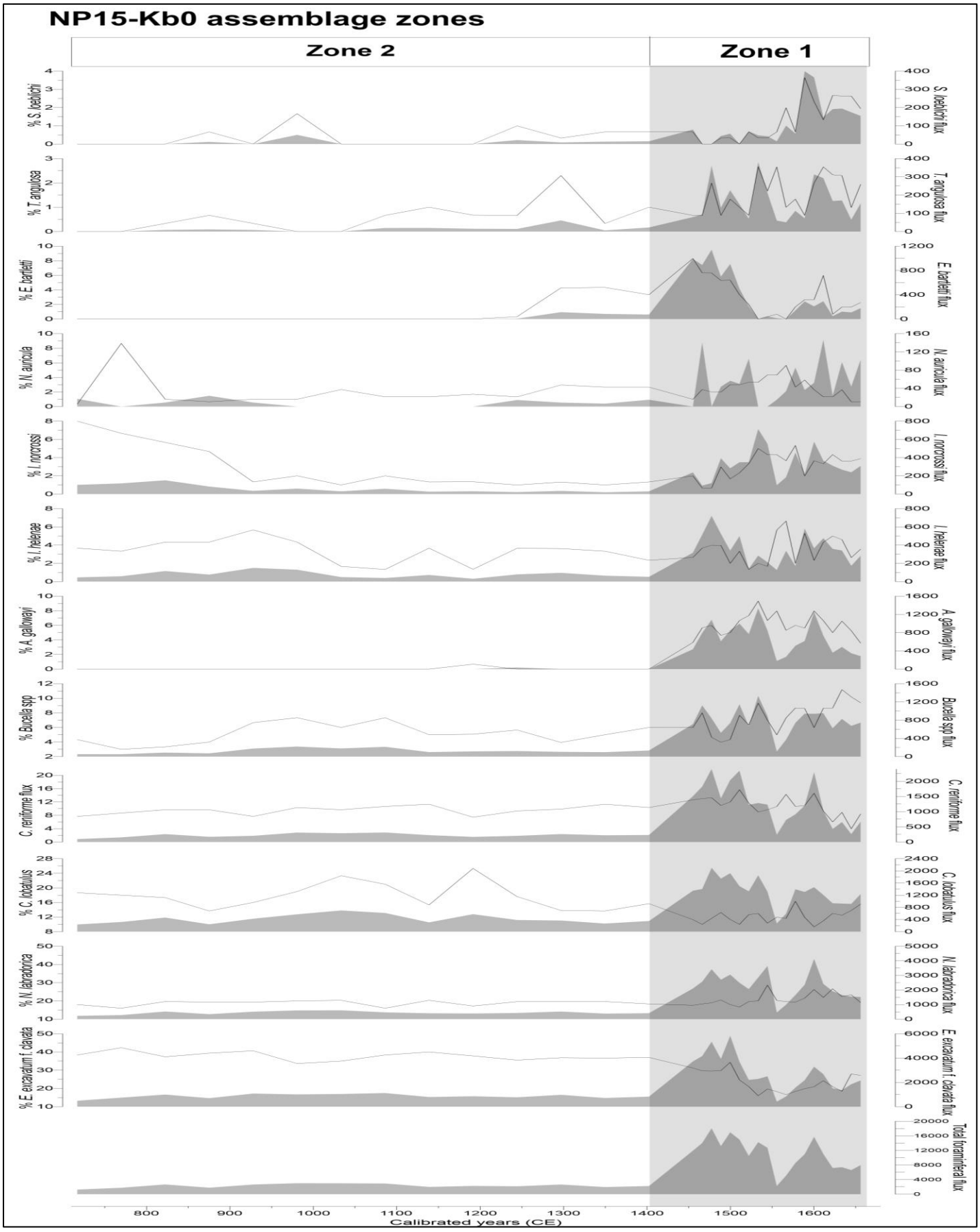

Figure 5.4: Relative abundances (left scale, line) and fluxes (right scale, shading) plotted against calibrated years for NP15-Kb0.

5.3 Biozones in core NP14-Kb3

In sediment core NP14-Kb3 32 species were identified (Table 5.4; Appendix 2.1) and five assemblage zones defined (Figure 5.5, 5.6).

5.3.1 Assemblage zone 5: *E. excavatum* f. *clavata – N. labradorica – C. reniforme zone* (~ 50 – 34 cm, ~ 350 – 880 CE)

The dominant species of assemblage zone 5 is *E. excavatum* f. *clavata*, with a mean value of 28 % (Figure 5.5, 5.6). The species has a maximum relative abundance of 50 % at 49,5 cm/ 351 CE, decreasing gradually towards 19 % at 42,5 cm/ 598 CE. This is followed by a rapid fluctuation, increasing to 30 % at 39, 5 cm/ 705 CE, and decreasing to 10 % towards the top of the zone at 34,5 cm/ 881 CE. The flux is generally following the same trend as the relative abundance, decreasing from a maximum of 1610 spec./cm2/yr. at 49,5 cm/ 351 CE to a minimum of 31 spec./cm2/yr. at the top of the zone.

N. labradorica is the second most abundant species, with an average relative abundance of 19 %. The species is frequently fluctuating towards 40,5 cm/ 669 CE, with values ranging between 16 and 32 %, and average fluctuations of ± 9 %. At 39,5 cm/ 705 CE the relative abundance abruptly decreases to 12 %, staying low towards the end of the zone. The flux follows the same trend as the relative abundance, going from 540 spec./cm2/yr. at 49,5 cm/ 351 CE to 47 spec./cm2/yr. at the top of the zone. Another abundant species is *C. reniforme*, with a relative abundance of 14 %. The species has a fluctuating but generally increasing trend, starting at 16 % at the start of the zone, increasing towards a maximum of 24 % at 36,5 cm/ 811 CE. The species flux decreases abruptly at the start of the zone, before stabilizing towards the top.

S. loeblichi is the most abundant of the least abundant species, with an average relative abundance of 9 %. The species has a clear increasing trend throughout the zone, starting at 2 % at 49,5 %/ 351 CE, increasing gradually to 17 % at 34,5 cm/ 881 CE. The species flux increasing at the start of the zone and stabilizes towards the top, with some minor fluctuations.
C. lobatulus remains stable around an average of 5 %, with minor fluctuations ranging from 2 – 3 %. The flux majorly follows the relative abundance. *I. helenae* and *I. norcrossi* are generally low with average abundances of 3 and 2 %, respectively. However, *I. norcrossi*, shows a clear increase from 2 % at 37,5 cm/ 775 CE to 8 % at 34,5 cm/ 881 CE. *I. helenae* remains at a low level throughout the core. The flux of *I. norcrossi* is low throughout the zone, while *I. helenae* follows the relative abundance. *A. gallowayi* and *N. auricula* are the least abundant species of the zone with average abundances of 2 %.

5.3.2 Assemblage zone 4: *E. excavatum* f. *clavata* zone (~ 34 – 26,5 cm, ~ 880 – 1165 CE)

E. excavatum f. *clavata* is increasing in the transition between zone 5 and 4, and continuous to increase abruptly into zone 4. Starting at 17 % at 33,5 cm/ 917 CE the species reaches a value of 62 % at 27,5 cm/ 1129 CE, which is the species maximum relative abundance throughout the entire core. The flux follows a similar trend, except from fluctuating rapidly at 28,5 cm/ 1094 CE.

N. labradorica remains stably low throughout the zone, with an average relative abundance of 8 % and an average flux of 87. The relative abundance of *C. reniforme* is generally lower in zone 4 compared to zone 5, with an average value of 7 %. The species is decreasing throughout the zone, from 13 % at 33,5 cm/ 917 CE to 7 % at 26,5 cm/ 1165 CE. The flux is relatively low throughout the zone, with a mean value of 70 spec./cm2/yr.

S. loeblichi is decreasing in relative abundance throughout the zone, reaching 6 % at 27,5 cm/ 1129 CE. The flux shows an opposite trend, increasing from 81 spec./cm2/yr. at 33,5 cm/ 917 CE to 135 spec./cm2/yr. at 27,5 cm/ 1129 CE. The average relative abundance of *I. norcrossi* increases to an average of 6 %, and fluctuates around this value throughout the zone. The flux is generally increasing throughout the zone, but shows a similar fluctuating trend as the relative abundance. *I helenae* shows higher values in both relative abundance and flux compared to zone 5, and is frequently fluctuating. *C. lobatulus*, *A. gallowayi* and *N. auricula* do not show any clear changes compared to zone 5.

5.3.3 Assemblage zone 3: *E. excavatum* f. *clavate* - *N. labradorica* – *S. loeblichi* zone (~ 26,5 – 15 cm, ~ 1165 – 1550 CE)

The relative abundance of *E. excavatum* f. *clavata* is gradually decreasing throughout the zone, from 44% at 25,5 cm/ 1200 CE to 13 % at 15,5 cm/ 1554 CE. The species flux follows the same trend as the relative abundance, with generally low values. *N. labradorica* is increasing in relative abundance throughout the zone, going from 7 % at 25,5 cm/ 1200 CE to 45% at 15,5 cm/ 1554 CE. The flux shows a similar increasing trend, going from 85 spec./cm2/yr. to 388 spec./cm2/yr. in the same depth interval.

C. reniforme decreases in both relative abundance and flux throughout the zone, going from 11 % and 132 spec./cm2/yr at 25,5 cm/ 1200 CE to 3 % and 26 spec./cm2/yr. at 15,5 cm/ 1554 CE. *S. loeblichi* shows a fluctuating trend in both relative abundance and flux, with mean values of 11% and 99 spec./cm2/yr. *I. norcrossi and I. helenae* are decreasing in relative abundance and flux throughout the zone. *C. lobatulus*, *A. gallowayi* and *N. auricula* remains low in abundance and flux.

5.3.4 Assemblage zone 2: *E. excavatum* f. *clavata* - *N. labradorica* zone (~ 15 – 5 cm, ~ 1590 – 1910 CE)

Going into zone 2, *E. excavatum* f. *clavata* is abruptly increasing throughout the first part of the zone, starting at 22 % at 14,5 cm/ 1589 CE, reaching 44 % at 10,5 cm/ 1731 CE. This is followed by a decrease towards 33 % at 6,5 cm/ 1872 CE, before a sudden increase to 44 % at 5,5 cm/ 1908 CE. The flux increases more moderately, but generally follows the trends of the relative abundance, with an average of 436 spec./cm2/yr. *N. labradorica* is abruptly decreasing to 12,5 cm/ 1660 CE, before gradually increasing towards the top, reaching a relative abundance of 25 % and a flux of 418 spec./cm2/yr. at 5,5 cm/ 1908 CE. *C. reniforme* remains unchanged compared to zone 3.

S. loeblichi decreases slightly towards 11,5 cm/ 1695 CE, before highly fluctuating towards the top of the zone, with average fluctuations of ± 5 %. *I. norcrossi* increases in relative abundance compared to zone 3. The species reaches 8 % at 11,5 cm/ 1695 CE, before decreasing to an average of 3 % towards the top. *C. lobatulus, A. gallowayi* and *I. helenae* remains low in relative abundance and flux.

5.3.5 Assemblage zone 1: *N. labradorica* zone (~ 5 – 2 cm, ~ 1940 – 2014 CE)

The relative abundance of *E. excavatum* f. *clavata* abruptly decreases throughout the zone starting at 34 % at 4,5 cm/ 1943 CE descending to 15 % at 2,5 cm/ 2014 CE. *N. labradorica* shows an opposite trend abruptly increasing in relative abundance and flux from 36 % and 204 spec./cm2/yr. at 4,5 cm/ 1943 CE to 56 % and 641 spec./cm2/yr. at 2,5 cm/ 2014 CE, which is the species maximum relative abundance throughout the entire core.

C. reniforme shows a decreasing trend going from 8 % at 4,5 cm/ 1943 CE to 5 % at 2,5 cm/ 2014 CE, while *S. loeblichi* gradually increases from 6 % at 4,5 cm/ 1943 CE to 8 % at 2,5 cm/ 2014 CE. *I. helenae* is nearly absent in the zone, and *I. norcrossi* reaches its lowest relative abundance. The remaining species *C. lobatulus, A. gallowayi* and *N. auricula* do not show any clear changes compared to zone 2.

SPECIES LIST

Benthic foraminiferal species identified in NP14-Kb3:

Astrononion gallowayi Loeblich & Tappan, 1953
Bolivina pseudopunctata Höglund, 1947
Buccella frigida (Cushman, 1922)
Buccella tenerrima (Bandy, 1950)
Casidulina neoteretis Seidenkrantz, 1995
Casidulina reniforme Nørvang, 1945
Cibicides lobatulus (Walker & Jacob, 1798)
Cornuspira involvens (Reuss, 1850)
Dentalina sp.
Elphidium bartletti Cushman, 1933
Elphidium excavatum forma *clavata* Cushman, 1930
Epistominella sp.
Globobulimina auriculata (Bailey, 1894)
Guttulina lactea (Walker & Jacob, 1798)
Islandiella helenae Feyling-Hanssen & Buzas, 1976
Islandiella norcrossi (Cushman, 1933)
Lagena sp.
Melonis barleeanum (Williamson, 1858)
Nodosariida sp
Nonionella auricula Heron-Allen & Earland, 1930
Nonionella labradorica (Dawson, 1860)
Nonionellina turgida (Williamson, 1858)
Oolina williamsoni (Alcock, 1865)
Patellina corrugata Williamson, 1858
Pullenia sp.
Quinqueloculina seminulum (Linnt, 1758)
Robertinoides arctica d'Orbigny, 1846
Stainforthia concava (Höglund, 1947)
Stainforthia fusiformis (Williamson, 1848)
Stainforthia loeblichi (Feyling-Hanssen, 1954)
Trifarina angulosa (Williamson, 1858)
Triloculina trihedral Loeblich & Tappan, 1953

Table 5.4: Species list including all the identified benthic taxa of core NP14-Kb3 (a total of 32 benthic taxa were identified)

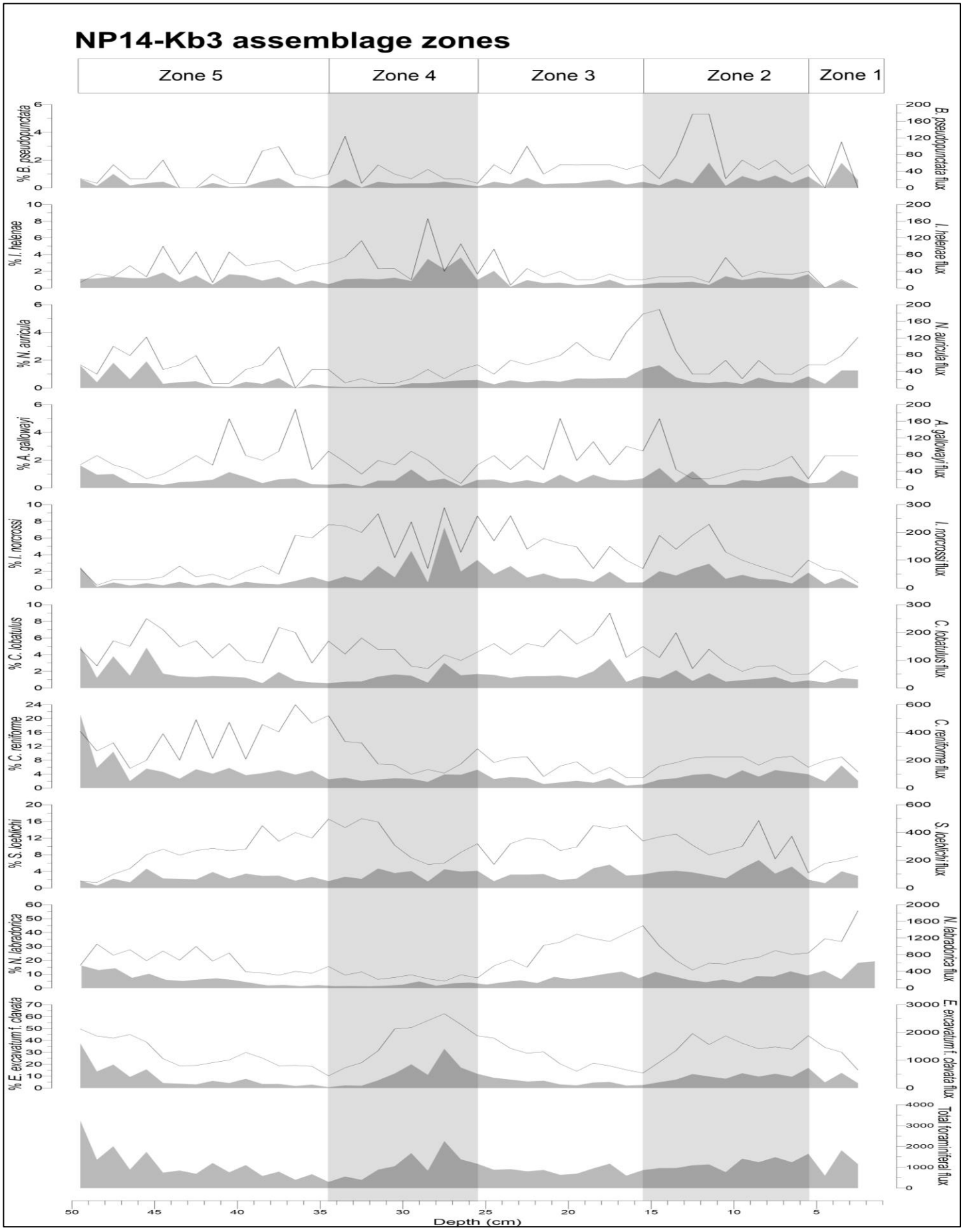

Figure 5.5: Relative abundances (left scale, line) and fluxes (right scale, shading) plotted against depth for NP14-Kb3

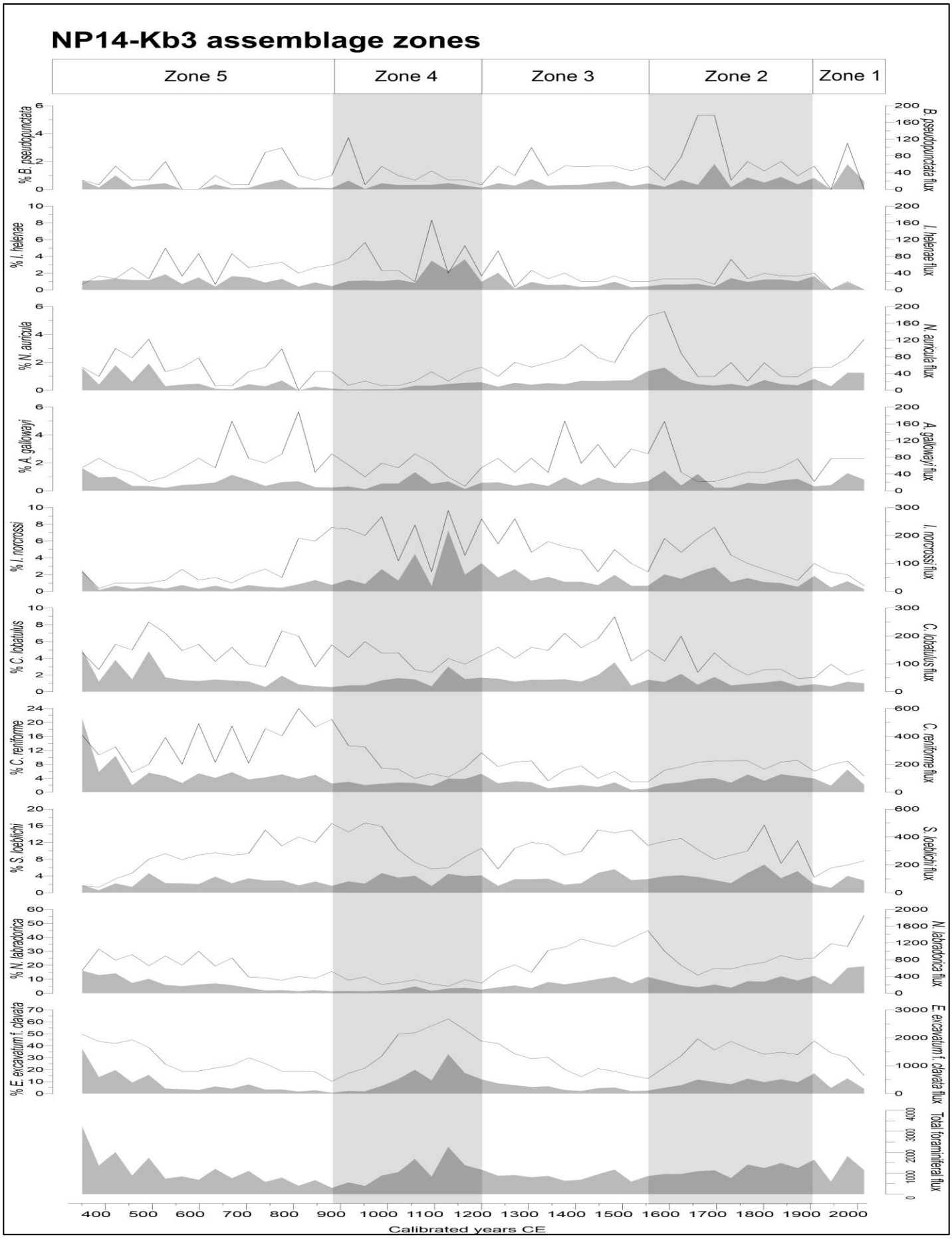

Figure 5.6: Relative abundances (left scale, line) and fluxes (right scale, shading) plotted against age for NP14-Kb3.

6 Discussion and correlations

In the first part of this section, the biozones of the NP15-Kb0 and NP14-Kb3 records will be interpreted and compared with respect to changes in the benthic foraminiferal fauna. These interpretations will further be investigated in making palaeoceanographic implications of the last ~ 2000 years in Kongsfjorden, and correlated with other similar studies from Svalbard and surrounding areas.

6.1 Interpretation of biozones in NP15-Kb0

6.1.1 Assemblage zone 2: *E. excavatum* f. *clavata* zone (~ 35 - 21 cm, ~ 720 – 1400 CE)

Assemblage zone 2 is characterized by a high relative abundance of *E. excavatum* f. *clavata* and a stable and relatively low benthic foraminiferal flux throughout the zone. Most of the species remains relatively unchanged in relative abundance, indicating stable conditions.

A generally high and stable relative abundance of *E. excavatum* f. *clavata,* is an indicator of cold water masses at the Kongsfjorden Trough. This is also supported by a stable % *C. reniforme* (Steinsund, et al., 1994; Hald & Korsun, 1997; Korsun & Hald, 1998; Korsun & Hald, 2000). Simultaneously, the moderate and stable relative abundance of *N. labradorica* indicates some influence of AW (Hald & Korsun, 1997; Korsun & Hald, 1998; Korsun & Hald, 2000; Rytter, et al., 2002; Jennings, et al., 2004). Cold water masses combined with a relatively low benthic foraminiferal flux are indications of unfavorable conditions at the Kongsfjorden Trough. Considering the local oceanography, this is likely related to high influence of relatively cold and fresh ArW from the CC, and could also indicate the presence of sea ice at the core site. However, the stable abundance of *N. labradorica* suggests some influence of AW and/ or TAW. A relatively high but fluctuating % *C. lobatulus* is an indicator of bottom currents with varying intensity throughout the zone (Steinsund, et al., 1994). This could indicate varying strength of submerged AW following the Kongsfjorden Trough.

6.1.2 Assemblage zone 1: *E. excavatum* f. *clavata* - *N. labradorica* zone (~ 21 – 0 cm, ~ 1400 – 1660 CE)

Assemblage zone 1 is characterized by an abrupt increase in the benthic foraminiferal flux and a gradual decrease in relative abundance of *E. excavatum* f. *clavata* and *C. reniforme*. The zone is otherwise characterized by increase in the relative abundance of the species *N. labradorica, Buccella spp., I. helenae* and *I. norcrossi*.

The gradual decrease of % *E. excavatum* f. *clavata* and *C. reniforme* indicates changing conditions from the previous zone, with decreasing influence of cold water masses at the Kongsfjorden Trough (Steinsund, et al., 1994; Hald, et al., 1994; Hald & Korsun, 1997; Korsun & Hald, 1998; Korsun & Hald, 2000). Simultaneously, a slightly increasing % *N. labradorica* indicates increased influence of AW (Hald & Korsun, 1997; Korsun & Hald, 1998; Korsun & Hald, 2000; Rytter, et al., 2002; Jennings, et al., 2004) Combined with the abruptly increasing benthic foraminiferal flux, the decreasing % *E. excavatum* f. *clavata* and *C. reniforme*, and slightly increasing % *N. labradorica*, suggest ameliorated conditions at the Kongsfjorden Trough. This implies less influence of ArW and increased influence of AW and/ or TAW at the Kongsfjorden Trough. There is a possibility that this could be related to increased seasonal influence of AW, and consequently the formation of a high productive oceanic fronts in proximity to the core site (Jernas, et al., 2013; Jernas, et al., In review).

6.2 Interpretation of biozones in NP14-Kb3

6.2.1 Assemblage zone 5: *E. excavatum* f. *clavata* – *N. labradorica* – *C. reniforme* zone (~50 – 34 cm, ~ 350 – 880 CE)

Assemblage zone 5 is generally characterized by a relatively high total benthic foraminiferal flux that gradually decreases throughout the zone, and a generally decreasing, but fluctuating, trend in the relative abundance of the species *E. excavatum* f. *clavata* and *N. labradorica*. *C. reniforme* and *S. loeblichi* are generally increasing throughout the zone, although *C. reniforme* is frequently fluctuating.

The high % *E. excavatum* f. *clavata* and moderate % *C. reniforme* at the start of the zone (~ 350 – 500 CE), indicates dominance of cold bottom water masses (Steinsund, et al., 1994; Hald & Korsun, 1997; Korsun & Hald, 1998; Korsun & Hald, 2000). In the inner part of Kongsfjorden this is likely related to high production of local water masses. The fluctuating moderate to high % *N. labradorica* indicates influence of AW (Hald & Korsun, 1997; Korsun & Hald, 1998; Korsun & Hald, 2000; Rytter, et al., 2002; Jennings, et al., 2004). Together with the relatively high benthic foraminiferal flux this indicates influence of AW and/ or TAW at the core site.

While % *E. excavatum* f. *clavata* decreases to a more moderate level throughout the remaining part of the zone, % *C. reniforme* is highly fluctuating, but generally increasing towards the top. This suggests somewhat improved conditions at the core site, although a relatively high influence of local water masses seems to prevail. Simultaneously, *N. labradorica* decreases, indicating less influence of AW and/ or TAW.

6.2.2 Assemblage zone 4: *E. excavatum* f. *clavata* zone (~ 34 – 26,5 cm, ~ 880 – 1200 CE)

Assemblage zone 4 is characterized by an abrupt increase in the total benthic foraminiferal flux and relative abundance of *E. excavatum* f. *clavata*. *E. excavatum* f. *clavata* reaches its maxima in relative abundance throughout the core, before decreasing towards the top of the zone. *C. reniforme, C. lobatulus, S. loeblichi* and *A. gallowayi* are clearly decreasing towards 1229 CE, before increasing towards the top of the zone, showing an opposite trend compared to *E. excavatum* f. *clavata. N. labradorica* is staying at a low level throughout the zone.

In the major part of the zone (900 – 1150 CE), an abrupt increase in the relative abundance of *E. excavatum* f. *clavata* indicates rapidly increasing influence of cold bottom water masses at the core site (Steinsund, et al., 1994; Hald & Korsun, 1997; Korsun & Hald, 1998; Korsun & Hald, 2000). The generally low relative abundance of *N. labradorica* throughout the zone, suggests minimal influence of AW (Hald & Korsun, 1997; Korsun & Hald, 1998; Korsun & Hald, 2000; Rytter, et al., 2002; Jennings, et al., 2004). The clear increase of % *E. excavatum* f. *clavata* and decrease in relative abundance of most other species indicates a transition to unfavorable conditions in the inner part of Kongsfjorden. This suggests increased influence of local water masses. Unfavorable conditions are further supported by the low % *N. labradorica*, indicating low influence of AW and/ or TAW at the core site. The combination a fluctuating % *N. norcrossi* and increased benthic foraminiferal flux during the period could possibly be related to increased production related to seasonal sea-ice and ice edge algal blooming (Steinsund, et al., 1994). However, this is speculative (Seidenkrantz, 2013). Apart from *N. labradorica* remaining low in abundance, the trend reverses towards the top of the zone (~ 1150 – 1200 CE), with % *E. excavatum* f. *clavata* decreasing and other species increasing. This is indicating a gradually decreased influence of local water masses in the inner part of Kongsfjorden and probably increased influence of AW and/ or TAW.

6.2.3 Assemblage zone 3: *E. excavatum* f. *clavata - N. labradorica – S. loeblichi* zone (~ 26,5 – 15 cm, ~ 1200 – 1550 CE)

Assemblage zone 3 is characterized by a gradual decrease in the relative abundance of *E. excavatum* f. *clavata*, simultaneously with a corresponding increase in relative abundance of *N. labradorica*. Less abundant species like *S. loeblichi, C. lobatulus, A. gallowayi* and *N. auricula* shows generally increasing trends, while the opposite is true for *C. reniforme, I. norcrossi* and *I. helenae*.

The clear increase in relative abundance of *N. labradorica* is an indicator of increased influence of AW (Hald & Korsun, 1997; Korsun & Hald, 1998; Korsun & Hald, 2000; Rytter, et al., 2002; Jennings, et al., 2004). At the same time the species *E. excavatum* f. *clavata, C. reniforme* and *I.*

norcrossi clearly decreases in relative abundance, indicating a decreasing influence of cold bottom water masses (Steinsund, et al., 1994; Hald & Korsun, 1997; Korsun & Hald, 1998; Korsun & Hald, 2000).
The gradually increasing % *N. labradorica* combined with a decrease in relative abundance of *E. excavatum* f. *clavata*, *C. reniforme* and *I. norcrossi* suggests ameliorated conditions in the inner part of Kongsfjorden, characterized by increased influence of AW and/ or TAW at the inner part of Kongsfjorden, and decreased influence of local water masses. It also possibly indicates decreasing amounts of sea-ice during the period. The increase in relative abundance of *C. lobatulus* and *A. gallowayi* indicates stronger bottom currents, possibly related to increased strength of inflowing AW and/ or TAW (Steinsund, et al., 1994).

6.2.4 Assemblage zone 2: *E. excavatum* f. *clavata* - *N. labradorica* zone (~ 15 – 5 cm, ~ 1590 – 1910 CE)

The first part of assemblage zone 2 (~ 1590 – 1660 CE) is characterized by a new abrupt increase in relative abundance of *E. excavatum* f. *clavata*, corresponding with a decreasing trend of % *N. labradorica*. In the second part of the zone (~ 1660 – 1910 CE) the general trend reverses, with a gradual increase of % *N. labradorica* and decrease of % *E. excavatum* f. *clavata*. The benthic foraminiferal flux is gradually increasing throughout the zone.

The abrupt increase of % *E. excavatum* f. *clavata* during the first part of the period, together with a slightly increasing % *C. reniforme*, indicates increased influence of cold water masses (Steinsund, et al., 1994; Hald & Korsun, 1997; Korsun & Hald, 1998; Korsun & Hald, 2000). This corresponds to the abrupt decrease of *N. labradorica*, suggesting less influence of AW (Hald & Korsun, 1997; Korsun & Hald, 1998; Korsun & Hald, 2000; Rytter, et al., 2002; Jennings, et al., 2004). The abrupt increase of % *E. excavatum* f. *clavata* and corresponding decrease of % *N. labradorica* suggests rapidly deteriorated conditions during the first part of the zone, with increased influence of local water masses, and diminished influence of AW and/ or TAW at the inner part of Kongsfjorden.
From 1660 - 1910 CE % *E. excavatum* f. *clavata* decreases slightly, but remains high in relative abundance throughout the zone, indicating slightly less influence of local water masses. This corresponds with a gradual increase in % *N. labradorica* together with the benthic foraminiferal flux, suggesting gradually increasing influence of AW and/ or TAW.

6.2.5 Assemblage zone 1: *N. labradorica* zone (~ 5 – 2 cm, ~ 1940 – 2014 CE)

Assemblage zone 1 is characterized by an accelerated increase in relative abundance of *N. labradorica* compared to the previous zone, reaching maxima in relative abundance of 56 % at the top of the core,

simultaneously with an abrupt decrease of *E. excavatum* f. *clavata*. *S. loeblichi* and *N. auricula* are also increasing, while other species decreases or remains largely unchanged.

The accelerated increase of % *N. labradorica* suggests increased influence of AW at the core site compared to the previous zone, and possibly the highest influence of AW throughout the entire core. The simultaneous abrupt decrease in % *E. excavatum* f. *clavata* and general decrease in % *C. reniforme* and *I. norcrossi*, indicates a rapidly decreasing influence of cold water masses (Hald & Korsun, 1997; Korsun & Hald, 1998; Korsun & Hald, 2000; Rytter, et al., 2002; Jennings, et al., 2004).
The accelerated increase and maxima of % *N. labradorica* combined with the decrease in relative abundance of *E. excavatum* f. *clavata*, *C. reniforme* and *I. norcrossi*, reaching the lowest relative abundance of the three species, indicates the most favorable environmental conditions throughout the entire core. This implies maxima in influence of AW and/ or TAW to the inner part of Kongsfjorden, and low influence of local water masses (Steinsund, et al., 1994; Hald & Korsun, 1997; Jernas, et al., 2013; Jernas, et al., In review)

6.3 Palaeoceanographic implications and correlations

The five assemblage zones from the NP14-Kb3 record show large centennial-scale fluctuations in climatic conditions. Assemblage zone 5 is characterized by dominantly cold conditions, including high influence of LW, IM and/ or WCW and possibly prolonged periods of sea ice cover. Further into the zone the sea-ice cover seems to diminish combined with a decreased influence of TAW. Assemblage zone 4 is characterized by deteriorated conditions related to increased influence of Arctic water masses and a new prolonged periods of sea ice cover. Going into assemblage zone 3, conditions are clearly improving, indicated by a gradual increase in advection of AW combined with decreasing influence of Arctic water masses. Assemblage zone 2 is characterized by a recurrence of unfavorable conditions. However, the trend reverses after ~ 100 years, indicating gradually improving conditions towards the top. The improving conditions seems to continue going into zone 1, with accelerated advection of AW and simultaneous decreasing influence of Arctic water masses. This suggests maxima in influence of AW during last ~ 100 years of the core.

Assemblage zone 2 (~ 700 – 1400 CE) of NP15Kb0 is characterized by a high and stable relative abundance of E. excavatum f. clavata and C. reniforme, and a corresponding low and stable abundance of N. labradorica. This indicates a cold environment throughout the zone with high influence of Arctic Water and an extensive sea ice cover. There is no clear change in these conditions until ~ 1400 CE, in the transition to assemblage zone 1 (~ 1400 – 1650 CE). This zone is characterized by an abrupt increase in foraminiferal flux and increase in relative abundance of *N. labradorica* and *Buccella* spp., congruently with a rapid decrease in relative abundance of *E. excavatum* f. *clavata* and *C. reniforme*. This is a clear indication of a sudden increase in biological production, likely related to seasonal influence of Atlantic Water in Kongsfjorden (Jernas, et al., 2013; Jernas, et al., In review).

6.3.1 Correlation of NP15-Kb0 and NP14-Kb3

The NP15-Kb0 record only covers parts of the same time interval as NP14-Kb3, much due to the missing core top, and thus limits the comparability of the two cores. The two assemblage zones from NP15-Kb0 show parts of the same environmental changes that is found in NP14-Kb3. There are clear resemblances in faunal composition between assemblage zone 2 of NP15-Kb0 and assemblage zone 5 and 4 of NP14-Kb3, and between assemblage zone 1 of NP15-Kb0 and assemblage zone 3 of NP14-Kb3, reflecting similar environmental conditions. Assemblage zone 2 and 1 of NP14-Kb3 is not present in the NP15-Kb0 record due to the missing core top. It should be noted that there is a time gap of 200 years between the onset of assemblage zone 1 of NP15-Kb0 (~ 1400 CE) compared to assemblage zone 2 of NP14-Kb0 (~ 1200 CE). The time gap can partly be explained by the uncertainty related to the 2σ range of the calibrated ^{14}C ages of NP15-Kb3 (Table 5.1), and partly by the different core locations of NP14-Kb3 and NP15-Kb0.

The similarities between assemblage zone 5 and 4 of NP14-Kb3 and assemblage zone 2 of NP15-Kb0 implies generally cold and unfavorable conditions at both core sites, with high influence of ArW at the Kongsfjorden trough and local masses in the inner part of Kongsfjorden, and generally low influence of AW and/ or TAW at both sites. This is interpreted from the relative high % *E. excavatum f. clavata* and low % *N. labradorica* in both cores. Similarly, assemblage zone 1 of NP15-Kb0 show clear similarities in faunal composition with assemblage zone 3 of NP14-Kb. This implies clearly improved conditions with increased influence of AW and/ or TAW at both core sites. In the NP15-Kb0 record this is mainly indicated by a rapid increase in the benthic foraminiferal flux and a slightly increase of % *N. labradorica*, while in the NP14-Kb3 records it is indicated by a clear increase in % *N. labradorica*. The generally higher benthic foraminiferal flux values in the NP15-Kb0 record is probably related to the core site location at the Kongsfjorden Trough, generally more affected by AW and/ or TAW than the inner parts of Kongsfjorden.

Another difference between the records is the stable high % *E. excavatum* f. *clavata* and stable low % *N. labradorica* in NP15-Kb0 compared to the clearly more fluctuating % *E. excavatum* f. *clavata* and generally decreasing % *N. labradorica* in NP14-Kb3. The highly fluctuating faunal trend in the NP14-Kb3 record suggests less stable environmental conditions. This is possibly owing to NP14-Kb3 being located further into the fjord than NP15-Kb0, being highly influenced by glacial activity from the tidewater glaciers at the fjord head in addition to the influence from inflowing coastal water

6.3.2 Regional correlation of centennial-scale changes

6.3.2.1 350 – 1200 CE

The time intervals 350 – 1200 CE (assemblage zone 5 and 4) in the NP14-Kb3 record and ~ 700 – 1400 CE (assemblage zone 2) in the NP15-Kb3 record are characterized by cold and unfavorable conditions with high influence of ArW at the Kongsfjorden Trough and high production of local water masses within Kongsfjorden, and low to moderate influence of AW at both core sites.

Similar conditions are described in Jernas et al. 2013 in the time interval ~ 300 – 700 CE, characterized by periods of cold conditions related to prolonged sea ice cover and high influence of ArW in Kongsfjorden, particularly after 550 CE. In the same time interval, more severe conditions are described for the Hinlopen Trough (Jernas, et al., 2013). In Jernas et al. 2013 the time interval from 700 to 1200 CE is characterized by ameliorated conditions at both the Kongsfjorden and the Hinlopen Strait with increased influence of AW and less influence of ArW. Jernas et al. 2013 correlates this time interval with an initial stage of the MWP. This deviates from the findings in this study, where generally unfavorable conditions characterize both records during the same time interval.

6.3.2.2 The Medieval Warm Period

The time intervals ~ 1200 – 1550 CE in the NP14-Kb3 record and ~ 1400 – 1650 CE in the NP15-Kb0 record is inferred to correlate to the MWP (Lamb, 1965; Bradley, 2000) (Figure 6.1). In the NP14-Kb3 record this correlation is based upon the clear increase in % *N. labradorica* and corresponding decrease in % *E. excavatum* f. *clavata* and *C. reniforme*, indicating increased influence of AW and/ or TAW and decreased influence of Arctic water masses. In the NP15-Kb0 record the correlation to the MWP is based upon the rapid increase in benthic foraminiferal flux and increase of % *N. labradorica* combined with decrease of % *E. excavatum* f. *clavata* and *C. reniforme*.

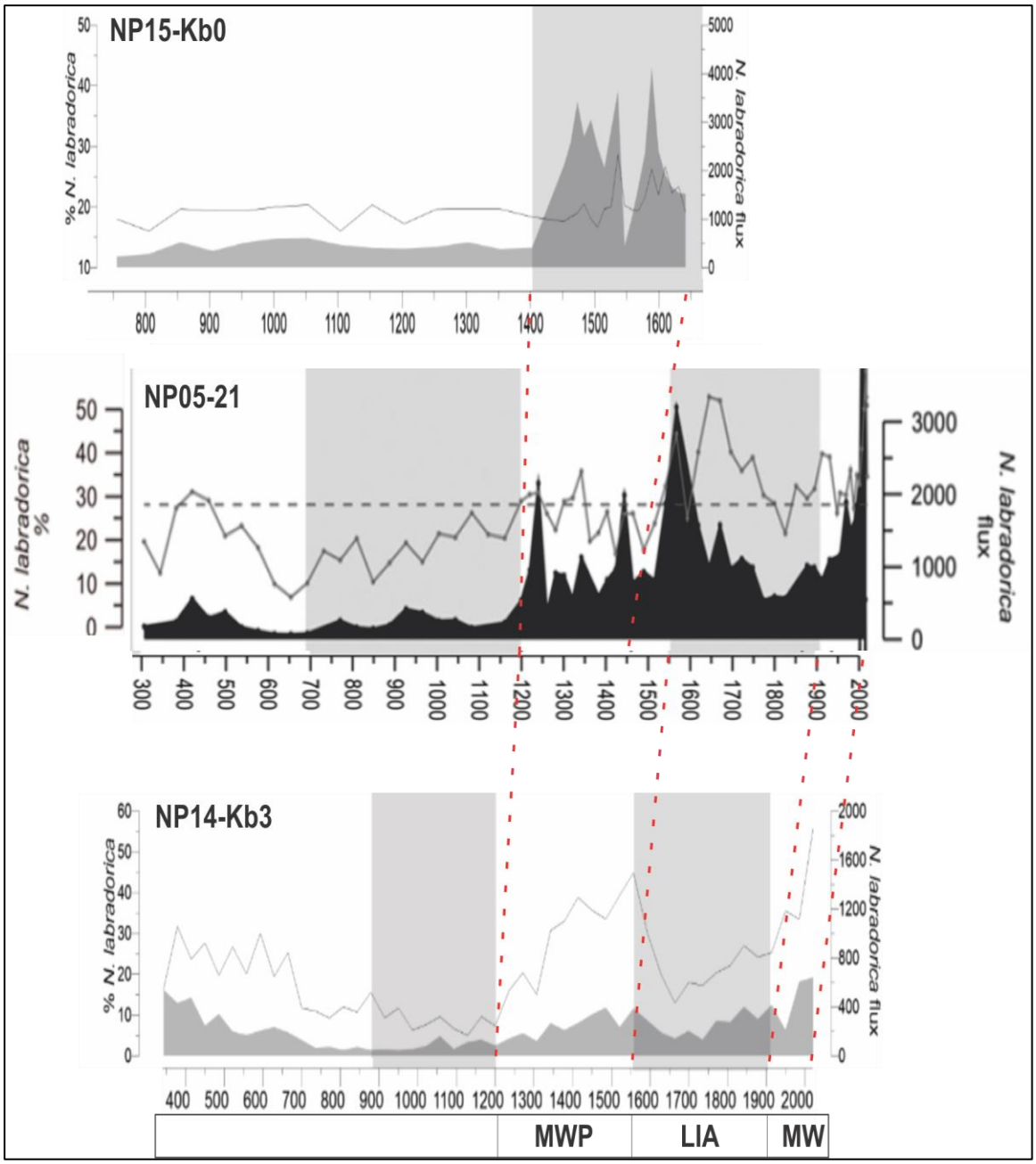

Figure 6.1: Correlation of centennial-scale climate changes based of the relative abundance and flux of N. labradorica in NP15-Kb0 and NP14-Kb3 from this study, and NP05-21 from Jernas et al. 2013. Relative abundances (left scale, line) and fluxes (right scale, shading). The plot for NP05-21 is adapted and modified from Jernas et al. 2013. The x-axis unit is "Calibrated years (CE)" for all plots.

In Jernas et al. 2013 the time interval from ~ 700 to 1500 CE is inferred to correlate with the MWP. The correlation is divided into two steps, ~ 700 – 1200 CE and ~ 1200 – 1500 CE, were the first step is characterized by warming and strong influence of AW in Kongsfjorden, and the second step by high seasonal productivity. There are no clear indications of a warmer period from ~ 700 – 1200 CE in the records from this study. However, a clear resemblance is observed between the second step of the MWP in the NP05-21 record from Jernas et al. 2013 and the time interval from ~1400 - 1650 CE in the NP15-Kb0 record (Figure 6.1). The resemblance mainly implies a similar trend, with rapid increase of the benthic foraminiferal flux in both records. Considering the proximity of the NP15-Kb0 and NP05-21 records, it is reason to believe that this trend occurred approximately simultaneously in both records. The difference in the dated onset of the increased flux event between NP15-Kb0 and NP05-21, can partly be explained by the uncertainty related to the sigma 2 range of the calibrated ^{14}C ages, and partly by the NP05-21 record being located slightly further northwest at 79°03.0'N; 11°05.5'E. There is no comparable increase in benthic foraminiferal flux in the NP14-Kb3 record. This is probably related to generally lower productivity within Kongsfjorden, owing to less influence of AW.

Indications of the MWP is also present in several other paleorecords from the North Atlantic/ Arctic region. Analysis of planktic foraminifera in paleorecords from the Fram Strait, located west of Kongsfjorden, shows increasing temperatures in the time interval 750 – 1300 CE, and increased productivity from 1300 to 1650 CE (Spielhagen, et al., 2011; Werner, et al., 2011).
In a paleorecord from Hornsund, a fjord located at the southwestern part of Spitsbergen, the MWP is inferred to occur from 900 to 1300 CE, based on generally lower $\delta^{18}O$ values (Majewski, et al., 2009). A paleorecord from Novaya Zemlya in the eastern Barents Sea discovered increased foraminiferal productivity related to warmer ocean temperatures during summer, and consequently, glacial retreat from 1170 to 1400 CE (Murdmaa, et al., 2004). In a paleorecord from the Canada Basin the MWP is inferred to correlate with the time interval ~ 1000 - 1250, characterized by a temperature maxima (Farmer, et al., 2011). A period of temperature maxima is also present in paleorecords from the Vøring Plateau in the Norwegian Sea, running from 1250 to 1400 CE, based on reconstructions of sea surface temperatures by applying planktic foraminifera in transfer functions (Andersson, et al., 2003, 2010; Risebrobakken, et al., 2003). A record from farther south in the Norwegian Sea, based on $\delta^{18}O$ values of planktic foraminifera, show warming from 1100 – 1300 CE (Sejrup, et al., 2010)

6.3.2.3 The Little Ice Age

Assemblage zone 2 (~1550 – 1900 CE) of NP14-Kb3 is inferred to correlate with the LIA (Bradley, 2000). This is inferred based on indications of cold conditions during this time interval. The first ~ 100 years of the zone (~1550 – 1650 CE) seems to reflect the most unfavorable climatic conditions, with a clear decrease in the influence of AW and increased production of local water masses within Kongsfjorden. From ~1650 CE onwards, the conditions seem to improve, with a gradual increasing influence of AW. A similar correlation was made by Jernas et al. 2013, were the time interval ~ 1500 – 1900 CE were inferred to correlate to the LIA. The study found different responses to the LIA between the Hinlopen Strait and Kongsfjorden records, suggesting harsh environmental conditions with extensive sea ice cover at the Hinlopen Strait compared to more favorable conditions in Kongsfjorden due to greater influence of Atlantic Water. The LIA conditions described for the Kongsfjorden record seems to coincide with the findings of this study.

Several other studies from the North Atlantic region indicates cold climatic conditions related to the LIA. Decreasing temperatures and productivity is found in paleorecords from the Fram Strait, by analyzing planktic foraminifera (Spielhagen, et al., 2011; Werner, et al., 2011).
In the study from Novaya Zemlya the first part of the LIA was characterized by advancing glacial fronts due to increased precipitation. This was followed by colder conditions from 1600 to 1800 CE, with prolonged periods of sea ice cover (Murdmaa, et al., 2004). Similar findings have also been made in the study from the Hornsund fjord, suggesting cold conditions related to high influence of ArW and presence of tidewater glaciers during the LIA (Majewski, et al., 2009).
The LIA is also present in several paleorecords from Northwestern Europe. A common period of cooling between 1400 and 1900 CE, inferred to correlate with the LIA, were found in paleorecords along a western European transect. The transect included open ocean and shallow marine records from the Iberian margin to the North Icelandic shelf (Eiríksson, et al., 2006). A similar correlation is found in several paleorecords from off the Norwegian coast (Berstad, et al., 2003; Andersson, et al., 2003).
In the Malangen fjord reconstruction of bottom water temperatures based on $\delta^{18}O$-values of benthic foraminifera show a period from ~ 1250 to 1800 CE of unparalleled cold temperatures, correlated to reflect the LIA (Hald, et al., 2011). In contrast, a period of ameliorated conditions during the LIA is discovered in marine paleorecords from the southwestern part of Greenland. This is connected to subsurface warming by the West Greenland Current (Lassen, et al., 2004).

6.3.2.4 The Modern Warming

Assemblage zone 1 (~1900 CE - present) of NP14-Kb3 is inferred to correlate with the Modern Warming (MW). This correlation is based on an accelerated increase in influence of Atlantic Water and benthic foraminiferal flux throughout this time interval. *N. labradorica* reaches its maxima during this time interval, suggesting the highest influence of Atlantic Water throughout the entire record. Similar conditions with increased relative abundance of *N. labradorica* during the last 100 years is described by Jernas et al. 2013, indicating increased influence of AW in both Kongsfjorden and the Hinlopen Strait.

Indications of increased inflow of Atlantic Water during the MW period is also found in paleorecords from the Fram Strait. This is inferred based on $\delta^{18}O$ values and dominance of subpolar planktic foraminiferal species as of 1860 CE (Spielhagen, et al., 2011; Werner, et al., 2011). In a record from Novaya Zemlya the recent warming is assumed to occur during the 20th century, indicated by warmer summers with increased productivity and glacial melting (Murdmaa, et al., 2004). Further south, in the Malangen fjord, by analyzing bottom water temperatures during the last ~ 2000 years, it is speculated that the occurrence of unprecedented warm temperatures after ~ 1800 CE may be related to the effect of Global Warming (Hald, et al., 2011).

6.3.3 Driving forces

This study agrees with Jernas et al. 2013 in that variations in the influence of AW is largely influencing the centennial-scale climatic changes found in Kongsfjorden and the Kongsfjorden Trough during the last ~ 2000 years. However, the production of local water masses within the fjord is also playing a major role, which is evident when comparing the Kongsfjorden and the Kongsfjorden Trough paleoenvironments. The changes in influence of AW found in this study correlates well with a positive state of the NAO and a consequently stronger AMOC to be the driving force behind the MWP, and an approximately neutral NAO state and a weaker AMOC corresponding with the LIA (Trouet, et al., 2009; Trouet, et al., 2011).

7 Conclusions

To map the paleoenvironmental development in Kongsfjorden during the last ~ 2000 years, the benthic foraminiferal fauna of two marine sediment cores, one from the Kongsfjorden Trough (NP15-Kb0) and one from the inner parts of Kongsfjorden (NP14-Kb3), were analyzed with respect to relative abundances and fluxes of each species. Climatic fluctuations on a centennial scale were discovered in both records, represented by five assemblage zones in NP14-Kb3 and two assemblage zones in NP15-Kb3. The faunal changes primarily reflect variations in the influence of AW and/ or TAW originating from the WSC and local water masses produced in the fjord, and how this impacts the inner parts of Kongsfjorden compared to the Kongsfjorden Trough.

From ~ 350 to 900 CE generally cold conditions with low to moderate influence of AW took place both in the Kongsfjorden Trough and the inner part of Kongsfjorden. In the inner parts of Kongsfjorden deteriorated conditions took place from ~ 900 to 1200 CE, related to increased production of LW, IM and/ or WCW. No changes in conditions is observed at the Kongsfjorden Trough during the same time interval. In the inner parts of Kongsfjorden, a gradually increasing influence of AW took place from 1200 to 1550 CE. Similar conditions are seen the Kongsfjorden Trough in the time interval from 1400 to 1650 CE, due to a rapid increase in the benthic foraminiferal flux. The difference in timing can partly be explained by the 2σ range of the calibrated ages and/ or a slightly different location of the core sites. The time interval from ~ 1200 to 1550 CE (1400 to 1650 CE in NP15-Kb0) is correlated to correspond to the MWP.

Deteriorated conditions prevailed in the inner parts of Kongsfjorden during the first ~ 100 years of the time interval from ~ 1550 to 1900 CE, with a sudden decrease in the influence of AW and dominance of local water masses. However, conditions gradually improved throughout the zone with increasing influence of AW. The time interval is inferred to correlate with the LIA.

During the last time interval of NP14-Kb3, from ~ 1900 to 2014 CE, an acceleration of the influence of AW to the inner part of Kongsfjorden took place. This represents a possible temperature maxima throughout the record. The time interval is inferred to correlate with the Modern Warming.

The results from this study supports the findings of Jernas et al. 2013, in concluding that advection of AW into Kongsfjorden and the Kongsfjorden Trough is largely impacting the oceanographic and climatic conditions in Kongsfjorden and the Kongsfjorden Trough. This study also concludes that there are clear paleoenvironmental differences between the Kongsfjorden Trough and the inner parts of Kongsfjorden, with generally more variable conditions within Kongsfjorden. This is probably related to production of local water masses within the fjord, combined with less influence of AW/ and or TAW. In accordance with Jernas et al. 2013, this study substantiates the hypotheses of the NAO and the AMOC being the driving forces behind several centennial-scale climatic fluctuations during the last ~ 2000 years. This implies a positive state of the NAO combined with a strong AMOC during the MWP, followed by a neutral NAO and a weaker AMOC during the LIA.

8 References

Aagaard, K., Foldvik, A. & Hillman, S. R., 1987. The West Spitsbergen Current: Disposition and Water Mass Transformation. *Journal of Geophysical Research*, pp. 3778-3784.

Aagaard-Sørensen, S., Husum, K., Hald, M. & Knies, J., 2010. Paleoceanographic development in the SW Barents Sea during the Late WeichselianeEarly - Holocene transition. *Quaternary Science Reviews 29*, pp. 3442-3456.

Aagaard-Sørensen, S. et al., 2014. Sub sea surface temperatures in the Polar North Atlantic during the Holocene: Planktic foraminiferal Mg/Ca temperature reconstructions. *The Holocene, vol 24*, pp. 93-103.

Ambaum, M. H. P., Hoskins, B. J. & Stephenson, D. B., 2001. Arctic Oscillation or North Atlantic Oscillation?. *American Meteorological Society Volume 14*, pp. 3495-3507.

Andersen, C., Koc, N., Jennings, A. & Andrews, J. T., 2004. Nonuniform response of the major surface currents in the Nordic Seas to insolation forcing: Implications for the Holocene climate variability. *Paleoceanography, Vol. 19*, pp. PA2003, doi:10.1029/2002PA000873.

Andersson, C. et al., 2010. Holocene trends in the foraminifer record from the Norwegian Sea and the North Atlantic Ocean. *Climate of the Past 6*, pp. 179-193.

Andersson, K., Risebrobakken, B., Jansen, E. & Dahl, S. O., 2003. Late Holocene surface ocean conditions of the Norwegian Sea (Vøring Plateau). *Palaeoceanography Vol. 18*, pp. 1044, doi:10.1029/2001PA000654.

Austin, W. E. N. & Evans, J. R., 2000. NE Atlantic benthic foraminifera: modern distribution patterns and paleoecological significance. *Journal of the Geological Society, Vol. 157*, pp. 679-691.

Berger, A. & Loutre, M. F., 1991. Insolation Values for the Climate of the Last 10 million years. *Quaternary Science Reviews, Vol 10*, pp. 297-317.

Bernhard, J. M. & Bowser, S. S., 1999. Benthic foraminifera of dysoxic sediments: chloroplast sequestration and functional morphology. *Earth-Science Reviews 46*, pp. 149-165.

Berstad, I. M., Sejrup, H. P., Klitgaard-Kristensen, D. & Haflidason, H., 2003. Variability in temperature and geometry of the Norwegian Current over the past 600 yr; stable isotope and grain size evidence from the Norwegian margin. *Journal of Quaternary Science 18*, pp. 591-602.

Birks, C. J. A. & Koc, N., 2002. A high-resolution diatom record of late-Quaternary sea-surface temperatures and oceanographic conditions from the eastern Norwegian Sea. *Boreas, Vol. 31*, pp. 323-344.

Björk, S., Rundgren, M., Ingolfsson, O. & Funder, S., 1997. The Preboreal oscillation around the Nordic Seas: terrestrial and lacustrine responses. *Journal of Quarternary Science*, July, pp. 455-465.

Bond, G. et al., 1997. A Pervasive Millennial-Scale in North Atlantic Holocene and glacial climates. *Science, 278 (5341)*, 14 November, pp. 1257-1266.

Bradley, R., 2000. 1000 Years of Climate Change. *American Association for the Advancement of Science*, pp. 1353-1355.

Calvo, E., Grimalt, J. & Jansen, E., 2002. High resolution UK′37 surface temperature reconstruction in the Norwegian Sea during the Holocene. *Quaternary Science Reviews 21*, p. 1385–1394.

Cedhagen, T., 1991. Retention of chloroplasts and bathymetric distribution in the Sublittoral Foraminiferan Nonionellina Labradorica. *Ophelia 33 (1)*, pp. 17-30.

Cisewski, B., Budéus, G. & Krause, G., 2003. Absolute transport estimates of total and individual water masses in the northern Greenland Sea derived from hydrographic and acoustic Doppler current profiler measurements. *Journal of Geophysical Research VOL. 108*, p. doi:10.1029/2002JC001530.

Cottier, F. R. et al., 2007. Wintertime warming of an Arctic shelf in response to large-scaleatmospheric circulation. *Geophysical Research Letters, Vol. 34*, 26 May, pp. 1-5.

Cottier, F. et al., 2005. Water mass modification in an Arctic fjord through cross-shelf exchange: The seasonal hydrography of Kongsfjorden, Svalbard. *Journal of Geophysical Research, Vol 110*, 8 December, pp. 1-18.

Crowley, T. J., 2000. Causes of Climate Change Over the Past 1000 Years. *Science Vol 289*, pp. 270-277.

Ebbesen, H., Hald, M. & Eplet, T. H., 2007. Lateglacial and early Holocene climatic oscillations on the western Svalbard margin, European Arctic. *Quaternary Science Reviews 26*, p. 1999–2011.

Eiríksson, J. et al., 2006. Variability of the North Atlantic Current during the last 2000 years based on shelf bottom water and sea surface temperatures along an open ocean/shallow marine transect in western Europe. *The Holocene 16*, pp. 1017-1029.

Elverhøi, A., Lønne, Ø. & Seland, R., 1983. Glaciomarine sedimentation in a modern fjord environment, Spitsbergen. *Polar Research 1*, pp. 127-149.

Farmer, J. R. et al., 2011. Western Arctic Ocean temperature variability during the last 8000 years. *Geophysical Research Letters, V. 38*, pp. L24602, doi: 10.1029/2011GL049714.

Fisher, T. G., Smith, D. G. & Andrews, J. T., 2002. Preboreal oscillation caused by a glacial Lake Agassiz flood. *Quaternary Science Reviews 21*, p. 873–878.

Gascard, J.-C., Richez, C. & Rouault, C., 1995. New Insights on Large-Scale Oceanography in Fram Strait: The West Spitsbergen Current. *Arctic Oceanography: Marginal Ice Zones and Continental Shelves Coastal and Estuarine Studies, Volume 49*, pp. 131-182.

Gerland, S. & Renner, A. H. H., 2007. Sea-ice mass-balance monitoring in an Arctic fjord. *Annals of Glaciology 46*, pp. 435-442.

Goosse, H. & Holland, M. M., 2005. Mechanisms of Decadal Arctic Climate Variability in the Community Climate System Model, Version 2 (CCSM2). *Journal of Climate Volume 18*, 9 February, pp. 3552-3570.

Graham, N. E. et al., 2011. Support for global climate reorganization during the ‘‘Medieval Climate Anomaly’’. *Clim Dyn 37*, pp. 1217-1245.

Groot, D. E., Aagaard-Sørensen, S. & K, H., 2014. Reconstruction of Atlantic water variability during the Holocene in the western Barents Sea.. *Climate of the past*, 10 January, pp. 51-62.

Grove, J. M., 1988. In: *The Little Ice Age.* London: Methuen, p. 520.

Hald, M. et al., 2007. Variations in temperature and extent of Atlantic Water in the northern North Atlantic during the Holocene. *Quaternary Science Reviews 26*, p. 3423–3440.

Hald, M. et al., 1994. Recent and Late Quaternary distribution of Elphidium excavarum f. clavata in Arctic seas. *Cushman Foundation, Special Publication no. 32*, pp. 141-153.

Hald, M. & Hagen, S., 1998. Early Preboreal cooling in the Nordic seas region triggered by meltwater. *Geology, v. 26*, pp. 615-618.

Hald, M. & Korsun, S., 1997. Distribution of modern bethic foraminifera from fjords of Svalbard, European Arctic. *Journal of Foraminiferal Research*, April, pp. 101-122.

Hald, M., Salomonsen, G. R., Husum, K. & Wilson, L. J., 2011. A 2000 year record of Atlantic Water temperature variability from the Malangen Fjord, northeastern North Atlantic. *The Holocene*, pp. 1049-1059.

Hald, M. & Steinsund, P. I., 1992. Distribution of surface sediment Benthic Foraminifera in the southwestern Barents Sea. *Jormrnol of Foraminiferal Research*, pp. 347-362.

Hald, M. & Steinsund, P. I., 1996. Benthic foraminifera and carbonate dissolution in the surface sediments of the Barents and Kara Seas. *Polarforsch., vol. 212*, pp. 285-307.

Hopkins, T. S., 1991. The GIN Sea - A synthesis of its physical oceanography and literature review 1972-1985. *Earth-Science Reviews 30*, pp. 175-318.

Howe, J. A., Moreton, S. G., Morri, C. & Morris, P., 2003. Multibeam bathymetry and the depositional environments of Kongsfjorden and Krossfjorden, western Spitsbergen, Svalbard. *Polar Research 22(2)*, pp. 301-316.

Hurrell, J. W., 1995. Decadal Trends in the North Atlantic Oscillation: Regional Temperatures and Precipitation. *Science, New Series, Vol. 269, No. 5224*, pp. 676-679.

Husum, K. & Hald, M., 2002. Early Holocene cooling events in Malangenfjord and the adjoining shelf, north-east Norwegian Sea. *Polar Research 21*, pp. 267-274.

Ito, H. & Kudoh, S., 1997. Characteristics of water in Kongsfjorden, Svalbard. *Proc. NIPR Symp. Polar Meteorol. Glaciol., 11*, pp. 211-232.

Jennings, A. E., Weiner, N. J., Helgadottir, G. & T, A. J., 2004. Modern foraminiferal faunas of the southwestern to northern Iceland shelf: oceanographic and environmental controls. *Journal of Foraminiferal Research*, 180-207 July.

Jernas, P. et al., 2013. Paleoenvironmental changes of the last two millennia on the western and northern Svalbard shelf. *Boreas*, pp. 236-255.

Jernas, P. et al., In review. Annual changes in Arctic fjord environment and modern benthic foraminiferal fauna: evidence from Kongsfjorden, Svalbard.. *Global and Planetary Change*.

Jiang, H. et al., 2005. Evidence for solar forcing of sea-surface temperature on the North Icelandic Shelf during the late Holocene. *Geology v. 33*, pp. 73-76.

Jiang, H. et al., 2015. Solar forcing of Holocene summer sea-surface temperatures in the northern North Atlantic. *Geology v. 43*, pp. 203-206.

Jiang, H., Seidenkrantz, M.-S., Knudsen, K. L. & Eiríksson, J., 2002. Late-Holocene summer sea-surface temperatures based on a diatom record from the north Icelandic shelf. *The Holocene 12*, pp. 127-147.

Kaufman, D. S. et al., 2004. Holocene thermal maximum in the western Arctic (0–180°W). *Quaternary Science Reviews 23*, pp. 529-560.

Kim, J.-H.et al., 2004. North Pacific and North Atlantic sea-surface temperature variability during the Holocene. *Quaternary Science Reviews 23*, p. 2141–2154.

Klitgaard-Kristensen, D., Sejrup, H. P. & Haflidason, H., 2001. The last 18 kyr fluctuations in Norwegian Sea surface conditions and implications for the magnitude of climatic change: Evidence from the North Sea. *Paleoceanography*, October, pp. 455-467.

Knorr, G. & Lohmann, G., 2007. Rapid transitions in the Atlantic thermohaline circulation triggered by global warming and meltwater during the last deglaciation. *Geochem. Geophys. Geosyst., 8*, p. doi:10.1029/2007GC001604.

Koc, N., Jansen, E. & Haflidason, H., 1993. Paleoceanographic reconstructions of surface ocean conditions in the Greenland, Iceland and Norwegian seas through the last 14 ka based on diatoms. *Quaternary Science Reviews 12*, p. 115–140.

Korsun, S. A., Pogodina, I. A., Forman, S. L. & Lubinski, D. J., 1995. Recent foraminifera in glaciomarine sediments from three arctic fjords of Novaja Zemlja and Svalbard. *Polar Research 14(1)*, pp. 15-31.

Korsun, S. & Hald, M., 1998. Modern Benthic Foraminifera off Novaya Zemlya Tidewater Glaciers, Russian Arctic. *Arctic and Alpine Research, Vol. 30, No. 1*, pp. 61-77.

Korsun, S. & Hald, M., 2000. Seasonal dynamics of Benthic Foraminifera in a glacially fed fjor of Svalbard, European Arctic. *Journal of Foraminiferal Research, v. 30, no. 4*, October, pp. 251-271.

Korsun, S. & Polyak, L., 1989. Distribution of benthic foraminiferal morphogroups in the Barents Sea. *Oceanology 29*, pp. 838-844.

Lamb, H. H., 1965. The early medieval warm epoch and its sequel. *Palaeogeography, Palaeoclimatology, Palaeoecology 1*, 22 January, pp. 13-37.

Laskar, J., 1990. The Chaotic Motion of the Solar System: A Numerical Estimate of the Size of the Chaotic Zones. *Icarus 88*, pp. 266-291.

Lassen, S. J. et al., 2004. Late-Holocene Atlantic bottom-water variability in Igaliku Fjord, South Greenland, reconstructed from foraminifera faunas. *The Holocene 14*, pp. 165-171.

Loeng, H., 1991. Features of the physical oceanographic conditions of the Barents Sea. *Polar Research 10(1)*, pp. 5-18.

Majewski, W., Szczucinski, W. & Zajaczkowski, M., 2009. Interactions of Arctic and Atlantic water-masses and associated environmental changes during the last millennium, Hornsund (SW Svalbard). *Boreas, Vol. 38*, pp. 529-544.

Mangerund, J. et al., 2006. Marine 14C reservoir ages for 19th century whales and molluscs from the North Atlantic. *Quaternary Science Reviews 25*, p. 3228–3245.

Mann, M. E. et al., 2011. Global Signatures and Dynamical Origins of the Little Ice Age and Medieval Climate Anomaly. *Science Vol 326*, pp. 1256-1260.

Miettinen, A., pers.com. s.l.:s.n.

Miller, G. H. et al., 2012. Abrupt onset of the Little Ice Age triggered by volcanism and sustained by sea-ice/ocean feedbacks. *Geophysical Research Letters Vol. 39*, p. doi:10.1029/2011GL050168.

Murdmaa, I., Polyak, L., Ivanova, E. & Khromova, N., 2004. Paleoenvironments in Russkaya Gavan' Fjord (NW Novaya Zemlya, Barents Sea) during the last millennium. *Palaeogeography, Palaeoclimatology, Palaeoecology 209*, pp. 141-154.

Murray, J. W., 2001. The niche of benthic foraminifera, critical thresholds and proxies. *Marine Micropaleontology 41*, pp. 1-7.

Nesje, A. et al., 2001. Holocene glacier fluctuations of Flatebreen and winter-precipitation changes in the Jostedalsbreen region, western Norvay, based on glaciolacustrine sediment records. *The Holocene 11,3*, pp. 267-280.

Nilsen, F., Cottier, F., Skogseth, R. & Mattsson, S., 2008. Fjord– shelf exchanges controlled by ice and brine production: The interannual variation of Atlantic Water in Isfjorden, Svalbard. *Continental Shelf Research 28*, p. 1838– 1853.

Olsen, J., Anderson, N. J. & Knudsen, M. F., 2012. Variability of the North Atlantic Oscillation over the past 5,200 years. *Nature Geoscience 5*, p. 808–812.

Polyak, L. et al., 2002. Benthic Foraminiferal assemblages from the southern Kara Sea, a river-influenced Arctic marine environment. *Journal of Foraminiferal Research, v. 32*, pp. 252-273.

Polyak, L. & Solheim, A., 1994. Late- and postglacial environments in the northern Barents Sea west of Franz Josef Land. *Polar Research 13 (2)*, pp. 197-207.

Rasmussen, T. L. et al., 2014. Spatial and temporal distribution of Holocene temperature maxima in the northern Nordic seas: interplay of Atlantic-, Arctic- and polar water masses. *Quaternary Science Reviews*, pp. 280-291.

Rasmussen, T. L. et al., 2007. Paleoceanographic evolution of the SW Svalbard margin (76°N) since 20,000 14C yr BP. *Quaternary Research 67*, pp. 100-114.

Reimer, P. J., Baillie, M. G. L. & Bard, E., 2009. IntCal09 and Marine09 radiocarbon age calibration curves, 0-50,000 years cal BP.. *Radiocarbon 51*, pp. 1111-1150.

Reimer, P. J., Reimer, W, R. & M, B., 2013. Calibration of the 14C Record. *Elsevier B.V.*, pp. 345-352.

Renssen, H. et al., 2009. The spatial and temporal complexity of the Holocene thermal maximum. *Nature Geoscience Vol 2*, pp. 411-414.

Risebrobakken, B. et al., 2011. Early Holocene temperature variability in the Nordic Seas: The role of oceanic heat advection versus changes in orbital forcing. *Paleoceanography, VOL. 26*.

Risebrobakken, B. et al., 2003. A high-resolution study of Holocene paleoclimatic and paleoceanographic changes in the Nordic Seas. *Paleoceanography Vol. 18*, pp. 1017, doi:10.1029/2002PA000764.

Risebrobakken, B. et al., 2010. Climate and oceanographic variability in the SW Barents Sea during the Holocene. *The Holocene 20(4)*, p. 609–621.

Rytter, F., Knudsen, K. L., Seidenkrantz, M.-S. & Eríksson, J., 2002. Modern distribution of benthic foraminifera on the north Icelandic shelf and slope. *Journal of Foraminiferal Research*, July, pp. 217-244.

Saloranta, T. M. & Hauan, P. M., 2001. Interannual variability in the hydrography of Atlantic water northwest of Svalbard. *Journal of Geophysical Research, 106(C7)*, 15 July, pp. 13,931-13,943.

Sarnthein, M. et al., 2003. Centennial-to-millennial-scale periodicities of Holocene climate and sediment injections off the western Barents shelf, 75°N. *Boreas, Vol. 32*, pp. 447-461.

Schauer, U., Fahrbach, E., Osterhus, S. & Rohardt, G., 2004. Arctic warming through the Fram Strait: Oceanic heat transport from 3 years of measurements. *Journal of Geophysical Research, Vol 109*.

Schleussner, C. F. et al., 2015. Indications for a North Atlantic ocean circulation regime shift at the onset of the Little Ice Age. *Climate Dynamics* , p. 3623–3633.

Seidenkrantz, M.-S., 2013. Benthic foraminifera as palaeo sea-ice indicators in the subarctic realm e examples from the Labrador SeaeBaffin Bay region. *Quaternary Science Reviews 79*, pp. 135-144.

Seidenkrantz, M. S. et al., 2007. Hydrography and climate of the last 4400 years in a SW Greenland fjord: implications for Labrador Sea palaeoceanography. *The Holocene 17*, pp. 387-401.

Sejrup, H. P. et al., 2010. Response of Norwegian Sea temperature to solar forcing since 1000 A.D.. *Journal of Geophysical Research, Vol. 115*, pp. C12034, doi:10.1029/2010JC006264.

Sejrup, H. P. et al., 2016. North Atlantic-Fennoscandian Holocene climate trends and mechanisms. *Quaternary Science Reviews 147*, pp. 365-378.

Shindell, D. T. et al., 2001. Solar Forcing of Regional Climate Change During the Maunder Minimum. *Science Vol 294*, pp. 2149-2152.

Shindell, D. T., Schmidt, G. A., Miller, R. L. & Mann, M. E., 2003. Volcanic and Solar Forcing of Climate Change during the Preindustrial Era. *Journal of Climate 16*, p. 4094–4107.

Skirbekk, K., Klitgaard Kristensen, D. & Rasmussen, T. L., 2010. Holocene climate variations at the entrance to a warm Arctic fjord: evidence. *Geological Society, London, Special Publications*, pp. 289-304.

Slubowska, M. A., Koc, N., Rasmussen, T. L. & Klitgaard-Kristensen, D., 2005. *Paleoceanography, VOL. 20*, 23 November, pp. 1-15.

Ślubowska, M. A., Koc, N., Rasmussen, T. L. & Klitgaard-Kristensen, D., 2005. Changes in the flow of Atlantic water into the Arctic Ocean since the last deglaciation: Evidence from the northern Svalbard continental margin, 80°N. *Paleoceanography, VOL. 20*, 23 November.

Slubowska-Woldengen, M. et al., 2007. Advection of Atlantic Water to the western and northern Svalbard shelf since 17,500 cal yr BP. *Quaternary Science Review 26*, 20 September, pp. 463-478.

Spielhagen, R. F. et al., 2011. Enhanced Modern Heat Transfer to the Arctic by Warm Atlantic Water. *Science V. 331*, January, pp. 450-453.

Steinsund, P. et al., 1994. Distribution of calcareous benthic foraminifera in recent sediments of the Barents and Kara Sea. *Benthic foraminifera in surface sediments of the Barents and Kara Seas: modern and late Quaternary application*, pp. 61-102.

Svendsen, H. et al., 2002. The physical environment of Kongsfjorden-Krossfjorden, an Arctic fjord system in Svalbard. *Polar Research 21*, pp. 133-166.

Svendsen, J. I. & Mangerud, J., 1997. Holocene glacial and climatic variations on Spitsbergen, Svalbard. *The Holocene*, 6 September, pp. 45-57.

Trouet, V. et al., 2009. Persistent Positive North Atlantic Oscillation Mode Dominated the Medieval Climate Anomaly. *Science 324 (5923)*, 3 April, pp. 78-80.

Trouet, V., Scource, J. D. & Raible, C. C., 2011. North Atlantic storminess and Atlantic Meridional Overturning Circulation during the last Millennium: Reconciling contradictory proxy records of NAO variability. *Global and Planetary Change 84-85*, pp. 48-55.

Tverberg, V. & Nøst, O. A., 2009. Eddy overturning across a shelf edge front: Kongsfjorden, west Spitsbergen. *Journal of Geophysical Research, VOL. 114, C04024*, 30 April.

Vinje, T., 2001. Anomalies and trends of sea-ice extent and atmospheric circulation in the Nordic seas during the period 1864–1998. *J. Climatol. 14*, pp. 255-267.

Walczowski, W., Piechura, J., Osinski, R. & Wieczorek, P., 2005. The West Spitsbergen Current volume and heat transport from synoptic observations in summer. *Deep-Sea Research I 52*, p. 1374–1391.

Werner, K. et al., 2011. Atlantic Water advection to the eastern Fram Strait — Multiproxy evidence for late Holocene variability. *Palaeogeography, Palaeoclimatology, Palaeoecology 308*, pp. 264-276.

Wilson, L. J., Hald, M. & Godtliebsen, F., 2011. Foraminiferal faunal evidence of twentieth-century Barents Sea warming. *The Holocene*, pp. 527-537.

Wohlfarth, B. et al., 1995. Early Holocene environment on Bjørnøya (Svalbard) inferred from multidisciplinary lake sediment studies. *Polar Research 14*, pp. 253-275.

Appendix 1.1: NP15-kb0 specimens count (p. 1-2)

Depth (cm):	Age (CE)	*E. excavatum*	*E. bartletti*	*N. labradorica*	*C. reniforme*	*C. lobatulus*	*I. norcrossi*	*I. helenae*	*Nodosariida sp*	*G. auriculata arctica*	*N. auricula*	*N. turgida*	*T. angulosa*	*Buccella spp*
2,5	1656	84	7	59	26	48	12	11	1	4	2	1	6	29
3,5	1645	85	5	71	12	42	11	8	1	2	2	0	3	31
4,5	1634	56	5	68	27	38	11	14	1	4	7	0	7	34
5,5	1623	63	2	80	18	39	13	15	3	1	4	1	7	26
6,5	1611	73	8	66	28	33	10	13	0	4	4	0	8	26
7,5	1600	63	4	79	44	28	11	7	0	1	7	0	6	18
8,5	1589	60	8	65	33	36	6	16	1	1	11	0	2	26
9,5	1578	55	5	58	32	49	16	6	1	3	8	0	4	26
10,5	1567	50	0	59	43	35	11	20	0	2	17	0	3	22
11,5	1556	55	2	61	32	36	13	17	2	2	13	0	8	15
12,5	1544	59	1	86	29	31	13	5	0	0	13	0	5	21
13,5	1533	48	0	60	27	39	15	6	0	0	10	1	8	28
14,5	1522	63	6	59	35	38	10	4	3	3	10	1	2	19
15,5	1511	74	10	50	47	30	7	10	1	1	9	0	3	23
16,5	1500	103	16	54	36	34	5	6	1	1	9	1	4	13
17,5	1489	90	16	62	33	40	9	12	1	1	6	0	3	12
18,5	1477	89	19	57	40	35	2	12	0	0	6	0	6	14
19,5	1466	89	19	55	39	30	2	11	2	3	7	0	2	24
20,5	1455	94	25	53	38	34	6	8	0	0	3	2	2	18
21,5	1402	111	10	55	31	47	4	7	1	2	8	0	3	18
22,5	1350	110	13	59	34	41	3	10	2	1	8	0	1	15
23,5	1297	112	13	60	30	42	4	11	0	1	9	0	7	12
24,5	1244	107	1	59	28	53	3	11	3	2	4	0	2	17
25,5	1191	112	0	51	22	75	4	4	0	0	5	0	2	15
26,5	1139	120	0	61	34	46	4	11	0	0	4	1	3	15
27,5	1086	115	0	48	32	63	6	4	0	0	4	1	2	22
28,5	1033	105	0	61	29	70	3	5	0	0	7	2	0	18
29,5	981	101	0	60	31	57	6	13	1	0	3	1	0	22
30,5	928	122	0	58	23	48	4	17	0	1	3	0	1	20
31,5	875	118	0	58	29	41	14	13	2	4	2	1	2	12
32,5	822	112	0	59	29	52	17	13	2	1	3	1	1	10
33,5	770	127	0	48	26	54	20	10	0	0	4	0	0	9
34,5	717	115	0	54	23	56	24	11	2	4	1	0	0	13
Sum		2940	195	1993	1020	1440	299	341	31	49	213	14	113	643

S. fusiformis	*S. loeblichi*	*A. gallowayi*	*O. williamsoni*	*O. melo*	*C. neoteretis*	*M. barleeanum*	*S. concava*	*B. pseudopunctata*	*P. osloensis*	Uidentifisert	Sum
0	6	11	0	0	2	0	0	0	0	0	309
0	8	16	1	0	5	0	1	0	0	0	304
0	8	20	0	0	2	0	1	1	0	0	304
3	8	15	0	0	1	0	1	0	0	0	300
0	4	20	0	0	0	1	1	0	1	1	301
0	7	24	0	0	1	1	0	0	0	0	301
0	11	17	0	0	0	7	2	0	0	0	302
0	2	18	0	1	3	12	1	0	0	0	300
0	6	16	1	0	0	14	2	0	0	0	301
4	2	24	0	0	2	12	1	0	0	0	301
1	1	20	0	0	2	13	0	0	0	0	300
3	1	28	0	0	6	19	1	0	0	0	300
1	2	22	0	1	4	15	2	0	0	0	300
1	0	20	0	0	4	10	0	0	0	0	300
0	1	15	0	0	0	0	0	0	0	1	300
2	1	14	0	0	0	0	0	0	0	0	302
3	0	18	0	0	0	0	0	0	0	0	301
0	0	17	0	0	0	0	0	0	0	0	300
4	2	11	1	0	0	0	0	0	0	0	301
1	2	0	0	0	0	0	0	0	0	0	300
1	2	0	0	0	0	0	0	0	0	0	300
1	1	0	1	0	0	0	0	0	0	0	304
3	3	5	0	0	0	0	0	0	0	0	301
0	0	0	2	0	0	0	0	0	0	4	296
1	0	0	0	0	0	0	0	0	0	0	300
2	0	0	1	0	0	0	0	0	0	0	300
0	0	0	0	0	0	0	0	0	0	0	300
0	5	0	0	0	0	0	0	0	0	0	300
3	0	0	0	0	0	0	0	0	0	0	300
2	2	0	0	0	0	0	0	0	0	0	300
0	0	0	0	0	0	0	0	0	0	0	300
2	0	0	0	0	0	0	0	0	0	0	300
0	0	0	0	0	0	0	0	0	0	0	300
38	85	351	7	2	32	104	13	1	1	6	9928

Appendix 1.2: NP15-kb0 sediment properties and calculations

Depth (cm):	Age (CE)	No. of splits	Squares counted	Sedimentation rate (cm/kyr)	Bulk density (g/cm3)	Total dry weight (g)	Total forams (x)	Foram concentration (x/dry weight)	Flux (x/cm2/year)
2,5	1656	16	12	89,55	0,5	104,35	99360	952	42635
3,5	1645	8	9	89,55	0,5	82,32	65793	799	35787
4,5	1634	8	9	89,55	0,5	73,61	65347	888	39750
5,5	1623	8	8	89,55	0,5	84,18	73013	867	38836
6,5	1611	16	8	89,55	0,5	110,05	145020	1318	59004
7,5	1600	32	15	89,55	0,5	82,30	153616	1867	83576
8,5	1589	16	16	89,55	0,5	55,52	71505	1288	57668
9,5	1578	16	19	89,55	0,5	59,63	59792	1003	44897
10,5	1567	16	21	89,55	0,5	91,00	53714	590	26430
11,5	1556	32	15	89,55	0,5	575,78	149328	259	11613
12,5	1544	32	33	89,55	0,5	46,09	67389	1462	65468
13,5	1533	32	14	89,55	0,5	96,86	157697	1628	72900
14,5	1522	16	8	89,55	0,5	115,27	136980	1188	53209
15,5	1511	32	18	89,55	0,5	71,80	120867	1683	75375
16,5	1500	32	12	89,55	0,5	94,98	179960	1895	84838
17,5	1489	32	23	89,55	0,5	64,27	93193	1450	64926
18,5	1477	32	11	89,55	0,5	97,65	193396	1981	88679
19,5	1466	32	11	89,55	0,5	125,27	191935	1532	68604
20,5	1455	16	7	89,55	0,5	116,28	149657	1287	57629
21,5	1402	16	8	18,97	0,5	114,31	126206	1104	10472
22,5	1350	16	9	18,97	0,5	116,74	107966	925	8772
23,5	1297	16	6	18,97	0,5	130,57	155623	1192	11305
24,5	1244	16	9	18,97	0,5	105,22	99531	946	8972
25,5	1191	16	6	18,97	0,5	148,37	142971	964	9140
26,5	1139	16	8	18,97	0,5	128,72	102484	796	7552
27,5	1086	16	6	18,97	0,5	116,70	130320	1117	10592
28,5	1033	16	6	18,97	0,5	114,36	123994	1084	10284
29,5	981	16	6	18,97	0,5	113,59	117669	1036	9826
30,5	928	32	13	18,97	0,5	118,78	102778	865	8207
31,5	875	32	21	18,97	0,5	109,88	60010	546	5180
32,5	822	32	11	18,97	0,5	139,50	107663	772	7320
33,5	770	16	11	18,97	0,5	105,99	50381	475	4509
34,5	717	16	10	18,97	0,5	162,08	51624	319	3021

Appendix 1.3: NP15-kb0 relative abundance (%)

Depth (cm):	Age (CE)	*E. excavatun*	*E. bartletti*	*N. labradori*	*C. reniforme*	*C. lobatulus*	*I. norcrossi*	*I. helenae*	*Nodosariida*	*G. auriculati*	*N. auricula*	*N. turgida*	*T. angulosa*	*Buccella spp*	*S. fusiformis*	*S. loeblichi*	*A. gallowayi*	*O. williamso*	*O. melo*	*C. neoteretis*	*M. barleean*	*Stainforthia*	*B. pseudopu*	*P. osloensis*	Uidentifiser
2,5	**1656**	27	2	19	8	16	4	4	0	1	1	0	2	9	0	2	4	0	0	1	0	0	0	0	0
3,5	1645	28	2	23	4	14	4	3	0	1	1	0	1	10	0	3	5	0	0	2	0	0	0	0	0
4,5	1634	18	2	22	9	13	4	5	0	1	2	0	2	11	0	3	7	0	0	1	0	0	0	0	0
5,5	1623	21	1	27	6	13	4	5	1	0	1	0	2	9	1	3	5	0	0	0	0	0	0	0	0
6,5	1611	24	3	22	9	11	3	4	0	1	1	0	3	9	0	1	7	0	0	0	0	0	0	0	0
7,5	1600	21	1	26	15	9	4	2	0	0	2	0	2	6	0	2	8	0	0	0	0	0	0	0	0
8,5	1589	20	3	22	11	12	2	5	0	0	4	0	1	9	0	4	6	0	0	0	2	1	0	0	0
9,5	1578	18	2	19	11	16	5	2	0	1	3	0	1	9	0	1	6	0	0	1	4	0	0	0	0
10,5	1567	17	0	20	14	12	4	7	0	1	6	0	1	7	0	2	5	0	0	0	5	1	0	0	0
11,5	1556	18	1	20	11	12	4	6	1	1	4	0	3	5	1	1	8	0	0	1	4	0	0	0	0
12,5	1544	20	0	29	10	10	4	2	0	0	4	0	2	7	0	0	7	0	0	1	4	0	0	0	0
13,5	1533	16	0	20	9	13	5	2	0	0	3	0	3	9	1	0	9	0	0	2	6	0	0	0	0
14,5	1522	21	2	20	12	13	3	1	1	1	3	0	1	6	0	1	7	0	0	1	5	1	0	0	0
15,5	1511	25	3	17	16	10	2	3	0	0	3	0	1	8	0	0	7	0	0	1	3	0	0	0	0
16,5	1500	34	5	18	12	11	2	2	0	0	3	0	1	4	0	0	5	0	0	0	0	0	0	0	0
17,5	1489	30	5	21	11	13	3	4	0	0	2	0	1	4	1	0	5	0	0	0	0	0	0	0	0
18,5	1477	30	6	19	13	12	1	4	0	0	2	0	2	5	1	0	6	0	0	0	0	0	0	0	0
19,5	1466	30	6	18	13	10	1	4	1	1	2	0	1	8	0	0	6	0	0	0	0	0	0	0	0
20,5	**1455**	31	8	18	13	11	2	3	0	0	1	1	1	6	1	1	4	0	0	0	0	0	0	0	0
21,5	1402	37	3	18	10	16	1	2	0	1	3	0	1	6	0	1	0	0	0	0	0	0	0	0	0
22,5	1350	37	4	20	11	14	1	3	1	0	3	0	0	5	0	1	0	0	0	0	0	0	0	0	0
23,5	1297	37	4	20	10	14	1	4	0	0	3	0	2	4	0	0	0	0	0	0	0	0	0	0	0
24,5	1244	36	0	20	9	18	1	4	1	1	1	0	1	6	1	1	2	0	0	0	0	0	0	0	0
25,5	1191	38	0	17	7	25	1	1	0	0	2	0	1	5	0	0	0	1	0	0	0	0	0	0	1
26,5	1139	40	0	20	11	15	1	4	0	0	1	0	1	5	0	0	0	0	0	0	0	0	0	0	0
27,5	1086	38	0	16	11	21	2	1	0	0	1	0	1	7	1	0	0	0	0	0	0	0	0	0	0
28,5	1033	35	0	20	10	23	1	2	0	0	2	1	0	6	0	0	0	0	0	0	0	0	0	0	0
29,5	981	34	0	20	10	19	2	4	0	0	1	0	0	7	0	2	0	0	0	0	0	0	0	0	0
30,5	928	41	0	19	8	16	1	6	0	0	1	0	0	7	1	0	0	0	0	0	0	0	0	0	0
31,5	875	39	0	19	10	14	5	4	1	1	1	0	1	4	1	1	0	0	0	0	0	0	0	0	0
32,5	822	37	0	20	10	17	6	4	1	0	1	0	0	3	0	0	0	0	0	0	0	0	0	0	0
33,5	770	42	0	16	9	18	7	3	0	0	1	0	0	3	1	0	0	0	0	0	0	0	0	0	0
34,5	**717**	38	0	18	8	19	8	4	1	1	0	0	0	4	0	0	0	0	0	0	0	0	0	0	0

Appendix 1.4: NP15-kb0 flux of each species (x/cm^2/year)

Depth (cm):	Age (CE)	Total flux	*E. excavatun*	*E. bartletti*	*N. labradori*	*C. reniforme*	*C. lobatulus*	*I. norcrossi*	*I. helenae*	*Nodosariida*	*G. auriculat*	*N. auricula*	*N. turgida*	*T. angulosa*	*Buccella spp*	*S. fusiformis*	*S. loeblichi*	*A. galloway*	*O. williamso*	*O. melo*	*C. neoteretis*	*M. barleean*	*Stainforthia*	*B. pseudopu*	*P. osloensis*	Uidentifisert
2,5	**1656**	7955	2163	180	1519	669	1236	309	283	26	103	51	26	154	747	0	154	283	0	0	51	0	0	0	0	0
3,5	1645	6614	1849	109	1545	261	914	239	174	22	44	44	0	65	674	0	174	348	22	0	109	0	22	0	0	0
4,5	1634	7397	1363	122	1655	657	925	268	341	24	97	170	0	170	827	0	195	487	0	0	49	0	24	24	0	0
5,5	1623	7181	1508	48	1915	431	934	311	359	72	24	96	24	168	622	72	191	359	0	0	24	0	24	0	0	0
6,5	1611	11022	2673	293	2417	1025	1208	366	476	0	146	146	0	293	952	0	146	732	0	0	0	37	37	0	37	37
7,5	1600	15721	3290	209	4126	2298	1462	575	366	0	52	366	0	313	940	0	366	1254	0	0	52	52	0	0	0	0
8,5	1589	10960	2178	290	2359	1198	1307	218	581	36	36	399	0	73	944	0	399	617	0	0	0	254	73	0	0	0
9,5	1578	8537	1565	142	1650	911	1394	455	171	28	85	228	0	114	740	0	57	512	0	28	85	341	28	0	0	0
10,5	1567	5078	844	0	995	725	590	186	337	0	34	287	0	51	371	0	101	270	17	0	0	236	34	0	0	0
11,5	1556	2247	411	15	455	239	269	97	127	15	15	97	0	60	112	30	15	179	0	0	15	90	7	0	0	0
12,5	1544	12718	2501	42	3646	1229	1314	551	212	0	0	551	0	212	890	42	42	848	0	0	85	551	0	0	0	0
13,5	1533	14265	2282	0	2853	1284	1854	713	285	0	0	475	48	380	1331	143	48	1331	0	0	285	903	48	0	0	0
14,5	1522	10488	2202	210	2063	1224	1328	350	140	105	105	350	35	70	664	35	70	769	0	35	140	524	70	0	0	0
15,5	1511	14967	3692	499	2494	2345	1497	349	499	50	50	449	0	150	1147	50	0	998	0	0	200	499	0	0	0	0
16,5	1500	16971	5827	905	3055	2037	1923	283	339	57	57	509	57	226	735	0	57	849	0	0	0	0	0	0	0	57
17,5	1489	13173	3926	698	2704	1439	1745	393	523	44	44	262	0	131	523	87	44	611	0	0	0	0	0	0	0	0
18,5	1477	18068	5342	1141	3422	2401	2101	120	720	0	0	360	0	360	840	180	0	1080	0	0	0	0	0	0	0	0
19,5	1466	14038	4164	889	2574	1825	1404	94	515	94	140	328	0	94	1123	0	0	795	0	0	0	0	0	0	0	0
20,5	**1455**	11922	3723	990	2099	1505	1347	238	317	0	0	119	79	79	713	158	79	436	40	0	0	0	0	0	0	0
21,5	1402	2240	829	75	411	232	351	30	52	7	15	60	0	22	134	7	15	0	0	0	0	0	0	0	0	0
22,5	1350	1950	715	84	383	221	266	19	65	13	6	52	0	6	97	6	13	0	0	0	0	0	0	0	0	0
23,5	1297	2650	976	113	523	262	366	35	96	0	9	78	0	61	105	9	9	0	9	0	0	0	0	0	0	0
24,5	1244	2171	772	7	425	202	382	22	79	22	14	29	0	14	123	22	22	36	0	0	0	0	0	0	0	0
25,5	1191	2271	859	0	391	169	575	31	31	0	0	38	0	15	115	0	0	0	15	0	0	0	0	0	0	31
26,5	1139	1990	796	0	405	225	305	27	73	0	0	27	7	20	99	7	0	0	0	0	0	0	0	0	0	0
27,5	1086	2926	1122	0	468	312	614	59	39	0	0	39	10	20	215	20	0	0	10	0	0	0	0	0	0	0
28,5	1033	2986	1045	0	607	289	697	30	50	0	0	70	20	0	179	0	0	0	0	0	0	0	0	0	0	0
29,5	981	3006	1012	0	601	311	571	60	130	10	0	30	10	0	220	0	50	0	0	0	0	0	0	0	0	0
30,5	928	2654	1079	0	513	203	425	35	150	0	9	27	0	9	177	27	0	0	0	0	0	0	0	0	0	0
31,5	875	1776	698	0	343	172	243	83	77	12	24	12	6	12	71	12	12	0	0	0	0	0	0	0	0	0
32,5	822	2670	997	0	525	258	463	151	116	18	9	27	9	9	89	0	0	0	0	0	0	0	0	0	0	0
33,5	770	1757	744	0	281	152	316	117	59	0	0	23	0	0	53	12	0	0	0	0	0	0	0	0	0	0
34,5	**717**	1264	485	0	228	97	236	101	46	8	17	4	0	0	55	0	0	0	0	0	0	0	0	0	0	0

Appendix 2.1: NP14-Kb3 specimens count (p. 6-7)

Core depth (cm)	Age (CE/BCE)	*E. excavatum* f. *clavata*	*N. labradorica*	*C. reniforme*	*C. lobatulus*	*I. norcrossi*	*I. helenae*	*Nodosariida sp.*	*G. auriculata arctica*	*B. tennerima*	*B. frigida*	*N. auricula*	*N. turgida*	*T. angulosa*
2,5	2014	46	168	14	8	2			10			11	1	
3,5	1979	91	101	27	6	6	3		4			7		
4,5	1943	104	108	24	10	7			1			5		3
5,5	1908	132	76	18	5	10	6					5	1	2
6,5	1872	100	74	28	5	4	5		1			3		
7,5	1837	104	81	26	8	6	5	1	1			3		
8,5	1802	100	67	20	8	8	6		3			6		
9,5	1766	113	61	27	6	10	4					2		
10,5	1731	132	52	27	9	13	11		1			6		
11,5	1695	110	54	27	14	23	2	1	1			3		
12,5	1660	138	39	26	7	19	4					4	1	
13,5	1625	95	60	22	20	14	4	2				8	1	1
14,5	1589	66	91	19	11	19	4		1			17		
15,5	1554	38	135	9	15	7	3	1	6			16	2	1
16,5	1519	46	118	9	11	10	3		13			12		1
17,5	1483	56	101	18	27	15	5		1			6		
18,5	1448	63	107	12	19	7	3		4			7		
19,5	1412	43	118	23	16	15	3	1	5			10	1	
20,5	1377	61	99	19	21	16	6		3			7	1	
21,5	1342	92	93	10	15	18	4		3			6	5	
22,5	1306	88	45	27	16	14	7		5			5	2	
23,5	1271	100	61	26	12	26	1		3			6	3	
24,5	1235	126	48	22	16	17	14		3			3	1	
25,5	1200	132	22	34	13	26	5		2			5		1
26,5	1165	162	29	21	10	13	16		2			4		
27,5	1129	188	15	13	12	29	6		2			2		
28,5	1094	170	20	16	7	7	25					4		
29,5	1058	154	29	12	8	24	3		3			2		
30,5	1023	150	23	20	14	11	7		2		1	1		1
31,5	988	95	19	21	14	27	7		4			1	2	
32,5	952	64	35	39	18	20	17		9	1	1	2		
33,5	917	46	25	36	11	20	10	1	11			1	2	
34,5	881	31	47	63	17	23	9		8			4	2	
35,5	846	55	32	56	9	18	8		7			4	1	1
36,5	811	57	36	72	20	19	6	1	4				1	
37,5	775	57	28	49	22	5	10		5			9		1
38,5	740	76	33	55	9	8	9		7			5	1	1
39,5	705	90	35	25	10	6	8		4			4		
40,5	669	71	76	57	16	3	13	2	10	1		1		
41,5	634	65	59	26	11	5	2		6			1	1	
42,5	598	57	90	59	17	4	13		10			7	2	
43,5	563	57	61	24	15	8	5		10			5		
44,5	528	74	80	47	21	4	15		6	1		4	1	
45,5	492	116	59	24	25	3	4		4			11		
46,5	457	135	83	17	15	3	8		2			7		
47,5	421	126	71	39	17	3	4		2			9		
48,5	386	131	95	32	8	1	5		1		2	3		
49,5	351	149	50	49	14	7	2		2			5	1	
Sum:		4552	3109	1386	638	583	320	10	192	3	4	259	33	13

S. fusiformis	*Buccella spp.*	*S. loeblichi*	*A. gallowayi*	*M. barleeanum*	*E. bartletti*	*C. neoteretis*	*B. pseudopu*	*Q. seminulum*	*P. corrugata*	*R. arctica*	*S. concava*	*Lagena sp.*	*P. osloensis*	*Dentalina sp*	*C. involvens*	*T. trihedra*	*G. lactea*	*O. williamso*	*E. epona*	Sum
		23	7			1	5	3			1		1		1					302
1	2	20	7				10	1					11		1	4				302
	3	18	7			1		2					7			3		1		304
2	1	11	2		1	1	5	1					17		2	2				300
1	1	38	7			1	3	3				1	27			2	1	1		306
1	2	21	5				6	5					24			1				300
2	1	49	4				4	4					21							303
2	1	30	4				6	6				2	23		1				2	300
2	1	27	3		1	1	2	2					9			1	1			301
2	3	24	2				16	2					15	1		1				301
1	1	31	11			1	3	1			2		10	1		1				301
4	3	39	4	2		2	7			1			9			1		1	1	301
	5	37	15	1	3	1	2	1		2		1	2			3				301
1	3	34	8				5			1		1	10		2	1		1	1	301
	2	45	9			1	4	3		1	1		8		1	2				300
3	1	43	5			2	5	2					10					1		301
	3	45	10		2		5	3		1			6			3				300
3	2	30	6	1		1	5	10		1		2	7			1				304
3	3	27	15			1	5	1		1			7	1		3				300
	2	35	4				3	4					6			2			1	303
1	6	36	7			2	9	7		3			20							300
2	2	32	4	2			3	2					9			3		2	1	300
3	4	17	7			1	5			2		2	6		2	1				300
	4	32	5				1	2	1				16							301
	5	26	1			2	2	4		1			4			1				303
	1	18	3				2						7		2			1		301
3	2	17	6	2		2	4	5		3		2	5							300
2	1	22	8				2	1		1			28			2			1	303
1	1	31	5		4		3	3	1	1			22							302
1	3	48	6			1	5	6		1			37			4			1	303
	4	50	3	5		1	1	11				1	16			2				300
2	3	39	5	2		1	10	25					15		1	2			1	269
	1	50	8	3			3	24		1			4	1	1	2				302
3	3	36	4			2	2	16		1			36		1	5				300
	1	40	17	1		3	3	12					7							300
1	3	34	8	2		1	9	9				1	47	1					1	303
	2	45	6	2		7	8	5				1	21							301
1	1	28	7				1	2				1	75			1		1		300
		27	15	1		4	1	1			1									300
		29	5	1			3						87	1		2				304
	2	27	7	1				3	1											300
1	1	24	5					2	1				81	2		2				304
	7	28	3			1	6	2												300
3	3	24	2			1	2	1					17						1	300
2	5	14	4			1	2	2												300
	3	10	5			2	5	1					3							300
1	3	4	7	1	3	2	1													300
1	4	5	5			2	2	1								1				300
56	115	1420	303	27	14	50	196	201	4	22	5	15	793	8	15	59	2	9	11	14427

Appendix 2.2: NP14-Kb3 sediment properties and calculations

Core depth (cm)	Age (CE/BCE)	No. of splits	Squares counted	Sedimentation rate (cm/kyr)	Bulk density (g/cm3)	Total dry weight (g)	Total forams (x)	Foram concentration (x/dry weigh	Total flux (x/cm2/year)
2,5	2014	4	14	28,26	0,5	47,59	25894	544	7687
3,5	1979	8	13	28,26	0,5	64,94	54792	844	11920
4,5	1943	2	11	28,26	0,5	58,86	15899	270	3816
5,5	1908	4	8	28,26	0,5	57,81	42926	743	10490
6,5	1872	4	10	28,26	0,5	62,52	33704	539	7616
7,5	1837	4	8	28,26	0,5	64,07	41333	645	9114
8,5	1802	4	9	28,26	0,5	68,69	36033	525	7411
9,5	1766	4	7	28,26	0,5	76,97	45418	590	8336
10,5	1731	2	7	28,26	0,5	71,21	22254	313	4415
11,5	1695	4	9	28,26	0,5	74,57	33910	455	6424
12,5	1660	4	10	28,26	0,5	69,73	29882	429	6054
13,5	1625	8	19	28,26	0,5	83,61	30784	368	5202
14,5	1589	8	23	28,26	0,5	69,25	24876	359	5075
15,5	1554	8	19	28,26	0,5	93,09	29443	316	4468
16,5	1519	4	16	28,26	0,5	79,42	17083	215	3039
17,5	1483	8	18	28,26	0,5	72,32	29663	410	5795
18,5	1448	8	19	28,26	0,5	84,53	27431	325	4585
19,5	1412	8	26	28,26	0,5	85,77	19556	228	3221
20,5	1377	8	26	28,26	0,5	91,81	19066	208	2934
21,5	1342	16	38	28,26	0,5	92,93	25419	274	3864
22,5	1306	16	45	28,26	0,5	84,00	20899	249	3515
23,5	1271	8	20	28,26	0,5	83,61	22874	274	3865
24,5	1235	8	30	28,26	0,5	57,84	14825	256	3621
25,5	1200	16	28	28,26	0,5	93,50	30857	330	4662
26,5	1165	8	14	28,26	0,5	79,68	29947	376	5310
27,5	1129	8	12	28,26	0,5	56,42	33877	600	8483
28,5	1094	8	20	28,26	0,5	91,27	19689	216	3048
29,5	1058	8	10	28,26	0,5	91,54	38104	416	5881
30,5	1023	4	8	28,26	0,5	91,06	23018	253	3571
31,5	988	8	17	28,26	0,5	101,79	20915	205	2903
32,5	952	8	38	28,26	0,5	101,46	9021	89	1256
33,5	917	16	45	28,26	0,5	108,39	14670	135	1912
34,5	881	4	36	28,26	0,5	71,02	4407	62	877
35,5	846	8	23	28,26	0,5	98,84	13243	134	1893
36,5	811	8	45	28,26	0,5	84,59	6486	77	1083
37,5	775	8	27	28,26	0,5	71,99	10337	144	2029
38,5	740	8	29	28,26	0,5	90,27	9185	102	1438
39,5	705	8	16	28,26	0,5	85,94	15852	184	2606
40,5	669	16	41	28,26	0,5	97,98	11751	120	1694
41,5	634	4	9	28,26	0,5	70,96	12675	179	2523
42,5	598	4	16	28,26	0,5	69,32	6731	97	1372
43,5	563	8	19	28,26	0,5	96,04	10667	111	1569
44,5	528	8	24	28,26	0,5	85,74	7913	92	1304
45,5	492	8	11	28,26	0,5	79,62	16108	202	2858
46,5	457	16	37	28,26	0,5	92,64	8889	96	1356
47,5	421	16	17	28,26	0,5	89,23	17847	200	2826
48,5	386	8	10	28,26	0,5	111,74	13896	124	1757
49,5	351	16	8	28,26	0,5	117,65	31555	268	3789

Appendix 2.3: NP14-Kb3 relative abundance (%) (p. 9-10)

Core depth (	Age (CE/ BCE	*E. excavatun*	*N. labradori*	*C. reniforme*	*C. lobatulus*	*I. norcrossi*	*I. helenae*	*Nodosariida*	*G. auriculata*	*B. tennerima*	*B. frigida*	*N. auricula*	*N. turgida*	*T. angulosa*
2,5	2014	15	56	5	3	1	0	0	3	0	0	4	0	0
3,5	1979	30	33	9	2	2	1	0	1	0	0	2	0	0
4,5	1943	34	36	8	3	2	0	0	0	0	0	2	0	1
5,5	1908	44	25	6	2	3	2	0	0	0	0	2	0	1
6,5	1872	33	24	9	2	1	2	0	0	0	0	1	0	0
7,5	1837	35	27	9	3	2	2	0	0	0	0	1	0	0
8,5	1802	33	22	7	3	3	2	0	1	0	0	2	0	0
9,5	1766	38	20	9	2	3	1	0	0	0	0	1	0	0
10,5	1731	44	17	9	3	4	4	0	0	0	0	2	0	0
11,5	1695	37	18	9	5	8	1	0	0	0	0	1	0	0
12,5	1660	46	13	9	2	6	1	0	0	0	0	1	0	0
13,5	1625	32	20	7	7	5	1	1	0	0	0	3	0	0
14,5	1589	22	30	6	4	6	1	0	0	0	0	6	0	0
15,5	1554	13	45	3	5	2	1	0	2	0	0	5	1	0
16,5	1519	15	39	3	4	3	1	0	4	0	0	4	0	0
17,5	1483	19	34	6	9	5	2	0	0	0	0	2	0	0
18,5	1448	21	36	4	6	2	1	0	1	0	0	2	0	0
19,5	1412	14	39	8	5	5	1	0	2	0	0	3	0	0
20,5	1377	20	33	6	7	5	2	0	1	0	0	2	0	0
21,5	1342	30	31	3	5	6	1	0	1	0	0	2	2	0
22,5	1306	29	15	9	5	5	2	0	2	0	0	2	1	0
23,5	1271	33	20	9	4	9	0	0	1	0	0	2	1	0
24,5	1235	42	16	7	5	6	5	0	1	0	0	1	0	0
25,5	1200	44	7	11	4	9	2	0	1	0	0	2	0	0
26,5	1165	53	10	7	3	4	5	0	1	0	0	1	0	0
27,5	1129	62	5	4	4	10	2	0	1	0	0	1	0	0
28,5	1094	57	7	5	2	2	8	0	0	0	0	1	0	0
29,5	1058	51	10	4	3	8	1	0	1	0	0	1	0	0
30,5	1023	50	8	7	5	4	2	0	1	0	0	0	0	0
31,5	988	31	6	7	5	9	2	0	1	0	0	0	1	0
32,5	952	21	12	13	6	7	6	0	3	0	0	1	0	0
33,5	917	17	9	13	4	7	4	0	4	0	0	0	1	0
34,5	881	10	16	21	6	8	3	0	3	0	0	1	1	0
35,5	846	18	11	19	3	6	3	0	2	0	0	1	0	0
36,5	811	19	12	24	7	6	2	0	1	0	0	0	0	0
37,5	775	19	9	16	7	2	3	0	2	0	0	3	0	0
38,5	740	25	11	18	3	3	3	0	2	0	0	2	0	0
39,5	705	30	12	8	3	2	3	0	1	0	0	1	0	0
40,5	669	24	25	19	5	1	4	1	3	0	0	0	0	0
41,5	634	21	19	9	4	2	1	0	2	0	0	0	0	0
42,5	598	19	30	20	6	1	4	0	3	0	0	2	1	0
43,5	563	19	20	8	5	3	2	0	3	0	0	2	0	0
44,5	528	25	27	16	7	1	5	0	2	0	0	1	0	0
45,5	492	39	20	8	8	1	1	0	1	0	0	4	0	0
46,5	457	45	28	6	5	1	3	0	1	0	0	2	0	0
47,5	421	42	24	13	6	1	1	0	1	0	0	3	0	0
48,5	386	44	32	11	3	0	2	0	0	0	1	1	0	0
49,5	351	50	17	16	5	2	1	0	1	0	0	2	0	0

S. fusiformis	*Buccella spp*	*S. loeblichi*	*A. gallowayi*	*M. barleean*	*E. bartletti*	*C. neoteretis*	*B. pseudopu*	*Q. seminulu*	*P. corrugata*	*R. arctica*	*S. concava*	*Lagena sp.*	*P. osloensis*	*Dentalina sp*	*C. involvens*	*T. trihedra*	*G. lactea*	*O. williamso*	*E. epona*
0	0	8	2	0	0	0	2	1	0	0	0	0	0	0	0	0	0	0	0
0	1	7	2	0	0	0	3	0	0	0	0	0	4	0	0	1	0	0	0
0	1	6	2	0	0	0	0	1	0	0	0	0	2	0	0	1	0	0	0
1	0	4	1	0	0	0	2	0	0	0	0	0	6	0	1	1	0	0	0
0	0	12	2	0	0	0	1	1	0	0	0	0	9	0	0	1	0	0	0
0	1	7	2	0	0	0	2	2	0	0	0	0	8	0	0	0	0	0	0
1	0	16	1	0	0	0	1	1	0	0	0	0	7	0	0	0	0	0	0
1	0	10	1	0	0	0	2	2	0	0	0	1	8	0	0	0	0	0	1
1	0	9	1	0	0	0	1	1	0	0	0	0	3	0	0	0	0	0	0
1	1	8	1	0	0	0	5	1	0	0	0	0	5	0	0	0	0	0	0
0	0	10	4	0	0	0	1	0	0	0	1	0	3	0	0	0	0	0	0
1	1	13	1	1	0	1	2	0	0	0	0	0	3	0	0	0	0	0	0
0	2	12	5	0	1	0	1	0	0	1	0	0	1	0	0	1	0	0	0
0	1	11	3	0	0	0	2	0	0	0	0	0	3	0	1	0	0	0	0
0	1	15	3	0	0	0	1	1	0	0	0	0	3	0	0	1	0	0	0
1	0	14	2	0	0	1	2	1	0	0	0	0	3	0	0	0	0	0	0
0	1	15	3	0	1	0	2	1	0	0	0	0	2	0	0	1	0	0	0
1	1	10	2	0	0	0	2	3	0	0	0	1	2	0	0	0	0	0	0
1	1	9	5	0	0	0	2	0	0	0	0	0	2	0	0	1	0	0	0
0	1	12	1	0	0	0	1	1	0	0	0	0	2	0	0	1	0	0	0
0	2	12	2	0	0	1	3	2	0	1	0	0	7	0	0	0	0	0	0
1	1	11	1	1	0	0	1	1	0	0	0	0	3	0	0	1	0	1	0
1	1	6	2	0	0	0	2	0	0	1	0	1	2	0	1	0	0	0	0
0	1	11	2	0	0	0	0	1	0	0	0	0	5	0	0	0	0	0	0
0	2	9	0	0	0	1	1	1	0	0	0	0	1	0	0	0	0	0	0
0	0	6	1	0	0	0	1	0	0	0	0	0	2	0	1	0	0	0	0
1	1	6	2	1	0	1	1	2	0	1	0	1	2	0	0	0	0	0	0
1	0	7	3	0	0	0	1	0	0	0	0	0	9	0	0	1	0	0	0
0	0	10	2	0	1	0	1	1	0	0	0	0	7	0	0	0	0	0	0
0	1	16	2	0	0	0	2	2	0	0	0	0	12	0	0	1	0	0	0
0	1	17	1	2	0	0	0	4	0	0	0	0	5	0	0	1	0	0	0
1	1	14	2	1	0	0	4	9	0	0	0	0	6	0	0	1	0	0	0
0	0	17	3	1	0	0	1	8	0	0	0	0	1	0	0	1	0	0	0
1	1	12	1	0	0	1	1	5	0	0	0	0	12	0	0	2	0	0	0
0	0	13	6	0	0	1	1	4	0	0	0	0	2	0	0	0	0	0	0
0	1	11	3	1	0	0	3	3	0	0	0	0	16	0	0	0	0	0	0
0	1	15	2	1	0	2	3	2	0	0	0	0	7	0	0	0	0	0	0
0	0	9	2	0	0	0	0	1	0	0	0	0	25	0	0	0	0	0	0
0	0	9	5	0	0	1	0	0	0	0	0	0	0	0	0	0	0	0	0
0	0	10	2	0	0	0	1	0	0	0	0	0	29	0	0	1	0	0	0
0	1	9	2	0	0	0	0	1	0	0	0	0	0	0	0	0	0	0	0
0	0	8	2	0	0	0	0	1	0	0	0	0	27	1	0	1	0	0	0
0	2	9	1	0	0	0	2	1	0	0	0	0	0	0	0	0	0	0	0
1	1	8	1	0	0	0	1	0	0	0	0	0	6	0	0	0	0	0	0
1	2	5	1	0	0	0	1	1	0	0	0	0	0	0	0	0	0	0	0
0	1	3	2	0	0	1	2	0	0	0	0	0	1	0	0	0	0	0	0
0	1	1	2	0	1	1	0	0	0	0	0	0	0	0	0	0	0	0	0
0	1	2	2	0	0	1	1	0	0	0	0	0	0	0	0	0	0	0	0

Appendix 2.4: NP14-Kb3 flux of each species (x/cm^2/year) (p. 11-12)

Core depth (cm)	Age (BCE/CE)	Total flux (x/	*E. excavatun*	*N. labradori*	*C. reniforme*	*C. lobatulus*	*I. norcrossi*	*I. helenae*	*Nodosariida*	*G. auriculata*	*B. tennerima*	*B. frigida*	*N. auricula*	*N. turgida*	*T. angulosa*
2,5	2014	1153	176	641	53	31	8	0	0	38	0	0	42	4	0
3,5	1979	1819	548	608	163	36	36	18	0	24	0	0	42	0	0
4,5	1943	597	204	212	47	20	14	0	0	2	0	0	10	0	6
5,5	1908	1650	726	418	99	27	55	33	0	0	0	0	27	5	11
6,5	1872	1245	407	301	114	20	16	20	0	4	0	0	12	0	0
7,5	1837	1488	516	402	129	40	30	25	5	5	0	0	15	0	0
8,5	1802	1246	411	276	82	33	33	25	0	12	0	0	25	0	0
9,5	1766	1416	533	288	127	28	47	19	0	0	0	0	9	0	0
10,5	1731	768	337	133	69	23	33	28	0	3	0	0	15	0	0
11,5	1695	1141	417	205	102	53	87	8	4	4	0	0	11	0	0
12,5	1660	1098	503	142	95	26	69	15	0	0	0	0	15	4	0
13,5	1625	964	304	192	70	64	45	13	6	0	0	0	26	3	3
14,5	1589	961	211	291	61	35	61	13	0	3	0	0	54	0	0
15,5	1554	866	109	388	26	43	20	9	3	17	0	0	46	6	3
16,5	1519	600	92	236	18	22	20	6	0	26	0	0	24	0	2
17,5	1483	1176	219	395	70	105	59	20	0	4	0	0	23	0	0
18,5	1448	950	200	339	38	60	22	10	0	13	0	0	22	0	0
19,5	1412	693	98	269	52	36	34	7	2	11	0	0	23	2	0
20,5	1377	639	130	211	40	45	34	13	0	6	0	0	15	2	0
21,5	1342	873	265	268	29	43	52	12	0	9	0	0	17	14	0
22,5	1306	807	237	121	73	43	38	19	0	13	0	0	13	5	0
23,5	1271	912	304	186	79	36	79	3	0	9	0	0	18	9	0
24,5	1235	879	369	141	64	47	50	41	0	9	0	0	9	3	0
25,5	1200	1170	513	85	132	51	101	19	0	8	0	0	19	0	4
26,5	1165	1381	739	132	96	46	59	73	0	9	0	0	18	0	0
27,5	1129	2261	1412	113	98	90	218	45	0	15	0	0	15	0	0
28,5	1094	836	474	56	45	20	20	70	0	0	0	0	11	0	0
29,5	1058	1683	856	161	67	44	133	17	0	17	0	0	11	0	0
30,5	1023	1054	524	80	70	49	38	24	0	7	0	3	3	0	3
31,5	988	891	279	56	62	41	79	21	0	12	0	0	3	6	0
32,5	952	396	84	46	51	24	26	22	0	12	1	1	3	0	0
33,5	917	561	96	52	75	23	42	21	2	23	0	0	2	4	0
34,5	881	300	31	47	63	17	23	9	0	8	0	0	4	2	0
35,5	846	671	123	72	125	20	40	18	0	16	0	0	9	2	2
36,5	811	401	76	48	96	27	25	8	1	5	0	0	0	1	0
37,5	775	793	149	73	128	58	13	26	0	13	0	0	24	0	3
38,5	740	585	148	64	107	17	16	17	0	14	0	0	10	2	2
39,5	705	1110	333	129	92	37	22	30	0	15	0	0	15	0	0
40,5	669	760	180	192	144	41	8	33	5	25	3	0	3	0	0
41,5	634	1210	259	235	104	44	20	8	0	24	0	0	4	4	0
42,5	598	688	131	206	135	39	9	30	0	23	0	0	16	5	0
43,5	563	847	159	170	67	42	22	14	0	28	0	0	14	0	0
44,5	528	741	183	198	116	52	10	37	0	15	2	0	10	2	0
45,5	492	1742	674	343	139	145	17	23	0	23	0	0	64	0	0
46,5	457	890	401	246	50	45	9	24	0	6	0	0	21	0	0
47,5	421	2012	845	476	262	114	20	27	0	13	0	0	60	0	0
48,5	386	1365	596	432	146	36	5	23	0	5	0	9	14	0	0
49,5	351	3242	1610	540	530	151	76	22	0	22	0	0	54	11	0

S. fusiformis	*Buccella spp.*	*S. loeblichi*	*A. gallowayi*	*M. barleeani*	*E. bartletti*	*C. neoteretis*	*B. pseudopu*	*Q. seminulu*	*P. corrugata*	*R. arctica*	*S. concava*	*Lagena sp.*	*P. osloensis*	*Dentalina sp*	*C. involvens*	*T. trihedra*	*G. lactea*	*O. williamso*	*E. epona*
0	0	88	27	0	0	4	19	11	0	0	4	0	4	0	4	0	0	0	0
6	12	120	42	0	0	0	60	6	0	0	0	0	66	0	6	24	0	0	0
0	6	35	14	0	0	2	0	4	0	0	0	0	14	0	0	6	0	2	0
11	5	60	11	0	5	5	27	5	0	0	0	0	93	0	11	11	0	0	0
4	4	155	28	0	0	4	12	12	0	0	0	4	110	0	0	8	4	4	0
5	10	104	25	0	0	0	30	25	0	0	0	0	119	0	0	5	0	0	0
8	4	202	16	0	0	0	16	16	0	0	0	0	86	0	0	0	0	0	0
9	5	142	19	0	0	0	28	28	0	0	0	9	109	0	5	0	0	0	9
5	3	69	8	0	3	3	5	5	0	0	0	0	23	0	0	3	3	0	0
8	11	91	8	0	0	0	61	8	0	0	0	0	57	4	0	4	0	0	0
4	4	113	40	0	0	4	11	4	0	0	7	0	36	4	0	4	0	0	0
13	10	125	13	6	0	6	22	0	0	3	0	0	29	0	0	3	0	3	3
0	16	118	48	3	10	3	6	3	0	6	0	3	6	0	0	10	0	0	0
3	9	98	23	0	0	0	14	0	0	3	0	3	29	0	6	3	0	3	3
0	4	90	18	0	0	2	8	6	0	2	2	0	16	0	2	4	0	0	0
12	4	168	20	0	0	8	20	8	0	0	0	0	39	0	0	0	0	4	0
0	10	143	32	0	6	0	16	10	0	3	0	0	19	0	0	10	0	0	0
7	5	68	14	2	0	2	11	23	0	2	0	5	16	0	0	2	0	0	0
6	6	58	32	0	0	2	11	2	0	2	0	0	15	2	0	6	0	0	0
0	6	101	12	0	0	0	9	12	0	0	0	0	17	0	0	6	0	0	3
3	16	97	19	0	0	5	24	19	0	8	0	0	54	0	0	0	0	0	0
6	6	97	12	6	0	0	9	6	0	0	0	0	27	0	0	9	0	6	3
9	12	50	21	0	0	3	15	0	0	6	0	6	18	0	6	3	0	0	0
0	16	124	19	0	0	0	4	8	4	0	0	0	62	0	0	0	0	0	0
0	23	119	5	0	0	9	9	18	0	5	0	0	18	0	0	5	0	0	0
0	8	135	23	0	0	0	15	0	0	0	0	0	53	0	15	0	0	8	0
8	6	47	17	6	0	6	11	14	0	8	0	6	14	0	0	0	0	0	0
11	6	122	44	0	0	0	11	6	0	6	0	0	156	0	0	11	0	0	6
3	3	108	17	0	14	0	10	10	3	3	0	0	77	0	0	0	0	0	0
3	9	141	18	0	0	3	15	18	0	3	0	0	109	0	0	12	0	0	3
0	5	66	4	7	0	1	1	15	0	0	0	1	21	0	0	3	0	0	0
4	6	81	10	4	0	2	21	52	0	0	0	0	31	0	2	4	0	0	2
0	1	50	8	3	0	0	3	24	0	1	0	0	4	1	1	2	0	0	0
7	7	81	9	0	0	4	4	36	0	2	0	0	81	0	2	11	0	0	0
0	1	53	23	1	0	4	4	16	0	0	0	0	9	0	0	0	0	0	0
3	8	89	21	5	0	3	24	24	0	0	0	3	123	3	0	0	0	0	3
0	4	87	12	4	0	14	16	10	0	0	0	2	41	0	0	0	0	0	0
4	4	104	26	0	0	0	4	7	0	0	0	4	277	0	0	4	0	4	0
0	0	68	38	3	0	10	3	3	0	0	3	0	0	0	0	0	0	0	0
0	0	115	20	4	0	0	12	0	0	0	0	0	346	4	0	8	0	0	0
0	5	62	16	2	0	0	0	7	2	0	0	0	0	0	0	0	0	0	0
3	3	67	14	0	0	0	0	6	3	0	0	0	226	6	0	6	0	0	0
0	17	69	7	0	0	2	15	5	0	0	0	0	0	0	0	0	0	0	0
17	17	139	12	0	0	6	12	6	0	0	0	0	99	0	0	0	0	0	6
6	15	42	12	0	0	3	6	6	0	0	0	0	0	0	0	0	0	0	0
0	20	67	34	0	0	13	34	7	0	0	0	0	20	0	0	0	0	0	0
5	14	18	32	5	14	9	5	0	0	0	0	0	0	0	0	0	0	0	0
11	43	54	54	0	0	22	22	11	0	0	0	0	0	0	0	11	0	0	0

Appendix 3: NP15-Kb3 dry weight

Paleo samples	Dry weight	63µm	1mm
NP15-Kb0-MC-A 2-3 cm	104,35	6,54	29,65
NP15-Kb0-MC-A 3-4 cm	82,32	5,77	20,69
NP15-Kb0-MC-A 4-5 cm	73,61	6,38	14,42
NP15-Kb0-MC-A 5-6 cm	84,18	5,97	11,19
NP15-Kb0-MC-A 6-7 cm	110,05	9,76	10,82
NP15-Kb0-MC-A 7-8 cm	82,30	9,39	7,11
NP15-Kb0-MC-A 8-9 cm	55,52	8,69	7,13
NP15-Kb0-MC-A 9-10 cm	59,63	9,00	8,98
NP15-Kb0-MC-A 10-11 cm	91,00	9,10	38,87
NP15-Kb0-MC-A 11-12 cm	575,78	8,77	467,07
NP15-Kb0-MC-A 12-13 cm	46,09	8,17	2,68
NP15-Kb0-MC-A 13-14 cm	96,86	10,21	14,68
NP15-Kb0-MC-A 14-15 cm	115,27	9,52	16,76
NP15-Kb0-MC-A 15-16 cm	71,80	10,44	0,48
NP15-Kb0-MC-A 16-17 cm	94,98	10,10	0,78
NP15-Kb0-MC-A 17-18 cm	64,27	9,41	0,53
NP15-Kb0-MC-A 18-19 cm	97,65	10,32	0,63
NP15-Kb0-MC-A 19-20 cm	125,27	9,99	0,93
NP15-Kb0-MC-A 20-21 cm	116,28	8,44	0,91
NP15-Kb0-MC-A 21-22 cm	114,31	8,28	1,72
NP15-Kb0-MC-A 22-23 cm	116,74	10,97	1,16
NP15-Kb0-MC-A 23-24 cm	130,57	10,74	3,06
NP15-Kb0-MC-A 24-25 cm	105,22	8,54	4,80
NP15-Kb0-MC-A 25-26 cm	148,37	12,41	2,80
NP15-Kb0-MC-A 26-27 cm	128,72	11,82	9,27
NP15-Kb0-MC-A 27-28 cm	116,70	11,81	2,15
NP15-Kb0-MC-A 28-29 cm	114,36	11,40	3,50
NP15-Kb0-MC-A 29-30 cm	113,59	10,92	1,36
NP15-Kb0-MC-A 30-31 cm	118,78	10,08	1,38
NP15-Kb0-MC-A 31-32 cm	109,88	10,58	1,46
NP15-Kb0-MC-A 32-33 cm	139,50	10,38	1,58
NP15-Kb0-MC-A 33-34 cm	105,99	10,62	1,15
NP15-Kb0-MC-A 34-35 cm	162,08	10,75	1,43

Appendix 4: NP14-Kb3 dry weight

Paleo samples	Dry weight	63µm	1mm
NP14-Kb3-MC-A 2-3 cm	47,59	1,88	0,97
NP14-Kb3-MC-A 3-4 cm	64,94	2,54	0,88
NP14-Kb3-MC-A 4-5 cm	58,86	2,70	0,78
NP14-Kb3-MC-A 5-6 cm	57,81	2,49	1,37
NP14-Kb3-MC-A 6-7 cm	62,52	2,59	1,02
NP14-Kb3-MC-A 7-8 cm	64,07	2,48	0,79
NP14-Kb3-MC-A 8-9 cm	68,69	2,80	0,76
NP14-Kb3-MC-A 9-10 cm	76,97	2,82	0,36
NP14-Kb3-MC-A 10-11 cm	71,21	2,36	3,29
NP14-Kb3-MC-A 11-12 cm	74,57	3,04	4,95
NP14-Kb3-MC-A 12-13 cm	69,73	3,11	3,30
NP14-Kb3-MC-A 13-14 cm	83,61	4,25	2,20
NP14-Kb3-MC-A 14-15 cm	69,25	4,08	0,47
NP14-Kb3-MC-A 15-16 cm	93,09	4,35	3,41
NP14-Kb3-MC-A 16-17 cm	79,42	3,41	1,63
NP14-Kb3-MC-A 17-18 cm	72,32	3,82	1,65
NP14-Kb3-MC-A 18-19 cm	84,53	4,06	1,56
NP14-Kb3-MC-A 19-20 cm	85,77	3,93	0,17
NP14-Kb3-MC-A 20-21 cm	91,81	3,92	0,80
NP14-Kb3-MC-A 21-22 cm	92,93	5,73	0,61
NP14-Kb3-MC-A 22-23 cm	84,00	6,11	11,21
NP14-Kb3-MC-A 23-24 cm	83,61	5,13	0,66
NP14-Kb3-MC-A 24-25 cm	57,84	3,74	0,95
NP14-Kb3-MC-A 25-26 cm	93,50	5,57	2,84
NP14-Kb3-MC-A 26-27 cm	79,68	4,66	3,56
NP14-Kb3-MC-A 27-28 cm	56,42	3,87	0,44
NP14-Kb3-MC-A 28-29 cm	91,27	4,51	2,26
NP14-Kb3-MC-A 29-30 cm	91,54	4,08	0,80
NP14-Kb3-MC-A 30-31 cm	91,06	3,45	2,17
NP14-Kb3-MC-A 31-32 cm	101,79	5,46	5,16
NP14-Kb3-MC-A 32-33 cm	101,46	7,48	7,72
NP14-Kb3-MC-A 33-34 cm	108,39	8,78	7,23
NP14-Kb3-MC-A 34-35 cm	71,02	4,35	1,31
NP14-Kb3-MC-A 35-36 cm	98,84	5,50	1,07
NP14-Kb3-MC-A 36-37 cm	84,59	4,69	0,92
NP14-Kb3-MC-A 37-38 cm	71,99	3,92	0,25
NP14-Kb3-MC-A 38-39 cm	90,27	4,95	0,44
NP14-Kb3-MC-A 39-40 cm	85,94	4,99	6,88
NP14-Kb3-MC-A 40-41 cm	97,98	5,67	4,53
NP14-Kb3-MC-A 41-42 cm	70,96	2,93	2,36
NP14-Kb3-MC-A 42-43 cm	69,32	2,20	1,55
NP14-Kb3-MC-A 43-44 cm	96,04	3,42	3,60
NP14-Kb3-MC-A 44-45 cm	85,74	4,25	4,30
NP14-Kb3-MC-A 45-46 cm	79,62	4,36	2,92
NP14-Kb3-MC-A 46-47 cm	92,64	6,02	11,83
NP14-Kb3-MC-A 47-48 cm	89,23	5,37	5,80
NP14-Kb3-MC-A 48-49 cm	111,74	6,40	5,40
NP14-Kb3-MC-A 49-50 cm	117,65	7,93	7,69

Appendix 5: C-14 report

POZNAN RADIOCARBON LABORATORY

Poznań, 06-09-2016

Report

on C-14 dating in the Poznań Radiocarbon Laboratory

Customer: **Arto Miettinen**
Norwegian Polar Institute

Fram Centre
N-9296- Tromsø
Norway

Job no.: 11294/16

Sample name	*Lab. no.*	*Age 14C*	*Remark*
NP15-Kb0-1	Poz-83769	**750 ± 50 BP**	0.12mgC
NP15-Kb0-2	Poz-83770	**980 ± 60 BP**	0.08mgC
NP15-Kb0-3	Poz-83771	**1780 ± 50 BP**	0.1mgC

Comments:

Head of the Laboratory
Prof. dr hab. Tomasz Goslar